

**The Peritoneal Cavity–Bone Marrow Axis:  
How Intraperitoneal Administration of  $\beta$ -Glucan Induces Central Trained Immunity**

Elizabeth Lapshina  
Supervisor: Dr. Maziar Divangahi

Faculty of Medicine and Health Sciences  
Department of Microbiology and Immunology  
Meakins-Christie Laboratories, RI-MUHC  
McGill University, Montreal, Quebec, Canada

August 2024

A thesis submitted to McGill University in partial fulfillment of the requirements of the degree of  
Master of Science (MSc).

© Elizabeth Lapshina 2024

## TABLE OF CONTENTS

Abstract .....	iv
Résumé.....	vi
Acknowledgements .....	viii
Author Contributions .....	ix
List of Figures .....	x
List of Abbreviations .....	xi
<b>Chapter 1: Introduction .....</b>	<b>1</b>
1.1. Trained immunity .....	1
1.1.1. Evidence for innate immune memory in plants and invertebrates.....	1
1.1.2. Evidence for innate immune memory in vertebrates .....	3
1.1.3. Peripheral trained immunity .....	4
1.1.4. Central trained immunity .....	6
1.2. Hematopoietic stem cells .....	8
1.2.1. Hematopoiesis .....	8
1.2.2. Regulation of steady-state hematopoiesis .....	10
1.2.3. Stress-induced hematopoiesis .....	12
1.2.4. Extramedullary hematopoiesis .....	14
1.3. $\beta$ -Glucan .....	15
1.3.1. $\beta$ -Glucan in nature .....	15
1.3.2. Immunomodulatory properties of $\beta$ -glucan .....	16
1.3.3. Cellular immune response to $\beta$ -glucan .....	17
1.4. Peritoneal cavity .....	19
1.4.1. Anatomy and physiology of the peritoneal cavity .....	19
1.4.2. Circulatory and lymphatic systems of the peritoneal cavity.....	20
1.4.3. Innate immunity in the peritoneal cavity .....	21
1.4.4. Adaptive immunity in the peritoneal cavity.....	23
1.5. Central Hypothesis and Aims .....	26

<b>Chapter 2: Methods and Materials</b> .....	27
2.1. Mice .....	27
2.2. $\beta$ -Glucan.....	27
2.2.1. Preparation of $\beta$ -glucan.....	27
2.2.2. Staining $\beta$ -glucan .....	28
2.3. <i>In vivo</i> training with $\beta$ -glucan .....	28
2.4. Cell isolations .....	28
2.4.1. Isolation of peritoneal cells .....	28
2.4.2. Isolation of bone marrow cells .....	29
2.4.3. Isolation of splenic cells .....	29
2.4.4. Isolation of cells from blood.....	29
2.5. Flow cytometry .....	29
2.5.1. Hematopoietic stem and progenitor (“LKS”) panel.....	30
2.5.2. Innate panel .....	30
2.5.3. Adaptive panel .....	31
2.5.4. Peritoneal B1 cell panel .....	31
2.6. Confocal microscopy .....	32
2.7. Splenectomy .....	32
2.8. Statistical analysis .....	33
<b>Chapter 3: Results</b> .....	34
3.1. $\beta$ -Glucan expands HSPC populations in the BM.....	34
3.2. $\beta$ -Glucan-induced HSC expansion is independent of adaptive immunity.....	35
3.3. Innate immune response to $\beta$ -glucan treatment in the peritoneal cavity, spleen and BM .....	36
3.4. $\beta$ -Glucan expands HSPC populations in the spleen .....	38
3.5. The role of the spleen in $\beta$ -glucan-mediated trained immunity .....	39
3.6. Peritoneal neutrophils and macrophages recognize and ingest $\beta$ -glucan .....	40
3.7. $\beta$ -Glucan is likely not directly accessing BM via a cell intermediate.....	41
3.8. $\beta$ -Glucan-induced LKS expansion is likely independent of dectin-1 signaling .....	42

<b>Chapter 4: Discussion</b> .....	44
<b>Chapter 5: Conclusion</b> .....	59
<b>References</b> .....	60
<b>Appendix A: Figures and Figure Legends</b> .....	74
<b>Appendix B: Supplementary Figures and Figure Legends</b> .....	83

## ABSTRACT

Immunological memory has been traditionally associated with the adaptive branch of immunity. However, growing evidence suggests that innate immune cells can elicit a more robust and broad immune response against a secondary homologous or heterologous insult, independent of adaptive immunity. This memory capacity of innate immunity is termed as “trained immunity”. Interestingly, adjuvants like  $\beta$ -glucan (a component derived from fungal cell walls) have been shown to significantly expand and epigenetically remodel hematopoietic stem cells (HSCs) in the bone marrow (BM) via interleukin-1 or type I interferon signaling, which generates functionally enhanced mature myeloid cells and increases host defense against pulmonary infections such as *Mycobacterium tuberculosis* or influenza A virus. The most common *in vivo* model of  $\beta$ -glucan-induced trained immunity employs an intraperitoneal (IP) injection of  $\beta$ -glucan. However, our understanding of how  $\beta$ -glucan in the peritoneal cavity trains HSCs in the BM is very limited. Here we describe the immunomodulatory effects of  $\beta$ -glucan in the peritoneal cavity and peripheral organs and aim to investigate the mechanisms by which IP administration of  $\beta$ -glucan generates central trained immunity in the BM. Similar to published studies, we found that one dose of  $\beta$ -glucan-IP induced central trained immunity by expanding the HSC compartment in the BM.  $\beta$ -Glucan dramatically altered the peritoneal immune composition; specifically, tissue-resident large peritoneal macrophages and B cells were rapidly depleted, while neutrophils, dendritic cells, monocytes and small peritoneal macrophages accumulated in the peritoneal cavity. We also showed that  $\beta$ -glucan was detected and engulfed by peritoneal macrophages and neutrophils, which were not responsible for shuttling  $\beta$ -glucan into the BM. Furthermore, the expansion of BM HSCs occurred independent of the spleen and dectin-1 signalling. Taken altogether, these results suggest that the induction of central trained immunity in the BM from an IP administration of  $\beta$ -

glucan does not rely on direct stimulation of HSCs by  $\beta$ -glucan and is likely driven by endocrine or paracrine signalling via soluble factors. Insights into the cellular and molecular mechanisms underlying  $\beta$ -glucan-induced trained immunity will advance our understanding of the immunomodulatory properties of  $\beta$ -glucan. Furthermore, delineating the key cellular players and signaling pathways required for the generation of trained immunity may contribute to the development of new therapeutics and vaccines against infectious diseases.

## RÉSUMÉ

La mémoire immunologique est traditionnellement associée à la branche adaptative de l'immunité. Cependant, de plus en plus de preuves suggèrent que les cellules immunitaires innées peuvent provoquer une réponse immunitaire plus robuste et plus large contre une agression homologue ou hétérologue secondaire, indépendamment de l'immunité adaptative. Cette capacité de mémoire de l'immunité innée est appelée « immunité entraînée ». Il est intéressant de noter qu'il a été démontré que des adjuvants tels que le  $\beta$ -glucane (un composant dérivé des parois cellulaires fongiques) augmentent et remodelent de manière significative les cellules souches hématopoïétiques (CSH) dans la moelle osseuse (MO) via la signalisation d'interleukine-1 ou interféron de type I, qui génère des cellules myéloïdes matures fonctionnellement améliorées et augmente la défense de l'hôte contre les infections pulmonaires telles que *Mycobacterium tuberculosis* ou le virus de la grippe A. Le modèle *in vivo* le plus courant d'immunité entraînée induite par le  $\beta$ -glucane utilise une injection intrapéritonéale (IP) de  $\beta$ -glucane. Cependant, notre compréhension de la manière dont le  $\beta$ -glucane présent dans la cavité péritonéale entraîne les CSH dans la MO est très limitée. Nous décrivons ici les effets immunomodulateurs du  $\beta$ -glucane dans la cavité péritonéale et les organes périphériques et visons à étudier les mécanismes par lesquels l'administration IP du  $\beta$ -glucane génère une immunité centrale entraînée dans la MO. Semblable aux études publiées, nous avons constaté qu'une dose de  $\beta$ -glucane-IP induisait une immunité centrale entraînée en élargissant le compartiment CSH dans la MO. Le  $\beta$ -glucane a considérablement modifié la composition immunitaire péritonéale ; plus précisément, les grands macrophages péritonéaux et les cellules B résidant dans les tissus ont été rapidement épuisés, tandis que les neutrophiles, les cellules dendritiques, les monocytes et les petits macrophages péritonéaux se sont accumulés dans la cavité péritonéale. Nous avons également montré que le  $\beta$ -glucane était détecté et englouti par les

macrophages péritonéaux et les neutrophiles, qui n'étaient pas responsables de la navette du  $\beta$ -glucane dans la MO. De plus, l'expansion des CSH MO s'est produite indépendamment de la signalisation de la rate et de la dectine-1. Dans l'ensemble, ces résultats suggèrent que l'induction d'une immunité centrale entraînée dans la MO à partir d'une administration IP de  $\beta$ -glucane ne repose pas sur la stimulation directe des CSH par le  $\beta$ -glucane et est probablement pilotée par la signalisation endocrinienne ou paracrine via des facteurs solubles. La compréhension des mécanismes cellulaires et moléculaires sous-jacents à l'immunité entraînée induite par le  $\beta$ -glucane fera progresser notre compréhension des propriétés immunomodulatrices du  $\beta$ -glucane. En outre, la définition des principaux acteurs cellulaires et des voies de signalisation nécessaires à la génération d'une immunité entraînée pourrait contribuer au développement de nouveaux traitements et vaccins contre les maladies infectieuses.

## ACKNOWLEDGEMENTS

First, I would like to thank my supervisor, Dr. Maziar Divangahi, for his mentorship and support throughout both of my undergraduate and graduate studies. He pushed me to become more persevering, open-minded and curious when things did not work out, and gave me numerous opportunities to test new ideas and learn various new techniques. His constructive feedback and insightful discussions have both challenged and helped me grow more confident as a scientist, presenter, and writer. I will always be grateful for my time and the opportunity in his lab.

Thank you to my advisory committee members, Dr. Irah King and Dr. Basil Petrof, for their advice and guidance that have helped me develop this project and engaged me in enlightening and productive discussions.

Next, I would like to express my gratitude to my lab members who have helped me and supported me during challenging times and celebrated with me in the good ones. The friendly and dynamic lab environment sparked many productive and entertaining discussions, which made me look forward to coming into lab and working with the group. Many thanks to Dr. Leonardo Jurado, Kristina Nikolaou, Dr. Zuzet Martinez Cordova and Oscar Tsai who have helped me with several experiments and bounced many scientific ideas around my project. And last, but certainly not least, thank you to Mina Sadeghi, Kim Tran and Julia Chronopoulos who always had my back during my highs and lows, both in and outside the lab, and have become some of my closest friends.

I would like to extend my gratitude to my family for their unconditional love and endless support. Thank you to my dearest friends Madison, Sunny, Hunter and Anda who were always there for me. To my family and friends, thank you for everything.

Finally, I would like to recognize the Canadian Institutes of Health Research (CIHR) and Fonds de Recherche du Québec – Santé (FRQS) for funding my Master's project and training.

## **AUTHOR CONTRIBUTIONS**

MD conceived the study. MD and EL designed the experiments. EL performed the experiments with technical assistance from KT, MS, LJ and NK. EL performed the data analysis. EL and MD wrote the thesis.

## LIST OF FIGURES

### Main figures

<b>Figure 1.</b> HSC fate and hematopoiesis.....	9
<b>Figure 2.</b> Neutrophil clearance in the BM .....	11
<b>Figure 3.</b> $\beta$ -Glucan expands HSPC populations in the BM .....	74
<b>Figure 4.</b> $\beta$ -Glucan-induced HSC expansion is independent of adaptive immunity .....	75
<b>Figure 5.</b> $\beta$ -Glucan increases innate cell populations in the peritoneal cavity.....	76
<b>Figure 6.</b> $\beta$ -Glucan expands HSPC populations in the spleen .....	77
<b>Figure 7.</b> The role of the spleen in $\beta$ -glucan-mediated trained immunity.....	78
<b>Figure 8.</b> Peritoneal neutrophils and macrophages recognize and ingest $\beta$ -glucan .....	79
<b>Figure 9.</b> $\beta$ -Glucan is likely not directly accessing BM via a cell intermediate .....	81
<b>Figure 10.</b> $\beta$ -Glucan-induced LKS expansion is likely independent of dectin-1 signaling .....	82
<b>Figure 11.</b> Working model .....	56

### Supplementary figures

<b>Figure S1.</b> Gating strategy for HSPC populations .....	83
<b>Figure S2.</b> Gating strategies for innate and adaptive immune cell subsets .....	84
<b>Figure S3.</b> Peritoneal B1 cells after $\beta$ -glucan treatment .....	85
<b>Figure S4.</b> Adaptive immune cell subsets in the BM and spleen after $\beta$ -glucan treatment .....	86
<b>Figure S5.</b> LPMs do not egress from the peritoneal cavity at day 1 post- $\beta$ -glucan treatment.....	87
<b>Figure S6.</b> Innate immune cell subsets in the spleen after $\beta$ -glucan treatment .....	88
<b>Figure S7.</b> Innate immune cell subsets in the BM after $\beta$ -glucan treatment .....	89

## LIST OF ABBREVIATIONS

DTAF	5-(4,6-dichlorotriazinyl) aminofluorescein
APC	Antigen presenting cell
BCG	Bacille Calmette-Guérin
BCR	B cell receptor
BM	Bone marrow
BMDM	Bone marrow-derived macrophages
CeLP	Cecal ligation and puncture
CLP	Common lymphoid progenitor
CMP	Common myeloid progenitor
CR3	Complement receptor 3
CSF	Colony stimulating factor
cDC	Conventional dendritic cell
DC	Dendritic cell
Dectin-1	Dendritic-associated C-type lectin-1
DNA	Deoxyribonucleic acid
EMH	Extramedullary hematopoiesis
GATA6	GATA-binding factor 6
G-CSF	Granulocyte colony stimulating factor
GM-CSF	Granulocyte-macrophage colony stimulating factor
GMP	Granulocyte-monocyte progenitor
H3K4me3	Histone 3 lysine 4 trimethylation
H3K9me3	Histone 3 lysine 9 trimethylation
HR	Hypersensitive response
HSC	Hematopoietic stem cell
HSPC	Hematopoietic stem and progenitor cell
IAV	Influenza A virus
IFN	Interferon
IL	Interleukin
Ig	Immunoglobulin

IP	Intraperitoneal
IRA	Innate response activator
IV	Intravenous
Lin	Lineage markers
LKS	Lineage- cKit <sup>+</sup> Sca1 <sup>+</sup>
LPM	Large peritoneal macrophage
LPS	Lipopolysaccharide
LT-HSC	Long-term hematopoietic stem cell
MDR	Macrophage disappearance reaction
MEP	Megakaryocyte-erythroid progenitor
moDC	Monocyte-derived dendritic cell
MPP	Multipotent progenitor
<i>Mtb</i>	<i>Mycobacterium tuberculosis</i>
MW	Molecular weight
NET	Neutrophil extracellular traps
NK	Natural Killer
PAMP	Pathogen-associated molecular pattern
pDC	Plasmacytoid dendritic cell
Poly(I:C)	Polyinosinic-polycytidylic acid
PRR	Pattern recognition receptor
RBC	Red blood cell
ROS	Reactive oxygen species
SAR	Systemic acquired resistance
SPM	Small peritoneal macrophage
SPX	Splenectomized
ST-HSC	Long-term hematopoietic stem cell
TB	Tuberculosis
TCR	T cell receptor
TLR	Toll-like receptor
TNF	Tumour necrosis factor
WT	Wild-type

## **CHAPTER 1: INTRODUCTION**

### **1.1. Trained immunity**

The vertebrate immune system is divided into two major branches: innate and adaptive immunity. Conventionally, the innate branch is responsible for invoking short-term, non-specific, and fast-acting responses that do not result in classical immunological memory due to the short lifespan of innate immune cells and the lack of somatically assembled antigen receptors (1). Thus, immunological memory has been historically characterized as a feature unique to the adaptive branch in vertebrates (2). Given that innate immunity is evolutionarily older than adaptive immunity and an overwhelming majority of species on Earth solely possess innate immune systems for host defense, sustained protection against reinfections cannot be exclusively ascribed to the adaptive immune system alone (1-3). In fact, it has been well documented that innate immune cells, such as monocytes, macrophages, neutrophils, dendritic cells (DCs) and natural killer (NK) cells, can be “trained” with a primary stimulation to generate greater and faster immune responses to subsequent homologous or heterologous infections (2). This memory-like phenomenon in innate immune cells is termed as “trained immunity” and it challenges the traditional dogma of adaptive immunological memory (4).

#### **1.1.1. Evidence for innate immune memory in plants and invertebrates**

Early evidence for trained immunity comes from immunological studies in plants and invertebrates, which lack an adaptive immune system. As a consequence, these organisms have developed an innate immune system with adaptive features to recall past infections and mount robust broad-spectrum responses to reinfections (4).

Systemic acquired resistance (SAR) is a well characterized disease resistance phenomenon in plants (5). The induction of SAR involves long-distance signaling between the local plant-microbe interface and distant non-infected cells (6). At the site of infection, the detection of necrotrophic plant pathogens and intracellular pathogenic effector molecules first activates the hypersensitive response (HR) in the infected plant cell (5, 7). HR is a localized defense mechanism that instructs programmed cell death and the release of antimicrobial molecules to prevent the dissemination of the pathogen (8). Induction of HR is also associated with the rapid generation and transport of mobile signals, such as salicylic acid and its methylated derivative (9), to distal parts of the plant, thereby inducing histone modifications at the promoters of defense genes (10). For example, inoculation of *Nicotiana tabacum* half-leaves with tobacco mosaic virus (TMV) protected the opposite half-leaves from secondary challenges with TMV, tobacco necrosis virus, turnip mosaic virus and tobacco ringspot virus (11). Thus, priming leaves with an infection or a salicylic acid analogue activates SAR and confers long-term non-specific resistance against same or different subsequent infections throughout the plant (11-13).

Like plants, the innate immune response in invertebrates is also capable of retaining immunological memory of previous insults (“immune priming”) and evoking a more efficient secondary response (“recall response”) (14, 15). Studies in arthropods (16, 17) and mollusks (18) have demonstrated that the recall response is regulated by metabolic and epigenetic rewiring, which in turn alter transcription and cellular function (19). Using *Drosophila melanogaster* (fruit fly) as an invertebrate model organism, one study showed that flies initially exposed to a sublethal dose of *Streptococcus pneumoniae* were protected against a subsequent lethal challenge with *S. pneumoniae* (17). This protective effect was independent of antimicrobial peptides and dependent on enhanced hemocyte-mediated phagocytosis (17). Similarly, in *Macrocyclus albidus*

(copepods), immune priming with its natural tapeworm revealed that the protective recall response to homologous and heterologous secondary infections both involved histone modifications, but differed in splicing patterns and metabolic changes (16).

These mechanisms of immune memory are key to the ability of plants and invertebrates to enhance host fitness and achieve evolutionary success in diverse environments. Taken together, studies in these organisms provide valuable evolutionary evidence for the existence of conserved innate immune memory.

### **1.1.2. Evidence for innate immune memory in vertebrates**

In addition to innate immunity, vertebrates have evolved an adaptive immune system to induce long-lived immunological memory and mount rapid antigen-specific responses to previously encountered pathogens (3). Due to its ability to generate memory T and B lymphocytes and produce antibodies, the adaptive immunity is often an attractive target for vaccines. However, certain vaccines confer cross-protection against unrelated pathogens, suggesting the involvement of the innate immune response in immunological memory.

Bacillus Calmette Guerin (BCG) is a live-attenuated *Mycobacterium bovis* vaccine against *Mycobacterium tuberculosis* (20). BCG is currently administered to infants and children in high risk communities and countries, and has been shown to be effective at protecting against disseminated extrapulmonary and meningeal forms of tuberculosis (TB) in early childhood (21). Following the introduction of neonatal BCG immunization a century ago, TB incidence in children has declined in TB-endemic regions (21, 22). More interestingly, epidemiological data found that BCG vaccination was also strongly associated with reduced overall morbidity and mortality to non-TB infectious deaths in children (23-26). For example, case-control studies in West Africa

showed that BCG-immunized infants were protected against acute lower respiratory tract infections, respiratory syncytial virus and leprosy (27, 28). Additionally, childhood BCG vaccination was linked with lower rates of bladder and lung cancer (29, 30). As a result, BCG became the standard of treatment care for non-muscle invasive bladder cancer and is currently investigated as a therapeutic treatment for other cancers (31, 32). In murine models, BCG vaccination also cross-protects against infections such as influenza A virus (IAV) (20, 33), *Plasmodium* (34), *Schistosoma mansoni* (35) and *Candida albicans* (36). Altogether, these studies provide strong evidence that BCG can exert long-lasting, non-specific protection against unrelated infections independent of adaptive immunity.

In addition to BCG, this off-target protective effect can be induced in vertebrates by other live attenuated vaccines (e.g., measles-mumps-rubella and oral polio vaccine) (2, 37), microbial ligands (e.g., chitin and  $\beta$ -glucan) (38, 39), infections (e.g., *Plasmodium falciparum*) (40) and endogenous stimuli (e.g., heme and palmitic acid) (41, 42). However, due to the non-specific nature of innate immunity, trained immunity has been attributed as one of the protective mechanisms offered by the BCG vaccine and other stimuli.

### **1.1.3. Peripheral trained immunity**

Trained immunity is defined as the long-term functional reprogramming of innate immune cells that enables cells to respond more strongly to non-specific subsequent insults (2). This phenomenon has been first and extensively described in mature myeloid cells, namely monocytes and macrophages (2). To induce trained immunity in the periphery, three events must occur: a primary stimulation, a resting stage, and a secondary stimulation (1).

The training program begins with exposure to a primary stimulus. The detection of pathogen-associated molecular patterns (PAMPs) by pattern recognition receptors (PRRs) triggers a cascade of intracellular signaling, resulting in the rewiring of metabolic pathways to meet the bioenergetic demands of the cell during a pro-inflammatory response (43). It has been shown that BCG and  $\beta$ -glucan activate the Akt/mTOR/HIF-1 $\alpha$  pathway, which upregulates aerobic glycolysis, glutaminolysis and fatty acid synthesis (44-46). These pathways supply metabolites, such as pyruvate and acetyl coenzyme A (acetyl-CoA), that feed into the tricarboxylic acid cycle to generate ATP or participate in epigenetic regulation as substrates and cofactors (4, 47). Accumulation of fumarate and acetyl-CoA from the TCA cycle inhibits multiple histone lysine-specific demethylases and activates histone acetyltransferases, respectively (2, 44). As a result, trained monocytes and macrophages show increased enhancer marks (histone 3 lysine 4 trimethylation; H3K4me3) and decreased repressor marks (histone 3 lysine 9 trimethylation; H3K9me3) at the promoters of glycolytic, *TNFA*, *IL1B* and *IL6* genes (48). Following the removal of the primary stimulus, the immune activation status and transcriptional activity of the cell return to baseline (49). However, the epigenetic modifications persist and the chromatin at the promoter sites of metabolic and pro-inflammatory genes remains accessible for rapid transcriptional activation (48). Finally, following a secondary related or unrelated stimulation, trained cells can elicit a more rapid and robust pro-inflammatory response (1). For example,  $\beta$ -glucan training of human and murine monocytes showed increased interleukin (IL)-6 and tumour necrosis factor- $\alpha$  (TNF- $\alpha$ ) production after *M. tuberculosis* (*Mtb*) and lipopolysaccharide (LPS) challenge (39, 50). Therefore, epigenetic and metabolic rewiring are the basis of trained immunity.

The induction of trained immunity is not limited to only the mononuclear phagocyte lineage. Growing evidence indicates that long-term functional reprogramming can also be induced

in neutrophils, DCs and NK cells (51). Moorlag *et al.* have found that neutrophils isolated from healthy BCG-vaccinated individuals exhibit an altered phenotype characterized by increased expression of activation markers, CD11b and CD66b, and enhanced antimicrobial activity against a *C. albicans* challenge. These functional changes were associated with enhanced H3K4me3 marks at promoter sites of genes involved in JAK-STAT signaling and pro-inflammatory cytokines (52). Another study revealed that neutrophils derived from  $\beta$ -glucan-treated mice acquired an anti-tumour phenotype that was linked with enhanced phagocytosis and reactive oxygen species (ROS) production (53). Dendritic cells are another myeloid cell that can also adopt a memory-like phenotype. Using a protective fungal vaccine model, immunization with *Cryptococcus neoformans* strain H99 $\gamma$  in mice induced pro-inflammatory DCs with strong production of interferon (IFN)- $\gamma$ , IL-2 and IL-4 upon subsequent wild-type (WT) *C. neoformans* challenge (54). Although NK cells are innate cells from the lymphoid lineage, experimental studies demonstrated that the activation of receptor Ly49H by murine cytomegalovirus generated memory NK cells with capacities to self-renew, rapidly degranulate and secrete cytokines upon reinfection (55).

One of the defining features of trained immunity is its ability to provide the long-term protection against homologous and heterologous infections. Depending on the primary stimulus, this protective effect can persist for several months and up to one year after its initial induction (2, 56), which paradoxically outlasts the lifespans of most innate immune cells (57). For this reason, it was unknown how protection from trained immunity was maintained in innate immune cells.

#### **1.1.4. Central trained immunity**

Hematopoietic stem cells (HSCs) are long-lived, multipotent, self-renewing cells that mainly reside in the bone marrow (BM). HSCs are responsible for maintaining the stem cell niche

and replenishing the myeloid and lymphoid cell populations via hematopoiesis (58). Lineage bias in HSCs can be tailored by direct infections and inflammatory signals from local and distal sources (59). In the recent years, several studies have demonstrated certain stimuli can epigenetically reprogram HSCs in the BM, giving rise to genomically imprinted progenitors and generating trained innate immune cells (39, 59). Therefore, HSCs are central to the induction and maintenance of trained immunity.

We have discovered that the presence of BCG in the BM altered the transcriptional landscapes, increased the proliferative capacity and induced myeloid-lineage commitment in hematopoietic stem and progenitor cells (HSPCs) via IFN- $\gamma$  signaling (59). Moreover, macrophages derived from BCG-educated HSCs acquired unique transcriptomic and epigenetically signatures (enhanced H3K4me and H3K27ac marks) that were associated with trained immunity and provided enhanced protection against virulent *Mtb* infection. In contrast, access of virulent *Mtb* to the BM impairs trained immunity via type I IFN signaling (56).

Using a different model of trained immunity, Mitroulis *et al.* demonstrated that one dose of  $\beta$ -glucan in mice drove the expansion of HSPCs and skewed a bias towards myelopoiesis (60). Transcriptomic and metabolomic analysis in HSPCs revealed that  $\beta$ -glucan rewired metabolic pathways, such as glycolysis and cholesterol biosynthesis, and increased levels of IL-1 $\beta$  and granulocyte-macrophage colony stimulating factor (GM-CSF). Importantly,  $\beta$ -glucan does not exhaust or functionally impair HSPC, but rather afforded protective response to a secondary challenge with LPS or chemotherapy-induced myeloablation (60). Similarly, we have shown that two doses of  $\beta$ -glucan in mice promotes an expansion in the myeloid-lineage in the BM and provided protection against pulmonary *Mtb* infection via IL-1 signaling (39). While we have

identified several key cytokines that are involved in training of HSCs, their cellular sources and their regulatory mechanisms remain vastly unknown.

## **1.2. Hematopoietic stem cells**

HSCs have been historically defined by two biological properties: multipotency and self-renewal (61). Multipotency is the ability to differentiate into any cell within a lineage, and self-renewal is the capacity of a parental cell to produce at least one identical daughter cell. At steady state, HSCs can undergo asymmetric divisions to maintain stem cell numbers while sustaining the constant replenishment of short-lived, terminally differentiated blood cells throughout adulthood (62). In addition, HSCs can divide symmetrically to replace HSCs lost to differentiation, death or exhaustion, or expand the HSC population in response to stress (63).

### **1.2.1. Hematopoiesis**

Hematopoiesis is a stepwise differentiation process by which specialized blood cells are generated from HSCs. The pool of HSCs comprises of two main subsets with varying levels of proliferative and differentiation potential: long-term HSCs (LT-HSCs) and short-term HSCs (ST-HSCs) (**Fig. 1D**). These HSC subsets and multipotent progenitors (MPPs) are also known as the LKS population due to the absence of surface markers that are normally found on lineage (Lin)-committed cells and the presence of stem cell factor receptor (cKit) and stem-cell antigen 1 (Sca1) (61). At the top of the hematopoietic hierarchy, LT-HSCs are the most primitive cells with the highest self-renewal capacity and longest multilineage reconstitution potential ( $\geq 16$  weeks) (64). At homeostasis, LT-HSCs enter a quiescent state in the endosteal niche, where they are metabolically inactive and rarely divide, but can re-enter the vascular niche to proliferate and

differentiate into ST-HSCs (61, 65). ST-HSCs have a shorter reconstitution capacity ( $\approx 8\text{--}12$  weeks) (64) compared to LT-HSC and can respond faster to activation and differentiate into MPPs, which lack self-renewal capacity. Based on transcriptional differences, MPPs can be categorized into myeloid-biased MPP (MPP3) and lymphoid-biased (MPP4) subsets (66). MPP3 give rise to the common myeloid progenitors (CMPs), which further differentiate to the granulocyte-monocyte progenitors (GMPs) and megakaryocyte-erythroid progenitors (MEPs). This arm of hematopoiesis is responsible for replenishing granulocytes, monocytes, macrophages, conventional dendritic

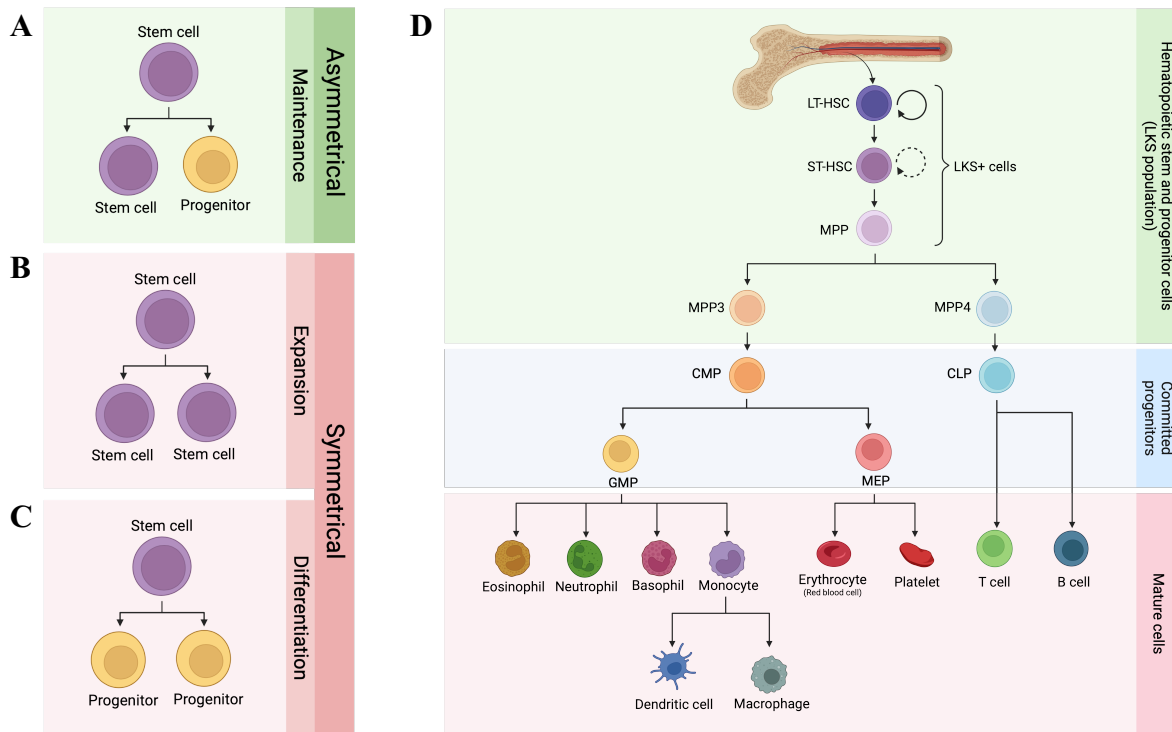


**Figure 1. HSC fate and hematopoiesis.** (A-C) HSCs can divide asymmetrically or symmetrically. (A) Asymmetric occurs to maintain the HSC population. One stem cell gives rise to two daughters: one stem cell and one progenitor cell that can commit to differentiation. (B-C) Symmetric division occurs to (B) expand the HSC population in the BM niche or (C) produce progenitor cells for differentiation. (D) The classical hematopoietic hierarchy in the bone marrow. LT-HSCs sit at the top of the hierarchy; they are quiescent, highly multipotent and have the highest self-renewing potential. LT-HSCs give rise to ST-HSCs, which have limited self-renewal capacity, and subsequently to MPPs. Myeloid-biased MPP3 produce lineage committed progenitors, CMP, GMP and MEP, which differentiate into mature myeloid cells. Lymphoid-biased MPP4 differentiate into CLPs, which generate T cells and B cells. Hematopoiesis is regulated by cellular and acellular components in the BM niche. Created with BioRender.com.

cells, red blood cells and platelets. In contrast, MPP4 give rise to common lymphoid progenitors (CLP), which differentiate into T and B cells (62).

### **1.2.2. Regulation of steady-state hematopoiesis**

Hematopoiesis is tightly regulated by various acellular and cellular components in the BM niche to maintain HSCs, meet demand during stress and prevent BM failure. For example, LT-HSCs primarily localize in the hypoxic endosteal niche where they shift from mitochondrial oxidative phosphorylation to glycolysis and arrest in G0 phase (67). The endosteal niche comprises different cell types, including osteoblasts and osteoclasts, that express various chemokines, growth factors and adhesion molecules to promote HSC quiescence, survival and retention in the BM niche (61). In contrast, the vascular niche regulates the self-renewal, differentiation and egress of activated HSCs through specialized supporting cells, such as vascular endothelial cells, CXCL12-abundant reticular cells, sympathetic neurons, macrophages, mesenchymal and perivascular stromal cells (68-70). Together, these components enable crosstalk between the endosteal and vascular niches, and regulate HSC fates through paracrine, endocrine and juxtacrine signaling (71).

Under steady state, more than  $10^9$  immune cells die by apoptosis and are cleared by phagocytes every day (72). Hence, HSCs are continuously provided various lineage-instructive differentiation signals to replace aged or dying blood cells and meet the demand of the organism. Erythropoiesis is the production of red blood cells that is activated by kidney-derived erythropoietin (Epo) during hypoxic conditions. High systemic levels of Epo transcriptionally reprograms HSCs and MPPs towards an erythroid fate, leading to increased erythroid and decreased myeloid output, and thus corrects anemia (73). On the other hand, signaling through Notch and IL-7 receptors and activation of Ikaros family of zinc finger transcription factors are essential for driving T and B cell lymphopoiesis (74-76). Furthermore, myeloid lineage

commitment is influenced by transcription factors (e.g., PU.1, GATA-1 and C/EBP $\alpha$ ) and myelopoietic colony stimulating factors (CSFs) (e.g., GM-CSF, granulocyte-colony stimulating factor (G-CSF), CSF-1) (77, 78).

The interplay between acellular and cellular components in the regulation of hematopoiesis is well illustrated by steady state granulopoiesis. Neutrophils are the most common granulocyte in peripheral blood (~50–70% of circulating leukocytes in human, ~10–25% in mice) (79) and have a short half-life of around 18h in humans and 6h to 8h in mice (57, 80). Due to their rapid turnover, tight regulation of the hematopoietic niche is required to control the continual production, release and clearance of neutrophils (**Fig. 2**). Under steady state conditions, BM stromal cells constitutively produce CXCL12 (also known as stromal cell-derived factor 1) which retains neutrophils in the BM through CXCR4 signaling (81). It is estimated that more than 90% of total

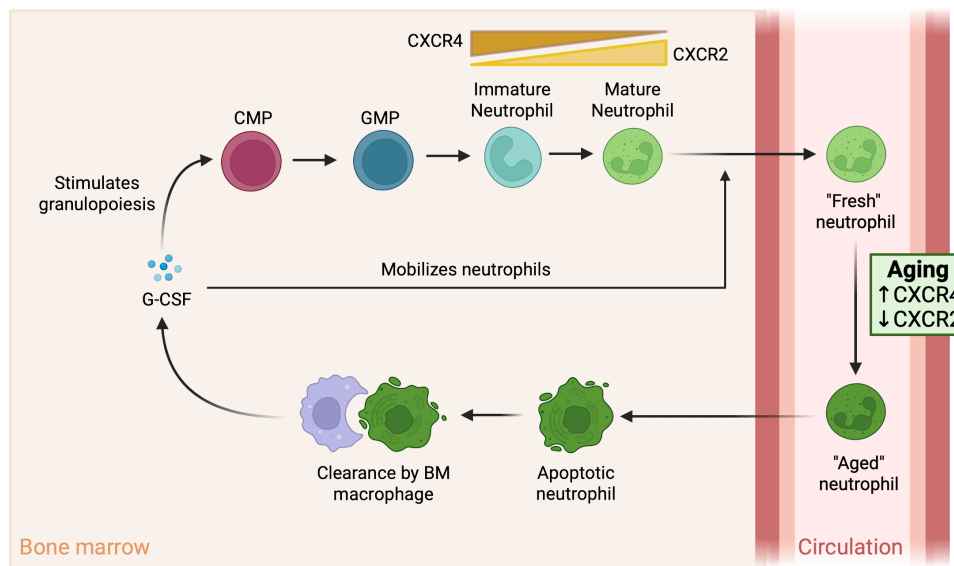


**Figure 2. Neutrophil clearance in the BM.** Mature neutrophils are retained in the BM reservoirs via CXCL12/CXCR4 signaling. As the expression of CXCR4 decreases and CXCR2 increases with maturity, mature neutrophils are released into circulation. In the periphery, neutrophils acquire an aging phenotype by upregulating CXCR4 and downregulating CXCR2. Following the CXCL12 gradient, aged neutrophils return to the BM, where they are cleared by stromal BM macrophages. Uptake of neutrophils by these macrophages stimulates the production of G-CSF, which further promotes granulopoiesis and can mobilize neutrophils from the BM reservoirs. Created with BioRender.com.

neutrophils reside in the BM, forming the neutrophil reservoir, while less than 2% are found in circulation (81). As neutrophils mature in the BM, upregulation of CXCR2 and downregulation of CXCR4 mobilize them into circulation (82). Within hours of their release into peripheral blood, neutrophils acquire an “aged” phenotype defined by CXCR4<sup>hi</sup> CXCR2<sup>low</sup> CD62L<sup>hi</sup> expression, allowing them to preferentially home back into the BM via the CXCL12 chemotactic gradient for clearance (83). In the BM, neutrophils undergo apoptosis and are cleared by stromal BM macrophages (84). Efferocytosis by these macrophages has been reported to stimulate G-CSF production, which drives granulopoiesis and maintains neutrophil homeostasis (83). However, during infection or inflammation, elevated IL-17 and G-CSF levels promote the excessive release of mature and immature neutrophils from the BM and activate emergency granulopoiesis (84, 85). Thus, granulopoiesis is tightly regulated by various acellular and cellular components but can be modulated by pro-inflammatory signals during stress (86).

### **1.2.3. Stress-induced hematopoiesis**

Growing evidence suggests that HSCs can respond to stress signals and infectious stimuli via direct or indirect mechanisms. It has been documented that HSPCs express a variety of PRRs to sense PAMPs or metabolites derived directly from microbes. For instance, numerous *in vivo* and *in vitro* studies have reported that HSPCs can respond to LPS via toll-like receptor (TLR) 4 (87), Pam<sub>3</sub>CSK<sub>4</sub> (synthetic bacterial lipopeptide) via TLR2 (87), CpG oligodeoxynucleotide (synthetic single-stranded DNA) via TLR9 (88), and zymosan via dectin-1 (89). It should be noted that dectin-1 expression is undetectable in primitive HSCs, but is acquired by Lin<sup>-</sup> progenitor cells in advanced stages of differentiation (90). Pathogens may also directly infect HSCs; however, this mechanism of activation does not commonly occur and has only been described in hematopoietic

progenitors during viral infections (91, 92). As a result, the establishment of a pathogen or presence of pathogen-derived products in the BM can directly activate PRRs on HSCs and provoke cell cycle entry and a bias towards myelopoiesis (93).

HSCs can indirectly respond to pathogens or inflammation by sensing cues emanated from cells in the BM niche or at the site of infection. In particular, IL-6, IL-1, type II IFN (IFN- $\gamma$ ) and type I IFN (e.g., IFN- $\alpha$ ) have been implicated as regulators of HSCs during inflammatory and infectious stress (93). In an animal model of systemic lupus erythematosus, high circulating levels of IL-6 were accompanied by a loss of CLPs and B cells and a corresponding accumulation of myeloid cells (94). Moreover, IL-6-stimulated LKS cells upregulated Id1 transcription factor, which is known to bias lineage commitment towards a myeloid fate at the expense of lymphopoiesis (95). IL-1 is another pro-inflammatory cytokine that plays a well-established role in hematopoietic aging, whereby IL-1 from damaged dysfunctional stromal cell in the BM directly accelerates cell division, drives myeloid differentiation and compromises self-renewal activity in HSCs (96, 97). IFN- $\gamma$  signaling has also been demonstrated to mediate proliferative activation of quiescent LT-HSCs in an *in vivo* infection with *Mycobacterium avium* and *in vitro* IFN- $\gamma$  exposure (98). Similar study demonstrated that IFN- $\alpha$  activated dormant HSCs in polyinosinic-polycytidylic acid (poly(I:C))-treated mice (99). Altogether, activation of PRRs and cytokine receptors on HSPCs induces proliferation and myeloid cell differentiation to rapidly replenish the innate immune populations that are consumed at the site of infection and to combat pathogens.

While acute inflammation is beneficial for shaping the demand-adapted hematopoietic response, chronic exposure to inflammatory signals can lead to HSC exhaustion, HSC depletion and myeloid oncogenic transformation (100, 101). For instance, long-term activation of IL-1, type I and type II IFN pathways were shown to limit HSC self-renewal and stemness, thus impairing

their function (96, 98, 99). A study by Matatall *et al.* also demonstrated that IFN- $\gamma$  depleted the HSC population in the BM through stress-induced terminal differentiation during chronic *M. avium* infection (102). Furthermore, excessive proliferation of HSCs during chronic inflammation can accumulate DNA damage, which may induce apoptosis, senescence or malignant transformations (103).

Acute and chronic inflammation have different effects on HSC quiescence, self-renewal, and differentiation. Therefore, a strict balance of signaling pathways, stimulus intensity and exposure period is required to dictate whether the long-term HSC response confers beneficial (i.e. trained immunity) or harmful (i.e. cell exhaustion) effects to the host. However, it is unknown how HSC exhaustion impacts trained immunity, and vice versa.

#### **1.2.4. Extramedullary hematopoiesis**

Extramedullary hematopoiesis (EMH) refers to hematopoiesis occurring in organs outside of the BM (104). During fetal development, fetal liver and spleen are important sites for EMH, after which HSCs migrate into the BM where they establish and sustain medullary hematopoiesis in adults (105). During adulthood, EMH becomes a compensatory mechanism to insufficient BM function and commonly occurs in the spleen and liver during severe infection and inflammation. In certain pathological circumstances, HSCs can mobilize from the BM into peripheral organs and re-establish a niche for EMH (104). Similarly, HSCs, which remained in the liver and spleen after the transition from fetal-to-adult hematopoiesis, can be reactivated (104).

Generally, EMH is primarily associated with emergency myelopoiesis and erythropoiesis (106). For example, a study by Burberry *et al.* showed that systemic *Escherichia coli* infection in mice mobilized functional HSCs to the spleen by increasing serum G-CSF through NOD1 and

TLR4 activation (104). In the spleen, mobilized HSPCs gave rise to neutrophils and monocytes to limit secondary infection with *E. coli*. In clinical practice, G-CSF is used as a mobilizing agent to increase circulating HSPCs by disrupting the CXCR4/CXCL12 retention signal, rendering HSPCs accessible for autologous and allogeneic stem cell transplants (107). Growing evidence suggests that EMH has been linked to several diseases, such as atherosclerosis and cancer (108, 109). Pro-inflammatory Ly6C<sup>hi</sup> monocytes produced by spleen have been reported to infiltrate and accumulate in atherosclerotic lesions, although it is unknown whether EMH drives the development of atherosclerosis (109). Interestingly, cancer induces and rewires splenic EMH to generate potent immunosuppressive myeloid cells, thus evading anti-tumour immunity and promoting tumour progression (108). Given that the spleen is a reservoir of HSPCs and a site for EMH, its role in the trained immunity is largely unknown.

### 1.3. $\beta$ -Glucan

#### 1.3.1. $\beta$ -Glucan in nature

$\beta$ -Glucans are a heterogenous class of  $\beta$ -linked glucose polymers that naturally occur in most fungi, bacteria, algae and cereal grains cell walls (110). Depending on the source, the structure of  $\beta$ -glucan strongly varies in the backbone and branching side chains. For instance,  $\beta$ -glucan found in the endosperm cell wall of cereal grains is composed of linear chains of glucose with  $\beta$ -1,3 and  $\beta$ -1,4 glycosidic linkages (111). Curdlan is a linear bacterial polysaccharide of high molecular weight (MW) that is exclusively made from repeating  $\beta$ -(1,3)-glucan and is typically produced by *Agrobacterium sp.*, *Rhizobium sp.*, and *Alcaligenes faecalis* (112). In contrast,  $\beta$ -glucan from fungal sources (e.g., mushrooms and yeast) consists of a  $\beta$ -(1,3)-glucan backbone with  $\beta$ -(1-6)-linked branches at various intervals (111).

Given the diversity in chemical structures and lengths,  $\beta$ -glucans also vary in physical and bioactive properties. Due to the lack of  $\beta$ -1,3-glucanase, which hydrolyzes  $\beta$ -1,3 and  $\beta$ -1,4 glycoside linkages, humans are unable to digest and absorb cereal  $\beta$ -glucan (113). As a result,  $\beta$ -glucan has been used as a dietary fiber prebiotic to improve the gut microbiota, promote the production of short-chain fatty acids, regulate appetite and reduce blood cholesterol (113, 114). In addition, the solubility of  $\beta$ -glucan is highly influenced by the composition and frequency of branches, degree of polymerization (DP) and conformation (113).  $\beta$ -Glucans with a  $\beta$ -1,6-linked monoglucose residue, such as lentinan and schizophyllan, are mostly soluble in water. However, yeast  $\beta$ -glucan with long  $\beta$ -1,6 branched side chains form a branched amorphous structure due to strong intermolecular interactions between the chains (115); hence, it is water insoluble. Similarly,  $\beta$ -glucan with high degree of polymerization (DP > 100), such as curdlan and zymosan (impure crude fungal cell wall extract containing  $\beta$ -glucan and mannan), is also insoluble (113). As such, different conformations of  $\beta$ -glucan impact its solubility and further dictate its biological function.

### **1.3.2. Immunomodulatory properties of $\beta$ -glucan**

Fungal  $\beta$ -glucans have repeatedly demonstrated to have potent immunomodulating effects. For centuries, various medicinal mushrooms species, containing biologically active  $\beta$ -glucans, have been long used in Chinese traditional medicine for its health benefits and therapeutic effects against acute and chronic conditions (116). In the recent decades,  $\beta$ -glucan has gained particular interest as adjuvant agents for cancers and infections (53, 117) because of its ability to induce trained immunity (60).

Anti-tumour activity of fungal  $\beta$ -glucan was first described in 1961 (118). Chikara et al. observed that  $\beta$ -glucan isolated from shiitake mushroom *Lentinus edodes* (“lentinan”) inhibited

the growth of sarcoma in mice. In 1983, Nakao *et al.* reported that intramuscular treatment with schizophyllan prolonged the lifespan of patients with inoperable or recurrent gastric cancer compared to the control group (119). Since then,  $\beta$ -glucan has been extensively tested as a potential adjuvant in combination with chemotherapy or immunotherapy (120), and has exhibited promising efficacy and safety in preclinical and clinical trials for various cancers (121), including colorectal (122), breast (123), pancreatic (124) and non-small cell lung cancer (125). To date, only two  $\beta$ -glucans have been clinically approved as adjuvants primarily for gastric and colorectal cancer therapy: polysaccharide-K (PSK), which is licensed in Japan (126), and lentinan, which is available in Japan and China (127). In addition to anti-tumour effects,  $\beta$ -glucan has also demonstrated to provide beneficial immunomodulatory activity and confer protection against experimental bacterial, viral and parasitic infections, such as *Mtb* (39), *Pseudomonas aeruginosa* (128), *Staphylococcus aureus* (129), IAV (130), alphaherpesvirus (131) and *Trichinella spiralis* (132). While there is strong evidence to support the anti-tumour and anti-infective effects of  $\beta$ -glucan, its specific mechanism of action varies with the route of administration and structural features of  $\beta$ -glucan and requires careful delineation. Notably, solubility of  $\beta$ -glucan strongly influences its functional activity; specifically, particulate and soluble  $\beta$ -glucans can both modulate the immune response, but via different pathways (133).

### **1.3.3. Cellular immune response to $\beta$ -glucan**

Numerous studies have indicated that  $\beta$ -glucan has no direct cytotoxic effects on tumours or pathogens, but instead, acts through the activation of immune cells (121).  $\beta$ -Glucan is a major fungal PAMP that is recognized mainly by mononuclear phagocytes and granulocytes through several important PRRs, such as dectin-1, TLR2/6 and complement receptor 3 (CR3; also known

as Mac-1, CD11b/CD18,  $\alpha_M\beta_2$ -integrin) (134-137). Interestingly, at least two other  $\beta$ -glucan receptors have been identified: scavenger receptor CD5 – which is expressed on mature T cells and B1a cells (138); and lactosylceramide – which is a glycosphingolipid found in the plasma membranes of leukocytes (139-141). Each receptor has varying degrees of affinity and specificity to  $\beta$ -glucan and are therefore capable of triggering different signaling cascades and immune responses.

Dectin-1 is the most well-studied receptor for  $\beta$ -glucan that is widely expressed on macrophages, DCs and neutrophils (137). Although dectin-1 recognizes both soluble and insoluble particulate  $\beta$ -(1,3)-glucan, only the latter can activate dectin-1 signaling by triggering the formation a “phagocytic synapse” and inducing phagocytosis (142). In macrophages and DCs, activation of NF- $\kappa$ B transcription factor through dectin-1/Syk and dectin-1/Raf-1 pathways can lead to increased production of pro-inflammatory cytokines (TNF- $\alpha$ , IL-6, IL-1 $\beta$ , IL-23), arachidonic acid and ROS (143-146). Furthermore, dectin-1 and TLR2/6 stimulation by  $\beta$ -glucan can synergistically enhance NF- $\kappa$ B activation and cytokine response, resulting in augment TNF- $\alpha$  production in macrophages and DCs compared to dectin-1 stimulation alone (147). As a result,  $\beta$ -glucan treatment can activate DCs to prime the cytotoxic T cell response (143) and convert immunosuppressive tumour-associated macrophages to classically activated macrophages (148), leading to an improved anti-tumour response.

In contrast, soluble low molecular weight  $\beta$ -glucan, such as laminarin ( $\beta$ -glucan extracted from algae), can also efficiently bind to dectin-1, but fail to induce phagocytosis and production of pro-inflammatory cytokines and ROS (142, 149). Thus, laminarin is regarded as a dectin-1 antagonist as it likely saturates dectin-1 and prevents productive downstream signaling. Instead, soluble  $\beta$ -glucan can be opsonized by inactive complement 3b (iC3b) and targeted for CR3-

mediated phagocytosis (134). The ligation of  $\beta$ -glucan to CR3 induces conformation changes (150) and downstream signaling, which stimulates degranulation by neutrophils, NK cells and macrophages through the CR3/Syk/PI3k pathway (151). As a result,  $\beta$ -glucan-primed CR3 promotes cytotoxic killing of iC3b-opsonized target cells, including microorganisms and tumour cells (135, 152-154).

It has been well established that  $\beta$ -glucan is an effective inducer of trained immunity (4). Upon receptor ligation, downstream signaling leads to the acquisition of histone modifications at promoter and repressor sites associated with gene activation of glycolytic genes and pro-inflammatory cytokines, such as IL-6, TNF- $\alpha$  and IL-1 $\beta$  (60, 155). These epigenetic modifications enable a faster and robust innate immune response upon restimulation, and thus are the basis of trained immunity. In the recent decades, the long-term anti-tumour and anti-infective effects of  $\beta$ -glucan were attributed to trained immunity (39, 53), however, our understanding of the cellular and molecular mechanisms underlying  $\beta$ -glucan-induced trained immunity still remains limited. Therefore, to study the immunomodulatory properties of  $\beta$ -glucan *in vivo*, we focused on insoluble  $\beta$ -glucan derived from *Saccharomyces cerevisiae* and employed one of the most common routes of administration for  $\beta$ -glucan via the peritoneal cavity. While many studies demonstrated that intraperitoneal (IP) injection of  $\beta$ -glucan induces central trained immunity, it is unclear how  $\beta$ -glucan in the peritoneal cavity reprograms HSCs in the BM.

## **1.4. Peritoneal cavity**

### **1.4.1. Anatomy and physiology of the peritoneal cavity**

Most multicellular organisms have a major body cavity that encloses vital organs, provides mechanical support and absorbs shock (156). This cavity is termed the *coelom*. The coelom is lined

by a single layer of mesothelial cells and filled with fluid which contains organic molecules and immune cells (157). In primordial species, such as sea urchins, the coelom is predominantly protected by a distinct population of macrophage-like cells, called *coelomocytes*, that participate in phagocytosis, encapsulation, pathogen clearance, cellular clotting and tissue repair (158). Throughout evolution, more complex vertebrate organisms retained the body cavity. In mammals, the coelom is further subdivided into three anatomically distinct compartments during embryonic development: the peritoneal cavity – which holds the digestive tract, liver, spleen and omentum; the pleural cavity – which contains the lungs; and the pericardial cavity – which encloses the heart (159). Importantly, the diaphragm develops between the peritoneal and pleural cavity during embryogenesis, and has a vital role in respiration and the lymphatic system (160).

The peritoneal cavity represents an excellent portal for substances to be quickly administered, absorbed and systemically circulated. The peritoneal cavity is lined with a highly vascular network of lymphatic and blood vessels along the sub-mesothelium, allowing fluid and solutes to enter and leave the peritoneal cavity (161). At homeostasis, the peritoneal cavity contains a small volume of fluid that ranges from 50 to 75 mL in humans and 0.02 to 0.1 mL in mice (162). This fluid serves to lubricate the organs and is continuously produced and drained into circulation.

#### **1.4.2. Circulatory and lymphatic systems of the peritoneal cavity**

There are two mechanisms by which fluid and molecules can reach systemic circulation: transcapillary absorption or lymphatic drainage (163). Majority of fluid and small molecules (MW < 20 kDa), such as caffeine, glucose and progesterone, can cross the semipermeable mesothelium via paracellular (between cells) or transcellular (through the cell) transport and diffuse into blood capillaries found within the tissue interstitium (164-166). Depending on whether the molecule was

absorbed through the visceral or parietal peritoneum, it can reach systemic circulation either directly by bypassing the liver or indirectly through the portal circulation (162, 165). In contrast, large size molecules (MW > 30 kDa) and cells primarily enter systemic circulation via lymphatics (162, 167). Unlike the circulatory system that relies on the heart, the lymphatic system uses one-way lymphatic valves and negative intrathoracic pressure to establish a unidirectional lymph flow (168). In fact, the pressure gradient generated by the diaphragm enables the peritoneal fluid to be absorbed through pore-like “stomata” and pass into the lymphatic lacunae, which are exclusively found on the peritoneal surface of the diaphragm (169). At the stomata, lymphatic fluid is filtered for antigens and pathogens by immune cells that form aggregates called *milky spots* or *fat-associated lymphoid clusters* (FALCs), which are embedded in the visceral adipose tissue (“omentum”) beneath the mesothelial cell layer (170, 171). Fluid within the lacunae then traverses the diaphragm through intrinsic lymphatics, passes through parasternal and/or mediastinal lymph nodes, and joins the thoracic duct or the right lymphatic duct before draining into systemic circulation (168, 172). Other absorption pathways exist; however, they account for less than 5% of lymphatic drainage of the peritoneal cavity (162). Thus, these intricate blood and lymphatic vascular systems and specialized lymphoid tissue allow substances to reach systemic circulation after IP administration and support immune surveillance in the peritoneal cavity (172).

#### **1.4.2. Innate immunity in the peritoneal cavity**

Similar to the coelom, the mammalian cavities are also surveilled and protected by suspended immune cells, notably macrophages that share strong functional similarities with sea urchin coelomocytes (157). In the peritoneal cavity, macrophages compose approximately 30 to 40% of all immune cells (173). Although murine peritoneal macrophages have been thoroughly

studied due to their abundance and accessibility in the peritoneal compartment (174), only recently, the co-existence of two morphologically, functionally, and developmentally distinct peritoneal macrophages subsets have been described (173). Large peritoneal macrophages (LPMs) are a unique and mobile population of tissue-resident macrophages characterized by high levels of CD11b and F4/80, and selectively express of zinc finger transcription factor GATA6 for proliferation and survival (173). GATA6<sup>+</sup> LPMs originate from embryonic precursors and can maintain locally in the cavity through self-renewal (175). Under steady state, GATA6<sup>+</sup> LPMs constitute approximately 90% of all peritoneal macrophages and have key roles in immune surveillance and cavity homeostasis (176). Conversely, small peritoneal macrophages (SPMs) are derived from bone marrow-derived myeloid precursors and are distinguished by the CD11b<sup>low</sup> F4/80<sup>low</sup> GATA6<sup>-</sup> phenotype. Under inflammatory conditions, SPMs predominate the peritoneal cavity and become a major source of pro-inflammatory mediators (176). For decades, the role of GATA6<sup>+</sup> LPMs in pathogen and cellular debris clearance has been well established (173, 177-179). However, recent studies have shown that GATA6<sup>+</sup> LPMs might also serve as a readily available reservoir of mature myeloid cells for infiltrating injured visceral organs, such as liver and intestines, and inducing tissue repair (180, 181). Similarly, GATA6<sup>+</sup> pericardial macrophages rapidly accumulate at the ischemic heart and prevent adverse cardiac fibrosis (182). Considering that LPMs have migration potential and are primary sentinel cells of the peritoneal cavity, their response to  $\beta$ -glucan and their role in the induction of trained immunity are unclear. Furthermore, it is unknown whether LPMs can traffic out of the peritoneal cavity and/or shuttle  $\beta$ -glucan into the BM to train HSCs.

In comparison to peritoneal macrophages, DCs represent a relatively small proportion of peritoneal immune cells (183). DCs are professional antigen presenting cells (APCs) that have

important roles in orchestrating the immune response and inducing T cell responses (184). Although all DCs originate from HSCs in the BM (except for Langerhans cells), they are heterogenous groups of cells that can be classified based on phenotype, function and development (185). Classical or conventional DCs (cDC) are derived from CMPs and display high expression of CD11c and MHC II (184). Depending on their function, cDCs can be further subdivided into type 1 cDCs (cDC1s) – which can potently prime CD8<sup>+</sup> T cells via cross-presentation and promote T<sub>H</sub>1 responses (186), and type 2 cDCs (cDC2s) – which can effectively induce T<sub>H</sub>2 and T<sub>H</sub>17 responses (187). At steady state, peritoneal cDCs are composed of approximately 20% cDC1s and 80% cDC2s (183) and can also be found in the omentum (171, 188). Plasmacytoid DCs (pDCs) are a rare subset of DCs that are known to be potent producers of type I IFN in response to viral infections and were shown to accumulate in peritoneal cavity of patients with malignant ascites (184, 189). Moreover, during infection or inflammation, monocytes can transmigrate in the peritoneal cavity and differentiate into inflammatory monocyte-derived DCs (moDCs), which act as local APCs in the periphery tissue (190, 191).

#### **1.4.3. Adaptive immunity in the peritoneal cavity**

B1 cells are a unique subset of B cells with innate-like features that reside in the peritoneal cavity where they comprise 35 to 70% of all peritoneal B cells (192). Unlike conventional B2 cells, B1 cells are derived from the fetal liver and are replenished independent of BM HSCs by self-renewal (193, 194). Peritoneal B1 cells are phenotypically different from their splenic counterpart as they express CD11b (195) and thus have phagocytic capacities to uptake and present antigen to T cells, as reported for DCs and macrophages (196). Based on CD5 expression, B1 cells can be further divided into B1a (CD5<sup>+</sup>) and B1b subsets (CD5<sup>-</sup>) (195). During fetal development, B1a

cells bypass the pre-BCR positive selection checkpoint and acquire a B cell receptor (BCR) repertoire skewed towards bacterial and self-antigen (197). Conversely, B1b cells can generate an antibody response in a T cell-independent (TI) manner; specifically, stimulation with a TI type I antigen (e.g. LPS) typically induces a short-lived antibody response, while TI type II antigens (e.g. capsular polysaccharide or antigens with highly repetitive epitopes) generate a long-lasting specific immunoglobulin (Ig) M response and immune memory (198, 199). Given their ability to spontaneously secrete polyreactive natural antibodies (primarily IgM) independent of T cell or microbial stimulation, B1 cells have important roles in promoting tissue homeostasis and microbial defense (200). For instance, autoreactive IgM can opsonize and facilitate the clearance of apoptotic and necrotic cell debris by mononuclear phagocytes through complement-dependent mechanisms. In murine models of sepsis, studies have demonstrated that peritoneal B1a cells migrate to the spleen and differentiate into innate response activator (IRA) B cells that then promote EMH via IL-3 and GM-CSF (201, 202). In addition, stimulation of TLRs by bacterial components in the peritoneal cavity can induce the migration of B1 cells into the intestinal lamina propria where they undergo IgA class switching and contribute to mucosal immunity against commensal bacterial and dietary antigens (192, 203). Many studies have shown that B1-cell-derived IgM provides the first line of defense against many bacterial pathogens (204), however, there is limited studies that investigate their response against fungal pathogens or components in the peritoneal cavity.

The peritoneal cavity is populated with various APCs, notably tissue-resident macrophages, DCs and B1 cells, that can drive different T cell responses against pathogens. In naïve mice, T cells make up between 10 to 20% of peritoneal immune cells, most of which are activated CD4<sup>+</sup> and CD8<sup>+</sup> T cells with an effector/memory phenotype (205). Prior studies have suggested that the omentum serves as the primary sites of T cell activation (188). In the omentum,

milky spots and FALCs are composed predominantly of macrophages (~50%), which monitor the peritoneal fluid and collect antigen for presentation (206, 207). After IP treatment with *Toxoplasma gondii*, infected peritoneal macrophages migrated into the FALCs and prime CD8<sup>+</sup> T cells, while resident cDC1 provided secondary signals to expand CD8<sup>+</sup> T cell and promote memory formation (207). Similarly, peritoneal T cells relocate to the omentum, particularly to the milky spots, where they become activated by resident DCs during bacterial peritonitis (188). Furthermore, bacterial infection of the peritoneal cavity has been associated with the accumulation of unconventional T cells, including  $\gamma\delta$  T cells (208) and mucosal-associated invariant T cells (209). Although the peritoneal T cell composition has been characterized, their precise function in coordinating anti-infective and anti-tumour immune responses in the peritoneal cavity is not well described. Therefore, understanding the adaptive immune response of the peritoneal cavity is important for designing novel vaccines and treatments that contain adjuvants, such as  $\beta$ -glucan.

## 1.5. Central Hypothesis and Aims

Given that  $\beta$ -glucan is intraperitoneally administered and the peritoneal cavity harbors a large reservoir of innate immune cells, *we hypothesized that peritoneal immune cells are required for the induction of  $\beta$ -glucan-mediated trained immunity in the BM.* To test this hypothesis, we designed two aims:

1. To assess the impact of  $\beta$ -glucan on the innate, adaptive and HSPC compartments in the peritoneal cavity, bone marrow and spleen.
2. To determine the effects of  $\beta$ -glucan on the migration of different peritoneal cell populations and their potential mechanism of accessing the BM.

## **CHAPTER 2: METHODS AND MATERIALS**

### **2.1. Mice**

C57BL/6, *Gata6*<sup>H2B-Venus</sup> knock-in reporter (*Gata6*<sup>tm1Hadj/J</sup>), *Rag1*<sup>-/-</sup> (B6.129S7-*Rag1*<sup>tm1Mom/J</sup>) and *Dectin-1*<sup>-/-</sup> (B6.129S6-*Clec7a*<sup>tm1Gdb/J</sup>) mice were purchased from Jackson Laboratory. *Rag1*<sup>-/-</sup> and *Dectin-1*<sup>-/-</sup> lines were on the C57BL/6 genetic background and inbred. Mice heterozygous for the *Gata6*<sup>H2B-Venus</sup> allele were bred with C57BL/6 mice to generate heterozygous mutants for experiments as homozygous mutants are non-viable. Mice were housed at the animal facility of the Research Institute of McGill University Health Centre, Montreal, QC, Canada. Experiments were performed using six- to ten-week-old male mice to study the mature immune response and to obtain sufficient number of cells for detecting rare populations in the bone marrow by flow cytometry. Mice were maintained under specific pathogen-free conditions with access *ad libitum* access to food and water. All animal studies complied with the guidelines of the Animal Research Ethics Board of McGill University and were approved by the Facility Animal Care Committee (protocol number: 2010-5860).

### **2.2. $\beta$ -Glucan**

#### **2.2.1. Preparation of $\beta$ -glucan**

Commercial  $\beta$ -glucan derived from *Saccharomyces cerevisiae* was purchased from Sigma-Aldrich (catalog #G5011). This glucan is composed of (1,3) linkages and (1,6) linked branches.  $\beta$ -Glucan was suspended in phosphate-buffered saline (PBS) to a final concentration of 10 mg/mL by repeated aspiration with a 25G needle and syringe.  $\beta$ -glucan was immediately used for injections.

### **2.2.2. Staining of $\beta$ -glucan**

5-(4,6-dichlorotriazinyl) aminofluorescein (DTAF) dye (ThermoFisher, catalog #D16) was dissolved in PBS at a concentration of 5 mg/mL.  $\beta$ -Glucan was then suspended in the DTAF solution at a concentration of 10 mg/mL and shaken for at least 8 hours at room temperature in the dark. After incubation,  $\beta$ -glucan was extensively washed at least five times with PBS to remove unbound dye. After the supernatant appeared clear,  $\beta$ -glucan was spun down at 5000 rpm for 5 minutes and the pellet was resuspended in sterile PBS at a concentration of 10 mg/mL. Stained  $\beta$ -glucan was immediately used or stored at 4°C up to 7 days.

### **2.3. *In vivo* training with $\beta$ -glucan**

Mice were injected intraperitoneally with 1 mg of  $\beta$ -glucan suspended in 100  $\mu$ L PBS or 100  $\mu$ L PBS control at day 0. Organs and peritoneal lavage fluid were collected at various timepoints following injection. Control mice represented by day 0 received 100  $\mu$ L of sterile PBS. All samples were collected between 10 am and 12 pm.

### **2.4. Cell isolations**

#### **2.4.1. Isolation of peritoneal cells**

The peritoneum of a mouse was lavaged with 5 mL ice-cold PBS using a 20G needle. Peritoneal cells were spun down (1500 rpm for 5 minutes) and red blood cells (RBCs) were lysed with 1 mL of ammonium-chloride-potassium (ACK) buffer for 2 minutes. After RBC lysis, cells were washed, resuspended in 0.5 mL of DMEM culture medium (Invitrogen) and counted with a hemocytometer at a 1:9 (control samples) or 1:40 (treated samples) dilution. Peritoneal lavages with blood contamination were excluded from the study.

#### **2.4.2. Isolation of bone marrow cells**

Right femora and tibiae from each mouse were harvested in 2 mL of RPMI culture medium (Invitrogen). Bones were cleaned from tissue, cut at both epiphyses, and centrifuged into 250  $\mu$ L RPMI in microcentrifuge tubes. BM cells were transferred into 15mL tubes, spun down and resuspended in 1 mL ACK buffer for 5 minutes. After RBC lysis, cells were washed, resuspended in 1 mL of RPMI and counted with a hemocytometer at a 1:40 dilution.

#### **2.4.3. Isolation of splenic cells**

Spleens were collected in 2mL RPMI medium and crushed through a 70- $\mu$ m nylon mesh. Cells were spun down, resuspended in 1 mL of ACK buffer for 5 minutes, washed, then resuspended in 1 mL of complete RPMI. Samples were counted with a hemocytometer at a 1:200 dilution.

#### **2.4.4. Isolation of cells from blood**

Blood was collected by cardiac puncture in a BD Microtainer tube. For flow cytometry, blood was directly stained with conjugated antibodies; then resuspended in 1 mL of ACK buffer to lyse RBCs.

### **2.5. Flow cytometry**

Bone marrow cells ( $6 \times 10^6$ ), peritoneal cells ( $2 \times 10^6$ ) or spleen cells ( $6 \times 10^6$ ) were seeded in 96-well plates and stained with fixable Viability Stain eFluor506 (BioScience) or Viability Stain eFluor780 (BioScience) at a concentration of 1:1000 in PBS for 30 minutes at 4°C. Cells were then washed

with FACS buffer (0.5% bovine serum albumin (BSA) in PBS). For staining of hematopoietic stem and progenitor cells, cells were incubated with the following biotinylated antibodies (all BD Bioscience) at a concentration of 1:100 for 30 minutes at 4°C: anti-Ter-119 (Ter119), anti-CD11b (M1/70), anti-CD5 (52-7.3), anti-CD4 (RM4-5), anti-CD8a (53-6.7), anti-CD45R (RA3-6B2), and anti-Ly6G/C (RB6-8C5). For staining of innate and adaptive immune cells, cells were resuspended in anti-CD16/32 (93; eBioscience) at a concentration of 1:200 in FACS buffer for 10 min at 4°C to block Fc receptor-mediated nonspecific binding. Subsequently, cells were washed with FACS buffer and then incubated the surface antibodies.

### **2.5.1. Hematopoietic stem and progenitor (“LKS”) panel**

Cells incubated with the following antibodies for 30 minutes at 4°C (all 1:100 dilution): APC-Cy7-conjugated streptavidin, APC-conjugated anti-cKit (2B8), PE-Cy7-conjugated anti-Sca1 (D7), FITC-conjugated anti-CD34 (RAMM34), PerCP-Cy5.5-conjugated anti-CD16/32 (93), BV786-conjugated anti-CD127 (SB/199), PE-conjugated anti-Ftl3 (A2F10), BUV737-conjugated anti-CD48 (HM48-1) and v450-conjugated anti-CD150 (mShad150).

### **2.5.2. Innate panel**

For staining of innate immune cells for the kinetic analysis, the following antibodies (all 1:200, unless otherwise stated) were used: BUV737-conjugated anti-CD45.2 (104), BUV395-conjugated anti-CD11b (M1/70), v450-conjugated anti-CD11c (N418), PE-conjugated anti-Ly6G (1A8), BV786-conjugated anti-SiglecF (E50-2440), PE-Cy7-conjugated anti-Ly6C (AL-21), AF700-conjugated anti-F4/80 (BM8), and FITC-

conjugated anti-pDCA1 (eB149). For the innate panel in *Dectin-1*<sup>-/-</sup> mice, the same antibodies as above were used, except for pDCA1 and the following antibodies were exchanged: PE-Cy7-conjugated anti-CD11b (M1/70), FITC-conjugated anti-Ly6C (AL-21), and APC-conjugated anti-F4/80 (BM8). For the innate panel with DTAF- $\beta$ -glucan, cells were stained with Viability Stain eFluor780 and the same antibodies as for the kinetic analysis were used, except for pDCA1 and the following antibodies were exchanged: APC-conjugated anti-F4/80 (BM8). For intracellular staining, the Foxp3 nuclear factor staining buffer set (eBioscience) was used and cells were stained with anti-GATA6-PE (D61E4; Cell Signaling Technology) at a 1:50 dilution for 1h at 4°C.

### **2.5.3. Adaptive panel**

For staining of innate immune cells, the following antibodies (all 1:200, unless otherwise stated) were used: BUV737-conjugated anti-CD45.2 (104), APC-conjugated anti-CD3 (145-2C11), BUV395-conjugated anti-CD19 (1D3), PE-Cy7-conjugated anti-CD4 (RM4-5), AF700-conjugated anti-CD8 (53-6.7), v450-conjugated anti- $\gamma\delta$ TCR (GL3; 1:100 dilution), and BV650-conjugated anti-NK1.1 (PK136).

### **2.5.4. Peritoneal B1 cell panel**

For staining of peritoneal B1 cells, the following antibodies (all 1:200, unless otherwise stated) were used: BUV737-conjugated anti-CD45.2 (104), BUV395-conjugated anti-CD19 (1D3), APC-conjugated anti-CD43 (S11), PE-conjugated anti-CD5 (53-7.3), PE-Cy7-conjugated anti-CD23 (B3B4) and BV711-conjugated anti-CD138 (281-2).

Following the staining of extracellular markers, cells washed with FACS buffer, fixed in 1% paraformaldehyde (PFA; ThermoFischer) overnight and acquired within 3 days. Samples were acquired on the Fortessa-X20 (BD) using FACSDiva software (BD) and analyzed using FlowJo software v.10.7.1.

## **2.6. Confocal microscopy**

Peritoneal and BM cells ( $4 \times 10^5$ ) were seeded in a glass chamber microscopy slide (Millipore) for 4h at 37°C. Cells were first fixed in 4% PFA for 10 minutes, and then permeabilized with 0.1% Triton X-100 in PBS for 10 minutes at 37°C. Samples were blocked with 3% BSA in PBS for 1h at 37°C, and then incubated with AF647-conjugated anti-F4/80 or AF594-conjugated anti-Ly6G (1:100 dilution in FACS buffer) overnight at 4°C. Slides were washed with PBS three times after each step. DAPI mounting medium was applied (ProLong Diamond Antifade; Invitrogen) and coverslips were placed onto microscope slides. Images were acquired using a Zeiss LSM 700 laser-scanning confocal microscope and analyzed with ImageJ.

## **2.7. Splenectomy**

Prior to surgery, the mid region of the abdomen of the mice was shaved and clean. Mice were induced and maintained under inhaled anesthesia (1.5% isoflurane) with its nose encased in the nosecone supplying the inhalation gas. All surgeries were performed on a heating pad. Using dissection scissors, a 0.5 cm skin vertical incision was made on the left lumbar region of the abdomen just below the last rib. A similar incision was made in the midline fascia which was directly under the skin incision. Lidocaine was applied to the open wound. Using smooth forceps, the spleen was brought out of the omentum and held out from the incision site without rupturing

the splenic artery and vein. A knot was tied around the vessels using non-absorbable 5-0 silk suture (Ethicon). The vessels were cut distal to the knot and the entire spleen was removed. For the closure of the abdomen, the parietal peritoneum was sewed together with 4-0 coated Vicryl absorbable sterile surgical sutures, and the skin was closed by wound clips. After the procedure, mice were administered 100  $\mu$ l of carprofen (5-10 mg/kg) subcutaneously and transferred into a clean, warm cage. Mice were monitored until they recovered from anesthesia. Two more doses of carprofen were subcutaneously administered at 24h and 48h post-surgery, and wound clips were removed after 7 days post-surgery. Mice were rested for 9 days before administrating one dose of  $\beta$ -glucan.

## **2.8. Statistical analysis**

Statistical analysis was performed using GraphPad Prism version 9 (GraphPad Software, San Diego, California, USA). All data are presented as mean  $\pm$  SEM, unless otherwise stated. Frequency refers to percentage of viable cells, unless otherwise stated. Statistical differences were determined by two-way ANOVA followed by Sidak's multiple comparison test or Kruskal-Wallis test followed by Dunn's multiple comparison test (FACS data), or two-tailed distribution independent Student T test (XY plots for FACS data). Asterisks indicate statistical significance (\* $p < 0.05$ ; \*\* $p < 0.01$ ; \*\*\* $p < 0.001$ ; \*\*\*\* $p < 0.0001$ ).

## CHAPTER 3: RESULTS

### 3.1. $\beta$ -Glucan expands HSPC populations in the BM.

$\beta$ -Glucan is a potent inducer of trained immunity that has been shown to drive the expansion of hematopoietic progenitor subpopulations in the BM (39). Previous work has reported that one dose of  $\beta$ -glucan promotes granulopoiesis (60), while our group has demonstrated that two doses of  $\beta$ -glucan skew HSCs towards monocytopoiesis (production of monocytes) (39). To validate our *in vivo* model of  $\beta$ -glucan-induced trained immunity, we treated wild-type (WT; C57BL/6) mice with one dose of intraperitoneal  $\beta$ -glucan ( $\beta$ -glucan-IP) or PBS control (PBS-IP) and evaluated the impact of  $\beta$ -glucan on the hematopoietic progenitor pool in BM at 1-, 3- and 5-days post-treatment by flow cytometry (**Fig. 3A** and **fig. S1**; hematopoietic stem and progenitor gating strategy). In line with previous studies,  $\beta$ -glucan-IP increased the frequency and number of HSCs (LKS; Lin<sup>-</sup> cKit<sup>+</sup> Sca1<sup>+</sup>) in BM (**Fig. 3B and 3C**). Specifically, the LKS expansion, which peaked at day 3, was primarily attributed to the significant increase in short-term HSCs (ST-HSCs) and multipotent progenitors (MPPs), and not due to long-term HSC (LT-HSCs) (**Fig. 3D-F**). Within the MPP population, the frequency and number of the myeloid-biased MPP3 subset were heightened (**Fig. 3G**), while lymphoid-biased MPP4 cells were decreased non-significantly at day 3 post- $\beta$ -glucan (**Fig. 3H**). At day 5, the MPP3 population then returned to baseline and MPP4s drastically increased. Downstream of MPP3 are lineage-restricted myeloid progenitors, which comprise of the common myeloid progenitor (CMP), granulocyte-monocyte progenitor (GMP) and megakaryocyte-erythrocyte progenitor (MEP) subsets. Among these progenitors, we observed a significant reduction of CMPs and MEPs (**Fig. 3I-K**), and interestingly, no expansion in GMPs (**Fig. 3K**). These results demonstrate that one dose of  $\beta$ -glucan-IP drives the expansion of HSPCs.

### 3.2. $\beta$ -Glucan-induced HSC expansion is independent of adaptive immunity.

Substances that are administrated through the peritoneal cavity eventually reach systemic circulation. To determine the effects of  $\beta$ -glucan on the local and global immune response, we first investigated the immune cell dynamic in the peritoneal cavity, spleen and bone marrow. At the site of administration, we observed a significant infiltration of CD45<sup>+</sup> leukocytes into the peritoneal cavity as early as day 1 after  $\beta$ -glucan-IP compared to PBS-IP, which gradually decreased by day 5 (**Fig. 4A**). Dynamic changes of immune cells were not limited to the peritoneal cavity, as there was an early drop in the number of CD45<sup>+</sup> leukocytes in the spleen on day 1 after  $\beta$ -glucan-IP, which returned to similar levels as PBS-IP by day 3 (**Fig. 4B**). In the BM, we found no significant differences between  $\beta$ -glucan-IP and PBS-IP groups (**Fig. 4C**). This indicates that  $\beta$ -glucan-IP treatment modulates the immune system at a local and splenic level.

Considering that  $\beta$ -glucan-IP significantly expanded peritoneal CD45<sup>+</sup> leukocytes, we next assessed the kinetic of adaptive immune cells in the peritoneal cavity following  $\beta$ -glucan treatment (**fig. S2A**; adaptive gating strategy). We showed that the frequency of peritoneal adaptive immune populations, namely B cells and T cells (including CD4<sup>+</sup> T cells, CD8<sup>+</sup> T cells and  $\gamma\delta$  T cells), were significantly reduced at all timepoints, while their numbers remained mostly unchanged except for day 3 post- $\beta$ -glucan treatment (**Fig. 4D-F**). Given that B1 cells represent a major subset of B cells in the peritoneal cavity, we assessed its kinetic at day 1 after  $\beta$ -glucan injection (**fig. S3A**; B1 cell gating strategy). While the counts of conventional B2 cells were unaltered (**fig. S3B**), we found that  $\beta$ -glucan treatment significantly contracted the B1 cells population (**fig. S3C**), specifically the B1a cells but not B2b cells (**fig. S3D and S3E**).

In the spleen, the frequencies of T cell subsets decreased over time, although a decline in the number of B and T cells was noted at day 1 and day 3 after  $\beta$ -glucan treatment (**fig. S4A-C**).

Additionally, T cell populations in the BM remained roughly constant except the B cells (**fig. S4D-G**), which were significantly lower in both frequency and number after day 3 post-treatment (**fig. S4H**). To assess the role of adaptive immune system in generating central trained immunity in the BM, we treated *Rag1*<sup>-/-</sup> (lacking T and B cells) with one dose of  $\beta$ -glucan-IP and analyzed the hematopoietic stem cell compartment at day 3 (**Fig. 4G**), when the LKS cells expansion peaks in the BM (**Fig. 3C**). The frequency and number of LKS cells and MPPs did not differ between WT and *Rag1*<sup>-/-</sup> mice after  $\beta$ -glucan injection (**Fig. 4H and 4I**). Despite a trending (yet not significant) increase in the frequency and number of LKS cells in *Rag1*<sup>-/-</sup> mice at 3 days post- $\beta$ -glucan treatment (**Fig. 4H**), we found that  $\beta$ -glucan-IP still expanded the MPP population in the BM (**Fig. 4I**). Together, these results indicate that the mechanism underlying the induction of  $\beta$ -glucan-mediated central trained immunity is independent of adaptive immunity.

### **3.3. Innate immune response to $\beta$ -glucan treatment in the peritoneal cavity, spleen and BM.**

Given that  $\beta$ -glucan is a well-known fungal PAMP, we hypothesized that mononuclear phagocytes and granulocytes accumulate in the peritoneal cavity in response to  $\beta$ -glucan. To address this, we profiled the innate immune response in the peritoneal cavity by flow cytometry post- $\beta$ -glucan treatment. At each timepoint, mice treated with  $\beta$ -glucan-IP exhibited a large expansion of innate immune cells into the peritoneal cavity (**Fig. 5A-C**). Notably, we observed increased numbers of peritoneal dendritic cells (**Fig. 5D**), monocytes, (**Fig. 5E**), F4/80<sup>+</sup> macrophages (**Fig. 5F**), and neutrophils (**Fig. 5G**), indicating that innate immune cells rapidly infiltrate the peritoneal cavity after  $\beta$ -glucan treatment.

Two major populations of resident macrophages occupy the peritoneal cavity: large peritoneal macrophages (LPMs; CD11b<sup>+</sup> F4/80<sup>hi</sup> GATA6<sup>+</sup>) and small peritoneal macrophages

(SPMs; CD11b<sup>+</sup> F4/80<sup>lo</sup> GATA6<sup>-</sup>). Considering that  $\beta$ -glucan-IP reduced the frequency while increased the number of F4/80<sup>+</sup> macrophages in the peritoneal cavity (**Fig. 5F**), we next examined the kinetic of LPMs and SPMs in response to  $\beta$ -glucan. We found a drastic depletion of LPMs at day 1 post- $\beta$ -glucan treatment (**fig. S5A and S5B**), which is accompanied by an accumulation of monocyte-derived SPMs (**fig. S5C**). To determine whether the decline in LPMs following  $\beta$ -glucan treatment was due to their egress from the peritoneal cavity, we utilized Gata6<sup>H2B-Venus</sup> knock-in reporter mice where the expression of GATA6 can be detected by flow cytometry to track the distribution of LPMs in peripheral blood and BM after 1 day of  $\beta$ -glucan treatment (**fig. S5D**). As previously shown, GATA6-Venus<sup>+</sup> LPMs significantly contracted in frequency and number after  $\beta$ -glucan-IP (**fig. S5E and S5F**), although less GATA6<sup>+</sup> LPMs were detected at baseline in PBS-IP control reporter mice compared to PBS-IP WT mice. There was no notable difference in SPMs in the peritoneal cavity of  $\beta$ -glucan-treated reporter mice (**fig. S5G**). Furthermore, flow cytometry analysis revealed low levels of GATA6-Venus<sup>+</sup> macrophages in peripheral blood (**fig. S5H**), and no detection of GATA6-Venus<sup>+</sup> macrophages in BM at day 1 post- $\beta$ -glucan-treatment (**fig. S5I**). Collectively, these findings suggest that the depletion of LPMs after  $\beta$ -glucan treatment is likely not due their migration out of the peritoneal cavity and thus, LPMs are not directly shuttling  $\beta$ -glucan from the peritoneal cavity into the BM to train HSCs.

We next continued to phenotype innate immune cells in the spleen and BM post- $\beta$ -glucan treatment. Spleens isolated from mice treated with  $\beta$ -glucan-IP showed an increase in DC frequency and a modest reduction in eosinophil at day 1 (**fig. S6A-E**), followed by with a gradual increase of splenic monocytes by day 5 after treatment (**fig. S6F**). We found no significant differences in the frequency or number of splenic macrophages between timepoints (**fig. S6G**). Additionally, BM from  $\beta$ -glucan-treated mice exhibited an expansion of DCs and monocytes at

day 1 (**fig. S7A-E**), an increase of eosinophils at day 3 (**fig. S7F**) and a decline in macrophages starting at day 1 (**fig. S7G**). Therefore,  $\beta$ -glucan-IP treatment accumulates DCs and monocytes in the spleen and BM, which may play a role in inducing central trained immunity in BM.

Neutrophils are the most abundant granulocyte in circulation and are critical for rapidly initiating an innate immune response against infections and tissue injury (210). Under physiological conditions, senescent neutrophils reverse migrate and home back to the bone marrow in a CXCR4-dependent manner and are cleared by bone marrow stromal macrophages (211). Other sites of neutrophil clearance occur in the spleen and liver (211). Assessment of the neutrophil kinetic revealed that following the peak in neutrophil frequency and absolute cell counts at day 1 in the peritoneal cavity (**Fig. 5G**), there was a subsequent increase of splenic and BM neutrophils at day 3 (**Fig. 5H and 5I**). These results suggest that peritoneal neutrophils may be returning to the BM and spleen for clearance or the activated BM and splenic granulopoiesis may be activated.

### **3.4. $\beta$ -Glucan expands HSPC populations in the spleen.**

Under “emergency” conditions, the spleen can serve as a secondary source of EMH (212). Given that the spleen is contained within the peritoneal cavity and  $\beta$ -glucan-IP alters the splenic innate immune repertoire, we next postulated that  $\beta$ -glucan treatment also expands splenic HSCs. To test this, we phenotyped splenic hematopoietic progenitors on day 1, 3 and 5 post- $\beta$ -glucan treatment by flow cytometry. Interestingly, mice exhibited significant expansion in the frequency and number of splenic LKS, LT-HSC, ST-HSC, MPP, myeloid-biased MPP3 and lymphoid-biased MPP4 subsets, which peaked at day 3 post- $\beta$ -glucan similar to BM (**Fig. 6A-G**). In addition,  $\beta$ -glucan-IP also increased splenic progenitor cell populations, including CMP, MEP and GMP (**Fig.**

**6H-J**). Thus,  $\beta$ -glucan treatment can activate EMH in the spleen, which may contribute to the accumulation of granulocytes in the peritoneal cavity and BM.

### **3.5. The role of the spleen in $\beta$ -glucan-mediated trained immunity.**

The spleen is a highly vascularized organ responsible for filtering blood, recycling iron from senescent or defective red blood cells, and maintaining immune homeostasis (213). The extensive network of vascular vessels of the spleen allows for bidirectional crosstalk between the spleen and BM via cellular and molecular mechanisms (214). For example, HSCs can mobilize from the BM and colonize the spleen to establish a site for extramedullary hematopoiesis during periods of stress (104). Moreover, IRA B cells (derived from peritoneal innate-like B cells known as B1a cells) in the spleen can produce GM-CSF and IL-3 and promote emergency granulopoiesis in the BM and spleen during sepsis (201).

Considering that  $\beta$ -glucan-IP treatment induces sterile inflammation of the peritoneal cavity and expands HSCs and progenitor cells in the spleen, we asked whether the spleen is required in the crosstalk between the peritoneal cavity and BM for the establishment of central trained immunity. To address this question, we splenectomized (SPX) mice, and subsequently administered one dose of  $\beta$ -glucan-IP or PBS-IP control (**Fig. 7A**). At day 5 post-treatment, the infiltration of innate immune cells, such as neutrophils, DCs and monocytes, into the peritoneal cavity of SPX mice was not impaired (**Fig. 7B-D**), whereas F4/80<sup>+</sup> peritoneal macrophages still significantly contracted in frequency (**Fig. 7E**). In the BM of both WT and SPX mice, the frequency of neutrophils and monocytes were elevated after  $\beta$ -glucan-IP compared to PBS-IP (**Fig. 7F-G**), while there were no differences in the DC populations between the two treatment groups (**Fig. 7H**). Upon FACS analysis of BM progenitors, although we did not observe any increase in

LKS or MPP in either WT or SPX mice (**Fig. 7I and 7J**), the expansion of ST-HSCs remained intact (**Fig. 7K**). Since  $\beta$ -glucan-IP did not expand the LKS or MPP populations in WT mice, one plausible explanation for these findings is the expansion of rare populations, in terms of frequency, may be masked by more abundant populations, such as neutrophils. To this end, we further validated whether  $\beta$ -glucan-IP expands BM HSCs independent of the spleen by assessing the HSC subsets as a frequency of  $\text{Lin}^-$  cells (**Fig. 7L**). We found increased frequency of LKS, MPP and ST-HSC, but not LT-HSC, of total  $\text{Lin}^-$  cells (**Fig. 7M-P**), potentially suggestive that the spleen is neither involved in the crosstalk between the peritoneal cavity and BM nor drives the expansion of hematopoietic progenitors.

### **3.6. Peritoneal neutrophils and macrophages recognize and ingest $\beta$ -glucan.**

The FACS analyses revealed that neutrophils are the most predominant immune cell to infiltrate into the peritoneal cavity in the early stages of  $\beta$ -glucan-induced inflammation. To determine whether neutrophils are the first cells to recognize and internalize  $\beta$ -glucan, we labelled  $\beta$ -glucan with 5-(4,6-dichlorotriazinyl) aminofluorescein (DTAF) and treated WT mice with one dose of DTAF- $\beta$ -glucan-IP. At early (1h, 4h and 12h) and intermediate (24h, 48h and 72h) timepoints post-injection, we assessed the distribution of DTAF- $\beta$ -glucan<sup>+</sup> cells in the peritoneal cavity by FACS (**Fig. 8A**). This experimental setup offers an efficient method for tracking  $\beta$ -glucan and cells that have internalized  $\beta$ -glucan *in vivo*. As early as 1h after treatment, DTAF- $\beta$ -glucan<sup>+</sup> cells were detected in the peritoneal cavity (**Fig. 8B**). Specifically, the percentage and absolute number of peritoneal CD45<sup>+</sup> leukocytes, which have phagocytosed  $\beta$ -glucan, peaked at 1h and 4h post-treatment, respectively (**Fig. 8C**). The same trends were observed for peritoneal neutrophils (**Fig. 8D**), whereby the internalization of  $\beta$ -glucan by neutrophils was also confirmed by confocal

imaging (**Fig. 8E**). In contrast, DTAF- $\beta$ -glucan<sup>+</sup> monocytes first appeared at 4h post-injection, which coincided with a depletion of macrophage (**Fig. 8F and 8G**). This was followed by a subsequent increase in macrophages starting at 24h (**Fig. 8G**), generating a second wave of macrophages where higher proportion of macrophages contained  $\beta$ -glucan particles (**Fig. 8H**). Therefore, we speculate that  $\beta$ -glucan-elicited inflammation may have quickly depleted tissue-resident LPMs and, in turn, activated the differentiation of monocytes into macrophages. Collectively, these data demonstrates that neutrophils and macrophages are among the first cells to recognize and ingest  $\beta$ -glucan in the peritoneal cavity.

### **3.7. $\beta$ -Glucan is likely not directly accessing BM via a cell intermediate.**

BCG is another agonist of trained immunity. Access of BCG into the BM is required for the reprogramming and expansion of HSCs (59). Because peritoneal neutrophils phagocytose  $\beta$ -glucan and have the capacity to return to the BM for clearance (211), we hypothesized that  $\beta$ -glucan gains access to the BM via neutrophils and directly induce central trained immunity. To address this hypothesis, we treated mice with DTAF- $\beta$ -glucan and the presence of DTAF- $\beta$ -glucan was evaluated in the BM by flow cytometry. While the DTAF- $\beta$ -glucan signal was drastically less pronounced in the BM compared to the peritoneal cavity, we detected similar levels of  $\beta$ -glucan<sup>+</sup> cells across all timepoints (**Fig. 9A**), including at 0 h which did not receive DTAF- $\beta$ -glucan-IP. The signal at 0h is likely due to autofluorescence. Furthermore, we measured negligible frequencies of DTAF- $\beta$ -glucan<sup>+</sup> cells (~0.020%), neutrophils (~0.015%) and macrophages (~0.0006%) at their highest peak at 24h post-treatment, whereas less than 5,000 cells in the BM were positive for DTAF- $\beta$ -glucan (**Fig. 9B-D**). It should be also noted that there was considerable variability in the frequency and number between timepoints of each BM cell populations.

Moreover, we failed to detect DTAF- $\beta$ -glucan as a free particle or in a cell in the BM by confocal microscopy (data not shown). In conclusion, these findings demonstrate that  $\beta$ -glucan is likely not directly shuttled into BM via neutrophils or macrophages and thus induces central trained immunity through indirect mechanisms.

### **3.8. $\beta$ -Glucan-induced LKS expansion is likely independent of dectin-1 signaling.**

Dectin-1 is widely expressed on myeloid cells, such as neutrophils, macrophages, monocytes and DCs, and participates in recognizing  $\beta$ -glucan particulates and inducing phagocytosis (137). Since we have previously shown that neutrophils rapidly recognize and engulf  $\beta$ -glucan in the peritoneal cavity, we sought to understand whether dectin-1 signaling and/or neutrophils are required for the expansion of HSCs in the BM. To disrupt the function of  $\beta$ -glucan sensing by neutrophils, we treated *Dectin1*<sup>-/-</sup> (dectin-1 deficient) mice with one dose of  $\beta$ -glucan-IP and analyzed the innate immune and hematopoietic stem cell compartments at day 3 (**Fig. 10A**). Mice with the loss of dectin-1 showed reduced recruitment of leukocytes, specifically neutrophils and monocytes, into the peritoneal cavity after  $\beta$ -glucan injection compared to  $\beta$ -glucan-treated WT mice (**Fig. 10B-D**). However, dectin-1 deficient mice displayed the similar trends in frequency and number of peritoneal DCs, macrophages, LPMs and SPMs after  $\beta$ -glucan treatment as their WT counterparts (**Fig. 10E-H**). In the BM, dectin-1-deficient mice treated with  $\beta$ -glucan still exhibited higher number of neutrophils and monocytes compared to the PBS control (**Fig. 10I and 10J**) and expanded the LKS and MPP3 populations to levels comparable to those of  $\beta$ -glucan-treated WT mice (**Fig. 10L and 10M**). FACS analysis of BM progenitors revealed that CMPs were not altered (**Fig. 10M**), while GMPs failed to increase independent of dectin-1 signaling (**Fig. 10N**). Taken together, these results indicate that dectin-1 is important for recruiting neutrophils

into the peritoneal cavity in response to  $\beta$ -glucan, but is not required for inducing the expansion of HSCs in the BM.

## CHAPTER 4: DISCUSSION

Trained immunity is an emerging concept in immunology that adds a new dimension to our understanding of innate immunity and immunological memory (1). Systemic administration of  $\beta$ -glucan via the IP route is a well-established model for inducing trained immunity *in vivo* (1, 60).  $\beta$ -Glucan treatment leads to long-term metabolic and epigenetic reprogramming of hematopoietic progenitors in the BM, allowing the “memory-like” phenotype to be transmitted to downstream myeloid cells (60). While numerous studies have demonstrated the therapeutic and prophylactic potential of  $\beta$ -glucan against infections, tumours and inflammatory disorders (39, 53, 215), the exact mechanisms underlying the establishment of central trained immunity by  $\beta$ -glucan are incompletely understood. Furthermore, it is unclear how  $\beta$ -glucan in the peritoneal cavity exerts its effects on HSCs in the BM. Here we characterized the immune response of the peritoneal cavity, spleen and BM in response to  $\beta$ -glucan, and explored the role of several cellular and molecular pathways in the induction of central trained immunity.

In this study, we followed a single dose of  $\beta$ -glucan regimen to induce trained immunity. Similar to the two dose  $\beta$ -glucan regimen (39), we observed an expansion of the LKS population, which is considered a hallmark of trained immunity. Our group has previously demonstrated that hematopoiesis is polarized towards enhanced monocytopoiesis with two doses of  $\beta$ -glucan (39) and granulopoiesis with one dose of  $\beta$ -glucan (130). Granulopoiesis involves a series of differentiation steps from CMPs to GMPs to neutrophils (216). Although we found no expansion of GMPs, there was an increase in granulocytes in BM, notably neutrophils and eosinophils, suggesting that our one-dose  $\beta$ -glucan model promoted granulopoiesis. However, due to the lack of epigenomic and transcriptomic analyses in this study, we cannot confirm whether the HSC expansion observed in  $\beta$ -glucan-treated mice was also accompanied by distinctive epigenetic and

metabolic reprogramming characteristic of trained immunity. Moreover, it remains unclear whether this  $\beta$ -glucan-induced granulopoiesis is mechanistically related to emergency granulopoiesis (217).

Emergency granulopoiesis is a hematopoietic response to systemic stress characterized by the accelerated and enhanced *de novo* production of granulocytes (218). Several studies have shown that HSCs can be activated directly by sensing pathogen through PRRs (e.g. TLR4 and/or TLR2) (87, 219) or indirectly by myelopoietic growth factors, such as G-CSF, GM-CSF and IL-3 (218-220). Thus, excessive inflammation leads to an expansion of LKS cells (221), transcriptional rewiring of HSCs to favor myeloid production (218), activation of extramedullary granulopoiesis (104) and rapid release of neutrophils from granulocytic marginated pools (83, 85). Similarly, we observed an increase in LKS cells in the BM peaking at day 3 post- $\beta$ -glucan injection, along with a heightened myeloid (MPP3) output, an expansion of HSPC populations in the spleen, and an early depletion of BM neutrophils in our model. Despite a significant expansion of lymphoid-biased MPP4 by day 5, this did not result in a corresponding increase in lymphoid cells, namely in T or B cells, in the BM or peripheral organs. Instead, we observed an expansion in mature myeloid cells, notably in granulocytes and monocytes, further supporting myelopoiesis. Furthermore, a study by Ueda *et al.* showed that during systemic inflammation, B cells egress from the BM to favour granulopoiesis and allow granulocytes to expand into abandoned niches (222, 223). This is consistent with our observation that  $\beta$ -glucan treatment reduced the pool of B cells in the BM while simultaneously accumulated neutrophils. Altogether, our findings illustrate that systemic administration of  $\beta$ -glucan activates HSPC proliferation and differentiation with a bias towards the generation of granulocytes and production of neutrophils. However, it is unknown whether this hematopoietic response is indicative of emergency granulopoiesis, trained immunity or both. For

instance, current evidence suggests that emergency granulopoiesis after BCG vaccination may represent the initial phase of trained immunity after BCG vaccination (224, 225). Thus, further experiments are needed to determine whether (i) HSCs acquired key epigenetic signatures (e.g. H3K27ac and H3K4me3) and rewired their metabolic pathways (e.g. increased glycolysis and cholesterol metabolism) by day 3 post- $\beta$ -glucan treatment, and (ii) myeloid cells derived from these  $\beta$ -glucan-treated HSCs produced higher amounts of pro-inflammatory cytokines against a secondary insult.

We propose three possible mechanisms through which central trained immunity can be induced by  $\beta$ -glucan from the peritoneal cavity. First,  $\beta$ -glucan disturbs the local immune homeostasis and triggers the migration of peritoneal immune cells into the BM where they interact with HSCs directly by physical contact (juxtacrine signaling) or indirectly by soluble factors (paracrine signaling). Second,  $\beta$ -glucan stimulates peritoneal immune cells to secrete soluble factors (e.g. cytokines), which enter systemic circulation and imprint HSCs (endocrine signaling). Third,  $\beta$ -glucan gains access to the BM as a free particle or via a cellular intermediate and activates signaling in HSCs. To determine whether peritoneal immune cells are required in this process, we performed kinetic analyses of the adaptive and innate immune compartments to  $\beta$ -glucan treatment in the peritoneal cavity.

Simple organisms that lack an adaptive immune system evolved trained immunity to improve responses to reinfections (226). Hence, in vertebrates with an adaptive immune response, protection against subsequent infections can also be achieved exclusively by innate immune cells (2). Using an adoptive transfer model, we have previously demonstrated that Rag1-deficient mice that received BCG-trained macrophages were protected against *Mtb* infection (59). Another study reported that a non-lethal inoculum of *C. albicans* trained monocytes provided protection against

a subsequent lethal *C. albicans* challenge in mice lacking T and B cells (227). In addition, Rag1<sup>-/-</sup> mice treated with  $\beta$ -glucan exhibited an expansion of LKS and MPP subsets and showed reduced IAV-mediated lung immunopathology (130) and melanoma tumour growth (53). In agreement with these studies, we observed a trending and significant increase in LKS and MPPs, respectively, after  $\beta$ -glucan treatment in Rag1<sup>-/-</sup> mice, supporting the notion that adaptive immune system does not contribute to HSC expansion in  $\beta$ -glucan-mediated trained immunity.

Although the induction of central trained immunity is not dependent on T and B cells (59),  $\beta$ -glucan is actively studied as a potential adjuvant agent for preventative vaccines and therapeutic treatments against infections and tumours. Therefore, it is important to not only study the immunomodulatory effect of  $\beta$ -glucan on the innate immune cells, but also the adaptive immune cells. We have shown that IP injection of  $\beta$ -glucan significantly reduced the number of peritoneal innate-like B1 cells, particularly B1a cells. These observations were further supported in murine models of septic peritonitis and endotoxemia models in which peritoneal B1a cells disappeared while B1b cells were maintained in mice that survived cecal ligation and puncture (CeLP) or LPS challenge (228). Another study also showed that severe sterile peritonitis elicited by high-dose zymosan treatment (1000  $\mu$ g) completely abrogated the accumulation of B1 cells in the peritoneal cavity, whereas low-dose zymosan treatment (10  $\mu$ g) led to a slight increase in B1 cells (229). This suggests that an injection with 1 mg of  $\beta$ -glucan induced severe peritoneal inflammation in our model of trained immunity. While the fate of these B1 cells was not explored in this study, their decline during peritonitis may be explained by the loss of peritoneal LPMs, which are important regulators of B1 cell proliferation and survival (230). These LPMs are also crucial for recruiting B1 cells from the omentum and circulation, and retaining them in the peritoneal cavity via CXCL12 signaling (229).

The peritoneal cavity provides a specialized niche for two populations of tissue resident macrophages: LPMs and SPMs (173). Under steady conditions, LPMs represent 90% of all peritoneal macrophages (173). However, in response to mild or severe inflammation in the peritoneal cavity, they rapidly disappear in an event known as “macrophage disappearance reaction” (MDR) (231), thereby opening the peritoneal niche for infiltrating blood-derived monocytes to differentiate into SPMs. The MDR phenomenon was first described in 1963 in tuberculin-treated guinea pigs with delayed-type hypersensitivity (231) and has since been recapitulated in various murine sepsis and peritonitis models induced by CeLP, (232), zymosan (233), LPS (192), thioglycollate (234) and *E. coli* (179). Consistent with previous findings, we demonstrated that MDR also occurred in the peritoneal cavity after  $\beta$ -glucan treatment. While the exact mechanisms behind MDR are unknown, studies have proposed that LPM become non-retrievable by peritoneal lavage due to their increased adherence to the peritoneal mesothelium (235), cell death (179) or migration into the omentum or other tissues (180, 181, 192, 207). In a model of abdominal sepsis, one group revealed that LPMs form aggregates around *E. coli* at the peritoneal mesothelium and underwent pyroptosis, resulting in the release of IL-1 $\beta$  (179). Thus, LPMs may use similar mechanisms to contain  $\beta$ -glucan (236) and represent be a source of IL-1 $\beta$  during peritoneal inflammation (**Fig. 11**). To determine whether  $\beta$ -glucan triggers the migration of LPMs into the BM, we used Gata6<sup>H2B-Venus</sup> knock-in reporter mouse system to track the expression of GATA6 as a marker for LPMs *in vivo*. In line with our previous findings (237), we did not detect GATA6-Venus<sup>+</sup> LPMs in the BM after  $\beta$ -glucan treatment, but we speculate that LPMs may be either downregulating GATA6 expression and undergoing apoptosis in the absence of local tissue-derived cues (182, 192, 238), migrating into the BM at a different timepoint or not egressing from the peritoneal cavity. Therefore, using markers whose expression is not regulated by environmental

signals, such as congenic markers CD45.1/CD45.2, will allow us to better track LPMs *in vivo* and elucidate their cellular fate after  $\beta$ -glucan treatment.

Neutrophils are classically regarded as the first line of defense; they are rapidly mobilized into sites of inflammation or injury where they perform their effector functions (239). It has been well documented that neutrophils are the predominant leukocytes that drive early inflammation in the peritoneal cavity after the introduction of a sterile stimulant (e.g. zymosan or thioglycollate) (233, 240) or an infection (e.g. *E. coli* or polymicrobial sepsis via CeLP) (241, 242). Here we also showed that  $\beta$ -glucan elicits a rapid infiltration of neutrophils into the peritoneal cavity followed by a gradual decline, which aligns with neutrophil kinetics reported in other murine models of peritonitis (233). Moreover, we observed that the number of neutrophils in the peritoneal cavity peaked at day 1 following treatment, coinciding with a decline in neutrophils counts in the BM. This implies that the mature neutrophils from the BM reservoir were rapidly released, likely in response to an inflammatory signal originating from the peritoneal cavity. In models of fungal infections caused by *Candida* and *Aspergillus* species, recruited neutrophils have been demonstrated to exert a variety of antimicrobial functions, such as phagocytosis, degranulation and neutrophil extracellular traps (NETs) release (239). Although we have not assessed the functional capacity of  $\beta$ -glucan-elicited peritoneal neutrophils in this study, previous work has described various neutrophil responses to  $\beta$ -glucan challenges. For instance, neutrophils from zymosan-treated mice exhibited enhanced reactive oxygen species production, myeloperoxidase activity, and phagocytosis following *Listeria* challenge (243). Moreover, Ratitong *et al.* has shown that IP injection of *Aspergillus fumigatus* spores (expressing surface  $\beta$ -glucan) in mice stimulated the secretion of bioactive IL-1 $\alpha$  and IL-1 $\beta$  from neutrophils in the peritoneal cavity (244). IL-1 $\alpha$  and IL-1 $\beta$  are pro-inflammatory cytokines that promote different stages of sterile inflammation; in

particular, IL-1 $\alpha$  attracts neutrophils in the initial phase, whereas IL-1 $\beta$  recruits macrophages in the later stages (245). Most importantly, IL-1 has been previously identified as a key mediator in promoting the expansion of HSCs and myelopoiesis after  $\beta$ -glucan treatment (39, 60). Therefore, it is possible that  $\beta$ -glucan-elicited neutrophils are one of the early cellular sources of IL-1, which is required to trigger a massive neutrophil infiltration into the peritoneal cavity and induce trained immunity via endocrine signaling (**Fig. 11**).

Historically, neutrophils have been viewed as a homogenous population of terminally differentiated effector cells with an inflammatory phenotype intended to respond to PAMPs and eliminate pathogens (239). However, for the last decade, mounting evidence has suggested that neutrophils are phenotypically heterogeneous. For example,  $\beta$ -glucan has been shown to epigenetically reprogramming granulopoiesis to promote an anti-tumour phenotype in neutrophils (53). In addition, recent data from our group showed that  $\beta$ -glucan training led to a generation of a unique subpopulation of regulatory neutrophils with less mature phenotype (Ly6C<sup>low</sup> CX101<sup>low</sup> CXCR2<sup>low</sup>) and rewired metabolism with heightened oxidative phosphorylation in a type I IFN-dependent, but IL-1-independent manner (130). These neutrophils promoted disease tolerance against pulmonary IAV infection by limiting lung tissue damage and thus improved survival. Another group reported that neutrophils isolated from the peritoneal cavity at 4h or 3 days following IP treatment with zymosan showed distinct transcriptional and proteomic profiles (246). 3-day neutrophils displayed an immature Ly6G<sup>low</sup> CD101<sup>low</sup> phenotype with neuroprotective/neuroregenerative properties and upregulated pathways involved in oxidative metabolism. In contrast, 4h neutrophils expressed higher levels of genes linked to immune responses and cytokine production, shared features with classically activated, mature Ly6G<sup>hi</sup> neutrophils and lacked neuroprotective/neuroregenerative properties. These studies reveal that

acute inflammation results in higher neutrophil heterogeneity, which may be a consequence of reprogrammed granulopoiesis associated with  $\beta$ -glucan-induced trained immunity or release of immature neutrophils from BM (“left shift”) due to emergency granulopoiesis (85). However, the techniques that were performed in this study were not adequate to characterize the phenotype of  $\beta$ -glucan-elicited neutrophils in the peritoneal cavity. Thus, the next step is to isolate neutrophils from these  $\beta$ -glucan-treated mice and perform transcriptomic, epigenomic and functional analyses to achieve an accurate assessment of neutrophil heterogeneity.

The spleen is the largest secondary lymphoid organ that is located within the peritoneal cavity. Given the spleen is a primary site for EMH (104) and  $\beta$ -glucan triggers HSC expansion in the BM, we investigated whether  $\beta$ -glucan promotes EMH. First, we showed that HSPCs were detectable in the spleen, but at lower levels compared to BM. As expected, the rarest population were LT-HSC. Unlike the quiescent LT-HSCs in the BM, most splenic HSCs and relocated BM-derived HSCs in the spleen have a pre-activated phenotype and are enriched for genes involved in the G0-G1 phase, allowing them to enter cell cycle and differentiate more rapidly in response to a stimulus (212). This may potentially explain the higher proportion of splenic ST-HSCs and downstream progenitors relative to LT-HSCs. Then, we demonstrated that  $\beta$ -glucan treatment increased HSPC subsets in the spleen, which is also in line with a recent study by Bono *et al.* (247). Together, our preliminary data indicates that EMH was activated after  $\beta$ -glucan treatment.

Because  $\beta$ -glucan modulated the hematopoietic and immune response in the spleen, we used a  $\beta$ -glucan-induced trained immunity model in SPX mice to assess the role of the spleen in the expansion of BM HSCs and the induction of trained immunity. To our knowledge, only one other group investigated the role of the spleen in trained immunity. Ferreira *et al.* showed that the removal of the spleen reduced neutrophils, but increased Ly6C<sup>hi</sup> monocytes levels in the blood

after  $\beta$ -glucan-IP compared to control SPX mice (248). Furthermore,  $\beta$ -glucan-treated SPX mice did not modulate G-CSF and GM-CSF plasma concentrations and showed unaltered IL-6, TNF- $\alpha$  and IL-6 plasma levels after a secondary LPS-IP challenge, suggesting that the spleen has a limited role in trained immunity. However, a general caveat to the study is that the induction of trained immunity was assessed by measuring cytokine production and innate immune cell populations in peripheral blood, which does not fully depict the training program that occurs in the BM. Thus, we evaluated the hematopoietic and innate immune cell compartments in the BM in SPX mice after  $\beta$ -glucan treatment. We found that  $\beta$ -glucan-treated SPX mice exhibited an expansion in the HSC subsets and an increase in BM neutrophils and monocytes frequencies, suggesting that granulopoiesis and monocytopoiesis were enhanced independent of the spleen. Furthermore, the peritoneal immune response to  $\beta$ -glucan-IP did not significantly differ between SPX and non-SPX groups. Therefore, our results support the limited role of spleen in trained immunity. Nevertheless, there were limitations to this experiment; we did not quantify the production of pro-inflammatory cytokines or analyzed chromatin remodelling in peritoneal and BM-derived myeloid cells before and after a secondary challenge to validate that  $\beta$ -glucan successfully induced peripheral and central trained immunity in our model.

$\beta$ -glucan cannot be digested by mammals due to the lack of  $\beta$ -1,3-glucanases (113). As a result, it is still unknown how long and where  $\beta$ -glucan persists in the system after an IP injection. Using DTAF-stained  $\beta$ -glucan, we demonstrated that neutrophils and macrophages are among the first immune cells to detect and internalize  $\beta$ -glucan in the peritoneal cavity as early as 1h post-treatment. Shortly after its peak,  $\beta$ -glucan<sup>+</sup> neutrophils gradually decline. Whether the reduction was due to cell death, aggregation or migration remains to be determined. Interestingly, we observed two waves of  $\beta$ -glucan<sup>+</sup> macrophages that peaked at 1h and 48h post-treatment. It is most

likely that the first wave of  $\beta$ -glucan<sup>+</sup> macrophages corresponded to LPMs because they are early sentinels of infection and reside in the peritoneal cavity. As neutrophils infiltrated the peritoneal cavity and drove inflammation, these LPMs rapidly disappeared due to MDR. The second wave of  $\beta$ -glucan<sup>+</sup> macrophages may be explained by the arrival of blood-derived monocytes into the peritoneal cavity, after which they subsequently differentiated into macrophages and continued to phagocytose  $\beta$ -glucan particulates. This observation was further supported by immunofluorescence microscopy analysis, where  $\beta$ -glucan was mainly engulfed by neutrophils in the early timepoints (4h), followed by macrophages in the later timepoints (72h). However, our approach for preparing peritoneal samples for imaging was not reliable as neutrophils are typically poorly adherent, have short lifespans and are particularly sensitive to manipulations *ex vivo*, which likely explains the variability in confluency between timepoints and renders them challenging to quantify. Therefore, immobilizing cells onto a slide by centrifugal forces, such as cytopsin, will improve cell preservation and reduce cell death of neutrophils and other cells (249).

As neutrophils age, they are recruited back into the BM for clearance. Previous studies have reported that sterile tissue-infiltrated neutrophils do not always die at the site of inflammation, but rather, can re-enter circulation and selectively return to the bone marrow to be recycled (250). Given the decline of neutrophils in the peritoneal cavity corresponded with an increase in the BM, we hypothesized that neutrophils are migrating back to the BM and may provide a mechanism for  $\beta$ -glucan to gain access to the BM and directly reprogram HSCs. In the BM, DTAF-stained  $\beta$ -glucan was used to identify cells that have internalized  $\beta$ -glucan, which has the caveat of not knowing the origin of these cells as we cannot exclude the potential that free  $\beta$ -glucan might also reach the BM via circulation and become engulfed by local phagocytes. Nevertheless, we failed to detect a strong signal in the BM in any cell type and each timepoint showed considerable variability

likely due to autofluorescence (**Fig. 10**). While the short-term and long-term reservoirs of  $\beta$ -glucan remain to be determined, a recent study characterized the early trafficking of particulate  $\beta$ -glucan after IP administration. Using DTAF-stained and radiolabelled whole  $\beta$ -glucan particles, Geller *et al.* demonstrated that  $\beta$ -glucan accumulated most prominently in the pancreas via dectin-1 signaling at day 3 following injection (251). Low levels of  $\beta$ -glucan were detected in the spleen, liver and intestinal system, and no signal was found in the blood, lung and bone. Taken together,  $\beta$ -glucan-IP does not appear to gain access into the BM as a free particle or via a cell intermediate. These results contradict a previous study that found that IP administration of soluble  $\beta$ -(1,3) (1,6)-glucan from maitake mushroom was detected in APCs in the spleen, peripheral blood and BM (252). Moreover, another group revealed that orally administered yeast- and barley-derived  $\beta$ -glucan were taken up and shuttled by gastrointestinal macrophages into the BM, where  $\beta$ -glucan was then degraded into smaller soluble fragments that activate marginated neutrophils via CR3 and enhance their anti-tumour activity (154). These discrepancies are most likely attributed to differences in the route of administration and the type of  $\beta$ -glucan used between these studies. Thus, further investigations are required to carefully delineate trafficking patterns of  $\beta$ -glucan and the mechanisms behind the immunomodulatory properties of  $\beta$ -glucan.

Numerous studies have demonstrated the importance of dectin-1 in antifungal immunity. Dectin-1 recognizes non-opsonized insoluble and soluble  $\beta$ -glucan and activates the Akt/mTOR/HIF-1 $\alpha$  pathway, which drives a metabolic shift towards aerobic glycolysis and ultimately induces epigenetic changes (45). Thus, dectin-1 signaling is considered as the basis of  $\beta$ -glucan-induced train immunity, at least in differentiated myeloid cells, namely monocytes and macrophages (45, 227). While most studies described the role of dectin-1 in the context of *peripheral* trained immunity (253), it is unclear whether dectin-1 signaling is essential for the

establishment of *central* trained immunity *in vivo* at the level of HSCs. Our data indicated that in the absence of dectin-1 signaling, HSC expansion still occurred with a bias towards myelopoiesis/granulopoiesis as MPP3, monocytes and neutrophil numbers were increased in the BM after  $\beta$ -glucan-IP treatment. Nevertheless, due to the technical limitations of this study, it is unknown whether this HSC expansion occurred with consequences on the epigenetic and metabolic status of the cells. If the induction of central trained immunity is dectin-1-independent, we expect to observe enhanced cytokine production by BMDMs derived from  $\beta$ -glucan-treated *Dectin-1*<sup>-/-</sup> mice in response to a secondary stimuli like LPS. A study by Stothers *et al.* also reported that linear  $\beta$ -glucan from *C. albicans* triggered metabolic alterations and a robust antimicrobial phenotype in macrophages, which afforded protection against intraperitoneal *P. aeruginosa* infection independent of dectin-1 (128). Further evidence indicated that intravenous administration of soluble  $\beta$ -glucan protected mice from systemic *S. aureus* infection in the absence of dectin-1 signaling (254). Taken together, our data supports the redundant role of dectin-1 in  $\beta$ -glucan trained immunity. In contrast, using a HSPC transplantation model, another study indicated that the production of trained macrophages by  $\beta$ -glucan (zymosan) *in vivo* involved direct dectin-1 ligation to activate HSPCs (89). However, this study did not rule out the contribution of alternative non-dectin-1 pathways in the training of HSPCs, considering that IFN- $\gamma$  and IL-1 $\beta$  has been shown to induce metabolic and epigenetic reprogramming, thereby generating trained immunity (3, 60, 255). Therefore, the role of dectin-1 in trained immunity is complicated by contradictory observations from previous studies and future studies are warranted to fully elucidate the specific mechanisms through which  $\beta$ -glucan acts on.

Consistent with previous studies (137), we showed that fewer neutrophils were recruited into the peritoneal cavity of *Dectin-1*<sup>-/-</sup> mice in response to  $\beta$ -glucan compared to WT mice, yet

HSC expansion still occurred, suggesting that neutrophils may not be the primary cellular driver of the  $\beta$ -glucan-induced HSC expansion. To test the contribution of neutrophils in generating trained immunity in the BM, we plan to deplete neutrophils globally with anti-Ly6G neutralizing antibody prior to  $\beta$ -glucan-IP and measure the functional and proliferative capacity of HSPCs and their downstream myeloid cells. Like WT mice, we found LPMs disappeared in the  $\beta$ -glucan-treated *Dectin-1*<sup>-/-</sup> mice. This drastic alteration of the peritoneal immune environment may represent a crucial event that must occur to trigger an HSC expansion in the BM. In the absence of LPMs, inflammatory monocytes colonize the vacant peritoneal niche and convert into mature

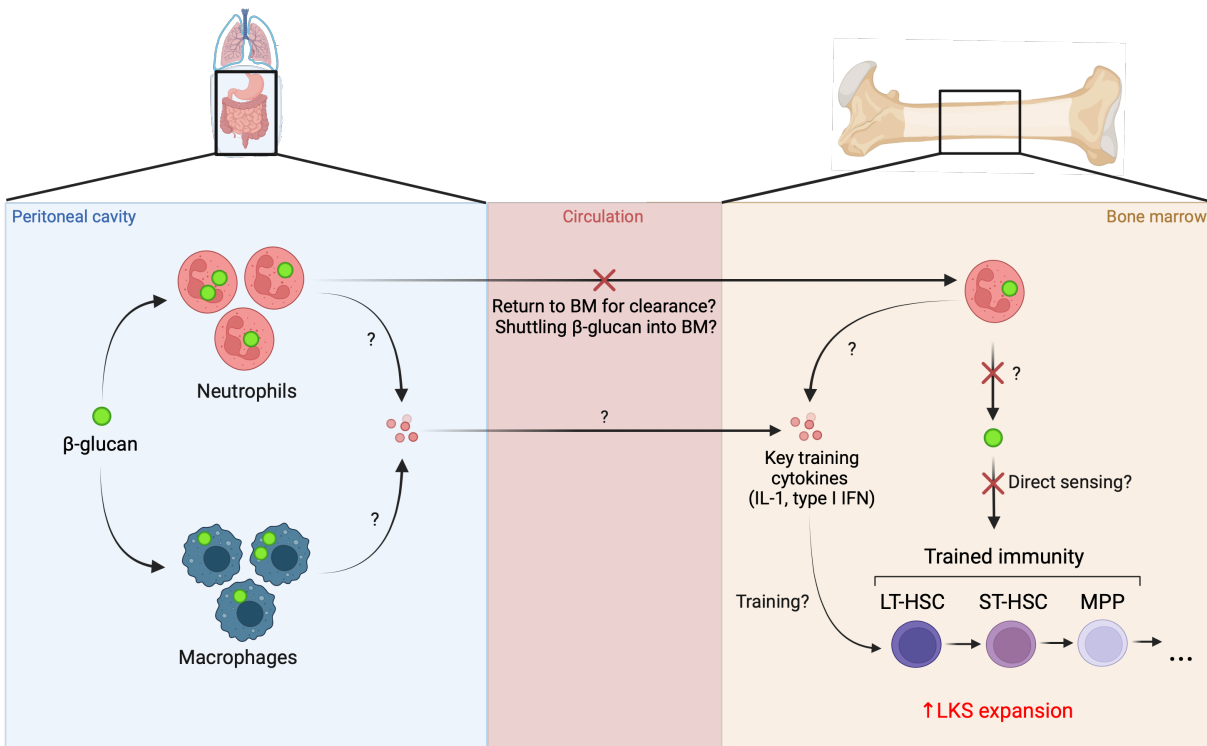


**Figure 11. Working model.** In response  $\beta$ -glucan-IP treatment, innate immune cells, notably neutrophils and monocytes, accumulate in the peritoneal cavity, while the adaptive immune cell populations remain mostly consistent and LPMs rapidly disappear. Neutrophils and mononuclear phagocytes are the earliest immune cells to detect and internalize  $\beta$ -glucan in the peritoneal cavity. In the BM,  $\beta$ -glucan treatment induces the expansion of HSCs and increases the neutrophil populations. Given that  $\beta$ -glucan was not detected in the BM after  $\beta$ -glucan-IP treatment, the direct access of  $\beta$ -glucan into the BM is not required for central trained immunity. Therefore, the induction of central trained immunity is likely mediated by key training cytokines, primarily IL-1 and type I IFN, secreted by other innate immune cells at the site of injection. Further studies are required to delineate the induction mechanism of central trained immunity.

inflammatory GATA6<sup>+</sup> macrophages with intrinsic and environment-dependent differences to LPMs (229). As consequence, the steady-state immune landscape of the peritoneal cavity before and after a primary stimulus is significantly different, and thus may produce distinct immune responses to a subsequent insult. Considering that one dose and two doses of  $\beta$ -glucan-IP promote different hematopoietic biases, notably granulopoiesis and monocytopoiesis, respectively, characterizing the peritoneal immune response will provide insight into the mechanisms of how  $\beta$ -glucan from the peritoneal cavity induces its distinct training effects in the BM.

## **Limitations**

Our study offers insight into the local and systemic immune response provoked by  $\beta$ -glucan-IP treatment and the possible mechanisms behind the induction of trained immunity in the BM. However, we also identify several limitations in our work:

- (1) Lack of complementary readouts for trained immunity.** Because we focused on an early timeframe to describe the peritoneal immune response after one dose of  $\beta$ -glucan treatment, it is difficult to determine whether the observed HSC expansion in the BM is a consequence of trained immunity or emergency granulopoiesis. The key difference between these two events is the long-term epigenetic and reprogramming of HSCs whose training signature is inherited by downstream progenitors and mature myeloid cells. To validate the induction of trained immunity, functional, transcriptional and epigenetic analyses must be done. Following a primary stimulus, we expect to observe (i) increased H3K4me3 and decreased H3K9me3 at the promoters of glycolytic, *TNFA*, *IL1B* and *IL6* genes in HSCs, (ii) upregulation of genes involved in glutaminolysis and

fatty acid synthesis in HSCs and BM-derived mature myeloid cells, and (iii) enhanced cytokine production (IL-6, IL-1 $\beta$  and TNF- $\alpha$ ) and function by trained mature myeloid cells after a secondary challenge.

(2) *Technical limitations of the  $\beta$ -glucan trafficking studies.* We utilized two techniques, flow cytometry and confocal microscopy, to assess the biodistribution of  $\beta$ -glucan in peritoneal and BM after IP injection. Our FACS data showed a low signal of DTAF- $\beta$ -glucan in the BM with significant variability, either due to autofluorescence or rare events. Our confocal microscopy data revealed few neutrophils and macrophages at 4h, which either accurately reflected the immune cell composition in the peritoneal cavity at that instant of time or highlighted the need for protocol optimization. Therefore, cell sorting prior and/or cytopsin will improve the sample preservation. Moreover, usage of live imaging systems using  $^{89}\text{Zr}$  radiolabelled or DTAF-stained  $\beta$ -glucan will address this limitation and elucidate the short-term and long-term distribution of particulate  $\beta$ -glucan after IP administration.

(3) *Unknown role of different immune cell types in trained immunity.* We did not directly test the contribution of neutrophils, monocytes/macrophages and DCs in the induction of trained immunity. Usage of conditional, rather than global, knockouts in these mature myeloid cells will address this question. Furthermore, proteome/secretome analysis (e.g. cytokines and growth factors) will provide valuable information about the cellular communication and state of peritoneal immune cells after  $\beta$ -glucan treatment, and identify cellular sources of key training cytokines, IL-1 $\beta$  and type I IFN.

## CHAPTER 5: CONCLUSION

In this study, we characterized the immune response of the peritoneal cavity, spleen and BM after  $\beta$ -glucan-IP treatment and explored the role of several cellular and molecular pathways in the induction of central trained immunity.  $\beta$ -Glucan significantly altered the peritoneal immune landscape by rapidly decreasing the resident LPM population and B1 cells while recruiting neutrophils, DCs, monocytes and SPMs. Furthermore, we showed that  $\beta$ -glucan treatment expanded the HSC population in the BM and spleen in dectin-1-independent manner. We proposed several mechanisms through which  $\beta$ -glucan in the peritoneal cavity may be exerting its effects on HSCs in the BM, one of which involved  $\beta$ -glucan gaining access into the BM to directly interact with HSCs. However, we failed to detect  $\beta$ -glucan in the BM as a free particle or via a cell intermediate, suggesting that the induction of central trained immunity is likely driven by soluble factors. While key training cytokines (e.g. IL-1 $\beta$  and type I IFN) have been identified, their cellular sources are still unknown, and thus requires further investigation. This study highlights the unique and dynamic immune response of the peritoneal cavity, which is largely forgotten, and demonstrates the various systemic immunomodulatory effects of  $\beta$ -glucan.  $\beta$ -Glucan is a potent adjuvant in infections and anti-cancer treatments because of its capacity to induce trained immunity. Therefore, delineating the cellular and molecular mechanisms of  $\beta$ -glucan-induced trained immunity will provide insight into harnessing the power of the innate immune system for clinical applications.

## REFERENCES

1. M. Divangahi *et al.*, Trained immunity, tolerance, priming and differentiation: distinct immunological processes. *Nature Immunology* **22**, 2-6 (2021).
2. M. G. Netea *et al.*, Defining trained immunity and its role in health and disease. *Nature Reviews Immunology* **20**, 375-388 (2020).
3. M. Sadeghi, M. Divangahi, Discovering adaptive features of innate immune memory. *Immunological Reviews* **323**, 186-196 (2024).
4. M. G. Netea *et al.*, Trained immunity: A program of innate immune memory in health and disease. *Science* **352**, aaf1098 (2016).
5. U. Conrath, Systemic acquired resistance. *Plant Signal Behav* **1**, 179-184 (2006).
6. A. Kachroo, P. Kachroo, Mobile signals in systemic acquired resistance. *Current Opinion in Plant Biology* **58**, 41-47 (2020).
7. H. Yakura, Cognitive and Memory Functions in Plant Immunity. *Vaccines (Basel)* **8**, (2020).
8. J. B. Morel, J. L. Dangl, The hypersensitive response and the induction of cell death in plants. *Cell Death Differ* **4**, 671-683 (1997).
9. Y. Zhang *et al.*, Control of salicylic acid synthesis and systemic acquired resistance by two members of a plant-specific family of transcription factors. *Proc Natl Acad Sci U S A* **107**, 18220-18225 (2010).
10. M. Jaskiewicz, U. Conrath, C. Peterhansel, Chromatin modification acts as a memory for systemic acquired resistance in the plant stress response. *EMBO reports* **12**, 50-55-55 (2011).
11. A. F. Ross, Systemic acquired resistance induced by localized virus infections in plants. *Virology* **14**, 340-358 (1961).
12. S. Gianinazzi, B. Kassanis, Virus Resistance Induced in Plants by Polyacrylic Acid. *Journal of General Virology* **23**, 1-9 (1974).
13. L. Friedrich *et al.*, A benzothiadiazole derivative induces systemic acquired resistance in tobacco. *The Plant Journal* **10**, 61-70 (1996).
14. Mihai G. Netea, J. Quintin, Jos W. M. van der Meer, Trained Immunity: A Memory for Innate Host Defense. *Cell Host & Microbe* **9**, 355-361 (2011).
15. M. Auguste *et al.*, Methodological Approaches To Assess Innate Immunity and Innate Memory in Marine Invertebrates and Humans. *Front Toxicol* **4**, 842469 (2022).
16. T. H. Ng, M. C. Harrison, J. P. Scharsack, J. Kurtz, Disentangling specific and unspecific components of innate immune memory in a copepod-tapeworm system. *Front Immunol* **15**, 1307477 (2024).
17. L. N. Pham, M. S. Dionne, M. Shirasu-Hiza, D. S. Schneider, A Specific Primed Immune Response in Drosophila Is Dependent on Phagocytes. *PLOS Pathogens* **3**, e26 (2007).
18. M. Lafont *et al.*, A Sustained Immune Response Supports Long-Term Antiviral Immune Priming in the Pacific Oyster, *Crassostrea gigas*. *mBio* **11**, 10.1128/mbio.02777-02719 (2020).
19. M. Zhao *et al.*, The mechanisms and factors that induce trained immunity in arthropods and mollusks. *Front Immunol* **14**, 1241934 (2023).

20. K. A. Tran *et al.*, BCG immunization induces CX3CR1hi effector memory T cells to provide cross-protection via IFN- $\gamma$ -mediated trained immunity. *Nature Immunology* **25**, 418-431 (2024).
21. P. Mangtani *et al.*, Protection by BCG vaccine against tuberculosis: a systematic review of randomized controlled trials. *Clin Infect Dis* **58**, 470-480 (2014).
22. G. A. Colditz *et al.*, Efficacy of BCG vaccine in the prevention of tuberculosis. Meta-analysis of the published literature. *Jama* **271**, 698-702 (1994).
23. M. L. Garly *et al.*, BCG scar and positive tuberculin reaction associated with reduced child mortality in West Africa. A non-specific beneficial effect of BCG? *Vaccine* **21**, 2782-2790 (2003).
24. I. Kristensen, P. Aaby, H. Jensen, Routine vaccinations and child survival: follow up study in Guinea-Bissau, West Africa. *Bmj* **321**, 1435-1438 (2000).
25. S. Prentice *et al.*, BCG-induced non-specific effects on heterologous infectious disease in Ugandan neonates: an investigator-blind randomised controlled trial. *The Lancet Infectious Diseases* **21**, 993-1003 (2021).
26. K. J. Jensen *et al.*, Seasonal variation in the non-specific effects of BCG vaccination on neonatal mortality: three randomised controlled trials in Guinea-Bissau. *BMJ Global Health* **5**, e001873 (2020).
27. L. G. Stensballe *et al.*, Acute lower respiratory tract infections and respiratory syncytial virus in infants in Guinea-Bissau: a beneficial effect of BCG vaccination for girls community based case-control study. *Vaccine* **23**, 1251-1257 (2005).
28. A. Bagshawe *et al.*, BCG vaccination in leprosy: final results of the trial in Karimui, Papua New Guinea, 1963-79. *Bull World Health Organ* **67**, 389-399 (1989).
29. N. T. Usher *et al.*, Association of BCG Vaccination in Childhood With Subsequent Cancer Diagnoses: A 60-Year Follow-up of a Clinical Trial. *JAMA Network Open* **2**, e1912014-e1912014 (2019).
30. A. Morales, D. Eidinger, A. W. Bruce, Intracavitary Bacillus Calmette-guerin in the Treatment of Superficial Bladder Tumors. *The Journal of Urology* **116**, 180-182 (1976).
31. F. Vaziri *et al.*, BCG as an Innovative Option for HCC Treatment: Repurposing and Mechanistic Insights. *Advanced Science* **11**, 2308242 (2024).
32. F. Cardillo *et al.*, Bacillus Calmette-Guérin Immunotherapy for Cancer. *Vaccines (Basel)* **9**, (2021).
33. J. C. Spencer, R. Ganguly, R. H. Waldman, Nonspecific protection of mice against influenza virus infection by local or systemic immunization with Bacille Calmette-Guérin. *J Infect Dis* **136**, 171-175 (1977).
34. I. A. Clark, A. C. Allison, F. E. Cox, Protection of mice against Babesia and Plasmodium with BCG. *Nature* **259**, 309-311 (1976).
35. R. H. Civil, K. S. Warren, A. A. F. Mahmoud, Conditions for Bacille Calmette-Guérin-Induced Resistance to Infection with Schistosoma mansoni in Mice. *The Journal of Infectious Diseases* **137**, 550-555 (1978).
36. J. Kleinnijenhuis *et al.*, BCG-induced trained immunity in NK cells: Role for non-specific protection to infection. *Clinical Immunology* **155**, 213-219 (2014).
37. L. C. J. de Bree *et al.*, Non-specific effects of vaccines: Current evidence and potential implications. *Seminars in Immunology* **39**, 35-43 (2018).

38. L. Rizzetto *et al.*, Fungal Chitin Induces Trained Immunity in Human Monocytes during Cross-talk of the Host with *Saccharomyces cerevisiae*. *J Biol Chem* **291**, 7961-7972 (2016).
39. S. Moorlag *et al.*,  $\beta$ -Glucan Induces Protective Trained Immunity against *Mycobacterium tuberculosis* Infection: A Key Role for IL-1. *Cell Rep* **31**, 107634 (2020).
40. M. A. Ataide *et al.*, Malaria-induced NLRP12/NLRP3-dependent caspase-1 activation mediates inflammation and hypersensitivity to bacterial superinfection. *PLoS Pathog* **10**, e1003885 (2014).
41. E. Jentho *et al.*, Trained innate immunity, long-lasting epigenetic modulation, and skewed myelopoiesis by heme. *Proc Natl Acad Sci U S A* **118**, (2021).
42. A. L. Seufert *et al.*, Enriched dietary saturated fatty acids induce trained immunity via ceramide production that enhances severity of endotoxemia and clearance of infection. *eLife* **11**, e76744 (2022).
43. N. P. Riksen, M. G. Netea, Immunometabolic control of trained immunity. *Mol Aspects Med* **77**, 100897 (2021).
44. R. J. Arts *et al.*, Glutaminolysis and Fumarate Accumulation Integrate Immunometabolic and Epigenetic Programs in Trained Immunity. *Cell Metab* **24**, 807-819 (2016).
45. S.-C. Cheng *et al.*, mTOR- and HIF-1 $\alpha$ -mediated aerobic glycolysis as metabolic basis for trained immunity. *Science* **345**, 1250684 (2014).
46. J. C. Xu *et al.*, Multi-omics analysis reveals that linoleic acid metabolism is associated with variations of trained immunity induced by distinct BCG strains. *Sci Adv* **10**, eadk8093 (2024).
47. A. V. Ferreira, J. Domínguez-Andrés, M. G. Netea, The Role of Cell Metabolism in Innate Immune Memory. *J Innate Immun* **14**, 42-50 (2022).
48. R. J. W. Arts *et al.*, Immunometabolic Pathways in BCG-Induced Trained Immunity. *Cell Rep* **17**, 2562-2571 (2016).
49. S. Fanucchi, J. Domínguez-Andrés, L. A. B. Joosten, M. G. Netea, M. M. Mhlanga, The Intersection of Epigenetics and Metabolism in Trained Immunity. *Immunity* **54**, 32-43 (2021).
50. P. Garcia-Valtanen, R. M. Guzman-Genuino, D. L. Williams, J. D. Hayball, K. R. Diener, Evaluation of trained immunity by  $\beta$ -1, 3 (d)-glucan on murine monocytes in vitro and duration of response in vivo. *Immunol Cell Biol* **95**, 601-610 (2017).
51. O. A. Acevedo, R. V. Berrios, L. Rodríguez-Guilarte, B. Lillo-Dapremont, A. M. Kalergis, Molecular and Cellular Mechanisms Modulating Trained Immunity by Various Cell Types in Response to Pathogen Encounter. *Front Immunol* **12**, 745332 (2021).
52. S. Moorlag *et al.*, BCG Vaccination Induces Long-Term Functional Reprogramming of Human Neutrophils. *Cell Rep* **33**, 108387 (2020).
53. L. Kalafati *et al.*, Innate Immune Training of Granulopoiesis Promotes Anti-tumor Activity. *Cell* **183**, 771-785.e712 (2020).
54. C. R. Hole *et al.*, Induction of memory-like dendritic cell responses in vivo. *Nature Communications* **10**, 2955 (2019).
55. J. C. Sun, J. N. Beilke, L. L. Lanier, Adaptive immune features of natural killer cells. *Nature* **457**, 557-561 (2009).

56. N. Khan *et al.*, M. tuberculosis Reprograms Hematopoietic Stem Cells to Limit Myelopoiesis and Impair Trained Immunity. *Cell* **183**, 752-770.e722 (2020).
57. A. A. Patel, F. Ginhoux, S. Yona, Monocytes, macrophages, dendritic cells and neutrophils: an update on lifespan kinetics in health and disease. *Immunology* **163**, 250-261 (2021).
58. A. P. Ng, W. S. Alexander, Haematopoietic stem cells: past, present and future. *Cell Death Discovery* **3**, 17002 (2017).
59. E. Kaufmann *et al.*, BCG Educates Hematopoietic Stem Cells to Generate Protective Innate Immunity against Tuberculosis. *Cell* **172**, 176-190.e119 (2018).
60. I. Mitroulis *et al.*, Modulation of Myelopoiesis Progenitors Is an Integral Component of Trained Immunity. *Cell* **172**, 147-161.e112 (2018).
61. A. Wilson, A. Trumpp, Bone-marrow haematopoietic-stem-cell niches. *Nature Reviews Immunology* **6**, 93-106 (2006).
62. E. Laurenti, B. Göttgens, From haematopoietic stem cells to complex differentiation landscapes. *Nature* **553**, 418-426 (2018).
63. M. Barile *et al.*, Hematopoietic stem cells self-renew symmetrically or gradually proceed to differentiation. *bioRxiv*, 2020.2008.2006.239186 (2020).
64. T. Hasan *et al.*, Homing and Engraftment of Hematopoietic Stem Cells Following Transplantation: A Pre-Clinical Perspective. *Curr Oncol* **31**, 603-616 (2024).
65. R. Thambyrajah *et al.*, I $\kappa$ B $\alpha$  controls dormancy in hematopoietic stem cells via retinoic acid during embryonic development. *Nature Communications* **15**, 4673 (2024).
66. E. M. Pietras *et al.*, Functionally Distinct Subsets of Lineage-Biased Multipotent Progenitors Control Blood Production in Normal and Regenerative Conditions. *Cell Stem Cell* **17**, 35-46 (2015).
67. P. Eliasson *et al.*, Hypoxia mediates low cell-cycle activity and increases the proportion of long-term-reconstituting hematopoietic stem cells during in vitro culture. *Experimental Hematology* **38**, 301-310.e302 (2010).
68. A. Mendelson, P. S. Frenette, Hematopoietic stem cell niche maintenance during homeostasis and regeneration. *Nat Med* **20**, 833-846 (2014).
69. T. Sugiyama, H. Kohara, M. Noda, T. Nagasawa, Maintenance of the hematopoietic stem cell pool by CXCL12-CXCR4 chemokine signaling in bone marrow stromal cell niches. *Immunity* **25**, 977-988 (2006).
70. A. N. Seyfried, J. M. Maloney, K. C. MacNamara, Macrophages Orchestrate Hematopoietic Programs and Regulate HSC Function During Inflammatory Stress. *Front Immunol* **11**, 1499 (2020).
71. P. Zhang *et al.*, The physical microenvironment of hematopoietic stem cells and its emerging roles in engineering applications. *Stem Cell Research & Therapy* **10**, 327 (2019).
72. Y. Peng *et al.*, Innate and adaptive immune response to apoptotic cells. *J Autoimmun* **29**, 303-309 (2007).
73. A. Grover *et al.*, Erythropoietin guides multipotent hematopoietic progenitor cells toward an erythroid fate. *J Exp Med* **211**, 181-188 (2014).

74. M. R. Clark, M. Mandal, K. Ochiai, H. Singh, Orchestrating B cell lymphopoiesis through interplay of IL-7 receptor and pre-B cell receptor signalling. *Nature Reviews Immunology* **14**, 69-80 (2014).
75. J. C. Pui *et al.*, Notch1 Expression in Early Lymphopoiesis Influences B versus T Lineage Determination. *Immunity* **11**, 299-308 (1999).
76. Y. Fan, D. Lu, The Ikaros family of zinc-finger proteins. *Acta Pharm Sin B* **6**, 513-521 (2016).
77. A. G. Rosmarin, Z. Yang, K. K. Resendes, Transcriptional regulation in myelopoiesis: Hematopoietic fate choice, myeloid differentiation, and leukemogenesis. *Experimental Hematology* **33**, 131-143 (2005).
78. J. A. Hamilton, A. Achuthan, Colony stimulating factors and myeloid cell biology in health and disease. *Trends in Immunology* **34**, 81-89 (2013).
79. J. Mestas, C. C. Hughes, Of mice and not men: differences between mouse and human immunology. *J Immunol* **172**, 2731-2738 (2004).
80. S. M. Rankin, The bone marrow: a site of neutrophil clearance. *J Leukoc Biol* **88**, 241-251 (2010).
81. N. Strydom, S. M. Rankin, Regulation of circulating neutrophil numbers under homeostasis and in disease. *J Innate Immun* **5**, 304-314 (2013).
82. K. J. Eash, A. M. Greenbaum, P. K. Gopalan, D. C. Link, CXCR2 and CXCR4 antagonistically regulate neutrophil trafficking from murine bone marrow. *J Clin Invest* **120**, 2423-2431 (2010).
83. R. C. Furze, S. M. Rankin, Neutrophil mobilization and clearance in the bone marrow. *Immunology* **125**, 281-288 (2008).
84. M. A. Stark *et al.*, Phagocytosis of apoptotic neutrophils regulates granulopoiesis via IL-23 and IL-17. *Immunity* **22**, 285-294 (2005).
85. B. Malengier-Devlies, M. Metzemaekers, C. Wouters, P. Proost, P. Matthys, Neutrophil Homeostasis and Emergency Granulopoiesis: The Example of Systemic Juvenile Idiopathic Arthritis. *Frontiers in Immunology* **12**, (2021).
86. J. L. Schultze, E. Mass, A. Schlitzer, Emerging Principles in Myelopoiesis at Homeostasis and during Infection and Inflammation. *Immunity* **50**, 288-301 (2019).
87. Y. Nagai *et al.*, Toll-like receptors on hematopoietic progenitor cells stimulate innate immune system replenishment. *Immunity* **24**, 801-812 (2006).
88. J. Megías *et al.*, Direct Toll-Like Receptor-Mediated Stimulation of Hematopoietic Stem and Progenitor Cells Occurs In Vivo and Promotes Differentiation Toward Macrophages. *Stem Cells* **30**, 1486-1495 (2012).
89. C. Bono *et al.*, Dectin-1 Stimulation of Hematopoietic Stem and Progenitor Cells Occurs In Vivo and Promotes Differentiation Toward Trained Macrophages via an Indirect Cell-Autonomous Mechanism. *mBio* **11**, (2020).
90. A. Yáñez, J. Megías, J.-E. O'Connor, D. Gozalbo, M. L. Gil, Candida albicans Induces Selective Development of Macrophages and Monocyte Derived Dendritic Cells by a TLR2 Dependent Signalling. *PLOS ONE* **6**, e24761 (2011).
91. M. F. Pascutti, M. N. Erkelens, M. A. Nolte, Impact of Viral Infections on Hematopoiesis: From Beneficial to Detrimental Effects on Bone Marrow Output. *Front Immunol* **7**, 364 (2016).

92. J. P. Maciejewski *et al.*, Infection of Hematopoietic Progenitor Cells by Human Cytomegalovirus. *Blood* **80**, 170-178 (1992).
93. A. Yáñez, H. S. Goodridge, D. Gozalbo, M. L. Gil, TLRs control hematopoiesis during infection. *Eur J Immunol* **43**, 2526-2533 (2013).
94. K. Maeda *et al.*, Interleukin-6 aborts lymphopoiesis and elevates production of myeloid cells in systemic lupus erythematosus-prone B6.Sle1.Yaa animals. *Blood* **113**, 4534-4540 (2009).
95. K. Maeda *et al.*, IL-6 blocks a discrete early step in lymphopoiesis. *Blood* **106**, 879-885 (2005).
96. E. M. Pietras *et al.*, Chronic interleukin-1 exposure drives haematopoietic stem cells towards precocious myeloid differentiation at the expense of self-renewal. *Nat Cell Biol* **18**, 607-618 (2016).
97. C. A. Mitchell *et al.*, Stromal niche inflammation mediated by IL-1 signalling is a targetable driver of haematopoietic ageing. *Nature Cell Biology* **25**, 30-41 (2023).
98. M. T. Baldrige, K. Y. King, N. C. Boles, D. C. Weksberg, M. A. Goodell, Quiescent haematopoietic stem cells are activated by IFN-gamma in response to chronic infection. *Nature* **465**, 793-797 (2010).
99. M. A. G. Essers *et al.*, IFN $\alpha$  activates dormant haematopoietic stem cells in vivo. *Nature* **458**, 904-908 (2009).
100. R. Bogeska *et al.*, Inflammatory exposure drives long-lived impairment of hematopoietic stem cell self-renewal activity and accelerated aging. *Cell Stem Cell* **29**, 1273-1284.e1278 (2022).
101. J. L. Zhao, D. Baltimore, Regulation of stress-induced hematopoiesis. *Curr Opin Hematol* **22**, 286-292 (2015).
102. K. A. Matatall *et al.*, Chronic Infection Depletes Hematopoietic Stem Cells through Stress-Induced Terminal Differentiation. *Cell Rep* **17**, 2584-2595 (2016).
103. S. Saluja, I. Bansal, R. Bhardwaj, M. S. Beg, J. K. Palanichamy, Inflammation as a driver of hematological malignancies. *Front Oncol* **14**, 1347402 (2024).
104. A. Burberry *et al.*, Infection mobilizes hematopoietic stem cells through cooperative NOD-like receptor and Toll-like receptor signaling. *Cell Host Microbe* **15**, 779-791 (2014).
105. D. Cenariu *et al.*, Extramedullary Hematopoiesis of the Liver and Spleen. *J Clin Med* **10**, (2021).
106. D. A. G. Barisas, K. Choi, Extramedullary hematopoiesis in cancer. *Experimental & Molecular Medicine* **56**, 549-558 (2024).
107. I. G. Winkler *et al.*, Hematopoietic stem cell mobilizing agents G-CSF, cyclophosphamide or AMD3100 have distinct mechanisms of action on bone marrow HSC niches and bone formation. *Leukemia* **26**, 1594-1601 (2012).
108. C. Wu *et al.*, Spleen mediates a distinct hematopoietic progenitor response supporting tumor-promoting myelopoiesis. *J Clin Invest* **128**, 3425-3438 (2018).
109. C. S. Robbins *et al.*, Extramedullary Hematopoiesis Generates Ly-6Chigh Monocytes That Infiltrate Atherosclerotic Lesions. *Circulation* **125**, 364-374 (2012).
110. B. Han, K. Baruah, E. Cox, D. Vanrompay, P. Bossier, Structure-Functional Activity Relationship of  $\beta$ -Glucans From the Perspective of Immunomodulation: A Mini-Review. *Frontiers in Immunology* **11**, (2020).

111. X. Zhong *et al.*, Immunomodulatory Effect and Biological Significance of  $\beta$ -Glucans. *Pharmaceutics* **15**, (2023).
112. M. Yuan, G. Fu, Y. Sun, D. Zhang, Biosynthesis and applications of curdlan. *Carbohydrate Polymers* **273**, 118597 (2021).
113. C. Caseiro, J. N. R. Dias, C. M. G. de Andrade Fontes, P. Bule, From Cancer Therapy to Winemaking: The Molecular Structure and Applications of  $\beta$ -Glucans and  $\beta$ -1, 3-Glucanases. *Int J Mol Sci* **23**, (2022).
114. R. P. Singh, A. Bhardwaj,  $\beta$ -glucans: a potential source for maintaining gut microbiota and the immune system. *Front Nutr* **10**, 1143682 (2023).
115. S. Nogami, Y. Ohya, in *Chemistry, Biochemistry, and Biology of 1-3 Beta Glucans and Related Polysaccharides*, A. Bacic, G. B. Fincher, B. A. Stone, Eds. (Academic Press, San Diego, 2009), pp. 259-282.
116. K. H. Lee *et al.*, Recent progress of research on medicinal mushrooms, foods, and other herbal products used in traditional Chinese medicine. *J Tradit Complement Med* **2**, 84-95 (2012).
117. G. C.-F. Chan, W. K. Chan, D. M.-Y. Sze, The effects of  $\beta$ -glucan on human immune and cancer cells. *Journal of Hematology & Oncology* **2**, 25 (2009).
118. G. Chihara, Y. Maeda, J. Hamuro, T. Sasaki, F. Fukuoka, Inhibition of mouse sarcoma 180 by polysaccharides from *Lentinus edodes* (Berk.) sing. *Nature* **222**, 687-688 (1969).
119. I. Nakao *et al.*, [Clinical evaluation of schizophyllan (SPG) in advanced gastric cancer--a randomized comparative study by an envelope method]. *Gan To Kagaku Ryoho* **10**, 1146-1159 (1983).
120. I. Sivanesan, M. Muthu, J. Gopal, J. W. Oh, Mushroom Polysaccharide-Assisted Anticarcinogenic Mycotherapy: Reviewing Its Clinical Trials. *Molecules* **27**, (2022).
121. E. J. Murphy, E. Rezoagli, I. Major, N. J. Rowan, J. G. Laffey,  $\beta$ -Glucan Metabolic and Immunomodulatory Properties and Potential for Clinical Application. *Journal of Fungi* **6**, 356 (2020).
122. N. H. Segal *et al.*, A Phase II Efficacy and Safety, Open-Label, Multicenter Study of Imprime PGG Injection in Combination With Cetuximab in Patients With Stage IV KRAS-Mutant Colorectal Cancer. *Clin Colorectal Cancer* **15**, 222-227 (2016).
123. A. S. H. Chan *et al.*, Imprime PGG Enhances Anti-Tumor Effects of Tumor-Targeting, Anti-Angiogenic, and Immune Checkpoint Inhibitor Antibodies. *Front Oncol* **12**, 869078 (2022).
124. K. Shimizu *et al.*, Efficacy of oral administered superfine dispersed lentinan for advanced pancreatic cancer. *Hepatogastroenterology* **56**, 240-244 (2009).
125. W. Engel-Riedel *et al.*, A randomized, controlled trial evaluating the efficacy and safety of BTH1677 in combination with bevacizumab, carboplatin, and paclitaxel in first-line treatment of advanced non-small cell lung cancer. *J Immunother Cancer* **6**, 16 (2018).
126. Y. Maehara *et al.*, Biological mechanism and clinical effect of protein-bound polysaccharide K (KRESTIN<sup>®</sup>): review of development and future perspectives. *Surg Today* **42**, 8-28 (2012).
127. Y. Zhang *et al.*, Lentinan as an immunotherapeutic for treating lung cancer: a review of 12 years clinical studies in China. *Journal of Cancer Research and Clinical Oncology* **144**, 2177-2186 (2018).

128. C. L. Stothers *et al.*,  $\beta$ -Glucan Induces Distinct and Protective Innate Immune Memory in Differentiated Macrophages. *J Immunol* **207**, 2785-2798 (2021).
129. N. R. Di Luzio, D. L. Williams, Protective effect of glucan against systemic *Staphylococcus aureus* septicemia in normal and leukemic mice. *Infect Immun* **20**, 804-810 (1978).
130. N. Khan *et al.*,  $\beta$ -Glucan Reprograms Neutrophils to Induce Disease Tolerance Against Influenza A Virus. *Nature Immunology [Under Revision]*, (2024).
131. J. Wang *et al.*, Yeast  $\beta$ -glucan promotes antiviral type I interferon response via dectin-1. *Veterinary Microbiology* **295**, 110107 (2024).
132. H. Mao *et al.*, The effect of  $\beta$ -Glucan induced intestinal trained immunity against *Trichinella spiralis* infection. *Veterinary Parasitology*, 110238 (2024).
133. Z. Wu *et al.*,  $\beta$ -Glucans in particulate and solubilized forms elicit varied immunomodulatory and apoptosis effects in teleost macrophages in a dosedependent manner. *Frontiers in Immunology* **14**, (2023).
134. Y. Zhang *et al.*, The phagocytic receptors of  $\beta$ -glucan. *International Journal of Biological Macromolecules* **205**, 430-441 (2022).
135. H. S. Goodridge, A. J. Wolf, D. M. Underhill, Beta-glucan recognition by the innate immune system. *Immunol Rev* **230**, 38-50 (2009).
136. P. R. Taylor *et al.*, The beta-glucan receptor, dectin-1, is predominantly expressed on the surface of cells of the monocyte/macrophage and neutrophil lineages. *J Immunol* **169**, 3876-3882 (2002).
137. P. R. Taylor *et al.*, Dectin-1 is required for beta-glucan recognition and control of fungal infection. *Nat Immunol* **8**, 31-38 (2007).
138. J. Vera *et al.*, The CD5 ectodomain interacts with conserved fungal cell wall components and protects from zymosan-induced septic shock-like syndrome. *Proc Natl Acad Sci U S A* **106**, 1506-1511 (2009).
139. S. Chatterjee, A. Balram, W. Li, Convergence: Lactosylceramide-Centric Signaling Pathways Induce Inflammation, Oxidative Stress, and Other Phenotypic Outcomes. *Int J Mol Sci* **22**, (2021).
140. V. Jimenez-Lucho, V. Ginsburg, H. C. Krivan, *Cryptococcus neoformans*, *Candida albicans*, and other fungi bind specifically to the glycosphingolipid lactosylceramide (Gal beta 1-4Glc beta 1-1Cer), a possible adhesion receptor for yeasts. *Infect Immun* **58**, 2085-2090 (1990).
141. J. W. Zimmerman *et al.*, A novel carbohydrate-glycosphingolipid interaction between a beta-(1-3)-glucan immunomodulator, PGG-glucan, and lactosylceramide of human leukocytes. *J Biol Chem* **273**, 22014-22020 (1998).
142. H. S. Goodridge *et al.*, Activation of the innate immune receptor Dectin-1 upon formation of a 'phagocytic synapse'. *Nature* **472**, 471-475 (2011).
143. S. LeibundGut-Landmann *et al.*, Syk- and CARD9-dependent coupling of innate immunity to the induction of T helper cells that produce interleukin 17. *Nature Immunology* **8**, 630-638 (2007).
144. M. J. Elder *et al.*,  $\beta$ -Glucan Size Controls Dectin-1-Mediated Immune Responses in Human Dendritic Cells by Regulating IL-1 $\beta$  Production. *Front Immunol* **8**, 791 (2017).

145. S. I. Gringhuis *et al.*, Dectin-1 directs T helper cell differentiation by controlling noncanonical NF-kappaB activation through Raf-1 and Syk. *Nat Immunol* **10**, 203-213 (2009).
146. S. Suram *et al.*, Regulation of cytosolic phospholipase A2 activation and cyclooxygenase 2 expression in macrophages by the  $\beta$ -glucan receptor. *Journal of Biological Chemistry* **281**, 5506-5514 (2006).
147. B. N. Gantner, R. M. Simmons, S. J. Canavera, S. Akira, D. M. Underhill, Collaborative induction of inflammatory responses by dectin-1 and Toll-like receptor 2. *J Exp Med* **197**, 1107-1117 (2003).
148. M. Liu *et al.*, Dectin-1 Activation by a Natural Product  $\beta$ -Glucan Converts Immunosuppressive Macrophages into an M1-like Phenotype. *J Immunol* **195**, 5055-5065 (2015).
149. P. Hernanz-Falc3n, O. Joffre, D. L. Williams, C. Reis e Sousa, Internalization of Dectin-1 terminates induction of inflammatory responses. *Eur J Immunol* **39**, 507-513 (2009).
150. X. M. O'Brien *et al.*, Lectin site ligation of CR3 induces conformational changes and signaling. *J Biol Chem* **287**, 3337-3348 (2012).
151. B. Li *et al.*, Yeast beta-glucan amplifies phagocyte killing of iC3b-opsonized tumor cells via complement receptor 3-Syk-phosphatidylinositol 3-kinase pathway. *J Immunol* **177**, 1661-1669 (2006).
152. L. Di Renzo, E. Yefenof, E. Klein, The function of human NK cells is enhanced by beta-glucan, a ligand of CR3 (CD11b/CD18). *Eur J Immunol* **21**, 1755-1758 (1991).
153. V. Vetvicka, B. P. Thornton, G. D. Ross, Soluble beta-glucan polysaccharide binding to the lectin site of neutrophil or natural killer cell complement receptor type 3 (CD11b/CD18) generates a primed state of the receptor capable of mediating cytotoxicity of iC3b-opsonized target cells. *The Journal of Clinical Investigation* **98**, 50-61 (1996).
154. F. Hong *et al.*, Mechanism by which orally administered beta-1,3-glucans enhance the tumoricidal activity of antitumor monoclonal antibodies in murine tumor models. *J Immunol* **173**, 797-806 (2004).
155. S. Saeed *et al.*, Epigenetic programming of monocyte-to-macrophage differentiation and trained innate immunity. *Science (New York, N.Y.)* **345**, 1251086-1251086 (2014).
156. R. Monahan-Earley, A. M. Dvorak, W. C. Aird, Evolutionary origins of the blood vascular system and endothelium. *J Thromb Haemost* **11 Suppl 1**, 46-66 (2013).
157. L. Salm, R. Shim, N. Noskovicova, P. Kubes, Gata6+ large peritoneal macrophages: an evolutionarily conserved sentinel and effector system for infection and injury. *Trends in Immunology* **44**, 129-145 (2023).
158. A. Pinsino, M. C. Thorndyke, V. Matranga, Coelomocytes and post-traumatic response in the common sea star *Asterias rubens*. *Cell Stress Chaperones* **12**, 331-341 (2007).
159. S. N. Zwicky, D. Stroka, J. Zindel, Sterile Injury Repair and Adhesion Formation at Serosal Surfaces. *Front Immunol* **12**, 684967 (2021).
160. C. Chatzigrigoriadis, A. Goulioumis, D. Sperdouli, K. Gyftopoulos, Embryological, anatomical and clinical considerations on pleuroperitoneal communication. *Pleura Peritoneum* **8**, 101-111 (2023).

161. W. Solass *et al.*, Functional vascular anatomy of the peritoneum in health and disease. *Pleura Peritoneum* **1**, 145-158 (2016).
162. A. Al Shoyaib, S. R. Archie, V. T. Karamyan, Intraperitoneal Route of Drug Administration: Should it Be Used in Experimental Animal Studies? *Pharm Res* **37**, 12 (2019).
163. R. A. Mactier, R. Khanna, Absorption of fluid and solutes from the peritoneal cavity. Theoretic and therapeutic implications and applications. *ASAIO Trans* **35**, 122-131 (1989).
164. E. Levai *et al.*, Human peritoneal tight junction, transporter and channel expression in health and kidney failure, and associated solute transport. *Scientific Reports* **13**, 17429 (2023).
165. G. Lukas, S. D. Brindle, P. Greengard, The route of absorption of intraperitoneally administered compounds. *J Pharmacol Exp Ther* **178**, 562-564 (1971).
166. M. F. Flessner, The importance of the interstitium in peritoneal transport. *Perit Dial Int* **16 Suppl 1**, S76-79 (1996).
167. D. Cortés-Guiral *et al.*, Primary and metastatic peritoneal surface malignancies. *Nature Reviews Disease Primers* **7**, 91 (2021).
168. M. F. Abu-Hijleh, O. A. Habbal, S. T. Moqattash, The role of the diaphragm in lymphatic absorption from the peritoneal cavity. *J Anat* **186 ( Pt 3)**, 453-467 (1995).
169. J. Li, Z. Zhao, J. Zhou, S. Yu, A study of the three-dimensional organization of the human diaphragmatic lymphatic lacunae and lymphatic drainage units. *Ann Anat* **178**, 537-544 (1996).
170. S. Meza-Perez, T. D. Randall, Immunological Functions of the Omentum. *Trends Immunol* **38**, 526-536 (2017).
171. M. Liu, A. Silva-Sanchez, T. D. Randall, S. Meza-Perez, Specialized immune responses in the peritoneal cavity and omentum. *J Leukoc Biol* **109**, 717-729 (2021).
172. A. Sarfarazi *et al.*, Therapeutic delivery to the peritoneal lymphatics: Current understanding, potential treatment benefits and future prospects. *International Journal of Pharmaceutics* **567**, 118456 (2019).
173. E. E. Ghosn *et al.*, Two physically, functionally, and developmentally distinct peritoneal macrophage subsets. *Proc Natl Acad Sci U S A* **107**, 2568-2573 (2010).
174. X. Zhang, R. Goncalves, D. M. Mosser, The isolation and characterization of murine macrophages. *Curr Protoc Immunol* **Chapter 14**, 14.11.11-14.11.14 (2008).
175. S. Yona *et al.*, Fate mapping reveals origins and dynamics of monocytes and tissue macrophages under homeostasis. *Immunity* **38**, 79-91 (2013).
176. P. Jayakumar, A. Laganson, M. Deng, GATA6+ Peritoneal Resident Macrophage: The Immune Custodian in the Peritoneal Cavity. *Frontiers in Pharmacology* **13**, (2022).
177. C. C. Bain, S. J. Jenkins, The biology of serous cavity macrophages. *Cell Immunol* **330**, 126-135 (2018).
178. A. W. Roberts *et al.*, Tissue-Resident Macrophages Are Locally Programmed for Silent Clearance of Apoptotic Cells. *Immunity* **47**, 913-927.e916 (2017).
179. A. Vega-Pérez *et al.*, Resident macrophage-dependent immune cell scaffolds drive anti-bacterial defense in the peritoneal cavity. *Immunity* **54**, 2578-2594.e2575 (2021).
180. J. Wang, P. Kubes, A Reservoir of Mature Cavity Macrophages that Can Rapidly Invade Visceral Organs to Affect Tissue Repair. *Cell* **165**, 668-678 (2016).

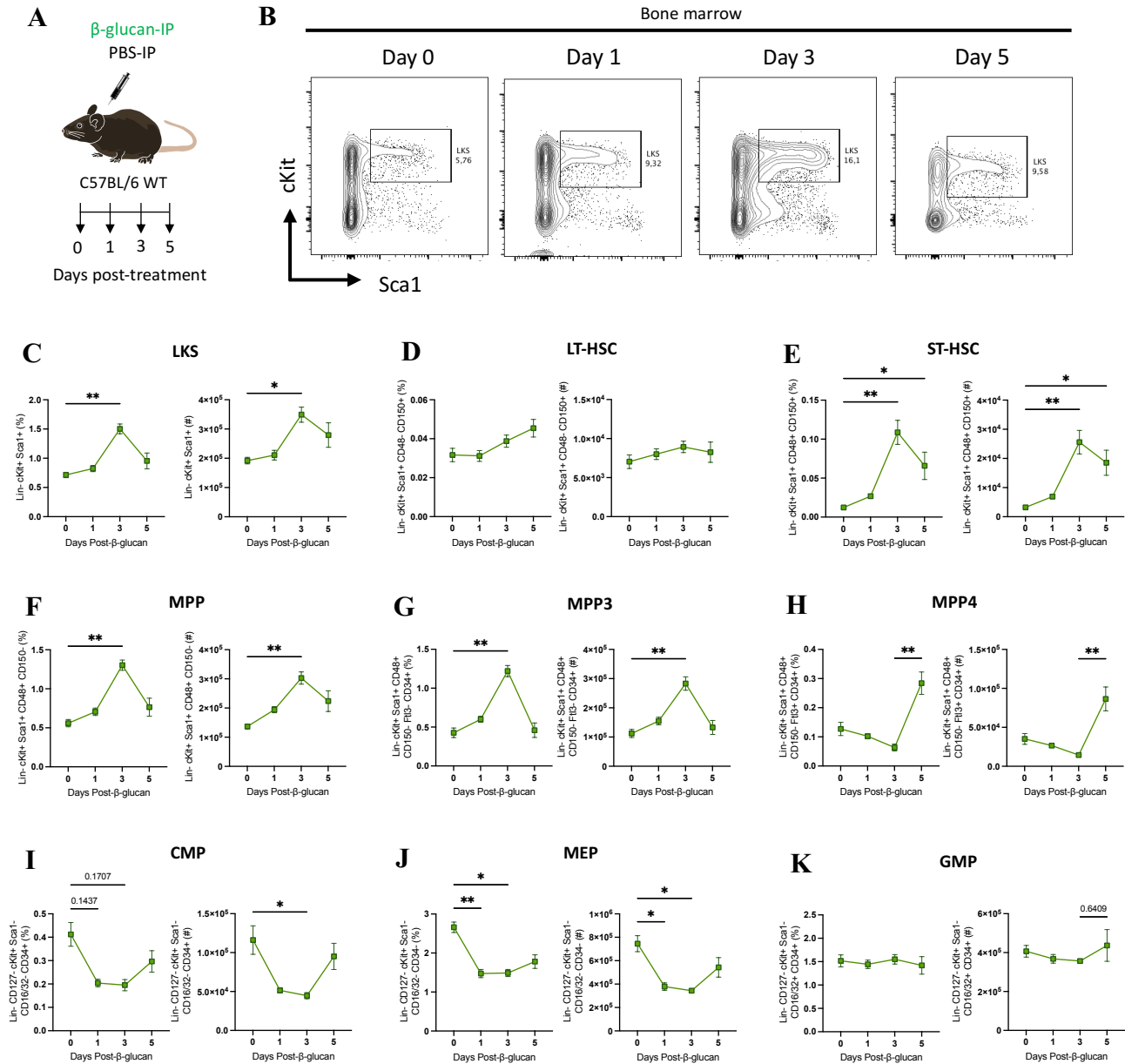
181. M. Honda, M. Kadohisa, D. Yoshii, Y. Komohara, T. Hibi, Directly recruited GATA6 + peritoneal cavity macrophages contribute to the repair of intestinal serosal injury. *Nature Communications* **12**, 7294 (2021).
182. J. F. Deniset *et al.*, Gata6(+) Pericardial Cavity Macrophages Relocate to the Injured Heart and Prevent Cardiac Fibrosis. *Immunity* **51**, 131-140.e135 (2019).
183. M. Sohn *et al.*, Two Distinct Subsets Are Identified from the Peritoneal Myeloid Mononuclear Cells Expressing both CD11c and CD115. *Immune Netw* **19**, e15 (2019).
184. S. Balan, M. Saxena, N. Bhardwaj, Dendritic cell subsets and locations. *Int Rev Cell Mol Biol* **348**, 1-68 (2019).
185. M. Guilliams *et al.*, Dendritic cells, monocytes and macrophages: a unified nomenclature based on ontogeny. *Nature Reviews Immunology* **14**, 571-578 (2014).
186. D. Theisen, K. Murphy, The role of cDC1s in vivo: CD8 T cell priming through cross-presentation. *F1000Res* **6**, 98 (2017).
187. J. Liu, X. Zhang, Y. Cheng, X. Cao, Dendritic cell migration in inflammation and immunity. *Cellular & Molecular Immunology* **18**, 2461-2471 (2021).
188. D. A. Carlow, M. R. Gold, H. J. Ziltener, Lymphocytes in the peritoneum home to the omentum and are activated by resident dendritic cells. *J Immunol* **183**, 1155-1165 (2009).
189. D. Repáraz, M. Hommel, F. Navarro, D. Llopiz, The role of dendritic cells in the immune niche of the peritoneum. *Int Rev Cell Mol Biol* **371**, 1-14 (2022).
190. R. A. Backer, H. C. Probst, B. E. Clausen, Classical DC2 subsets and monocyte-derived DC: Delineating the developmental and functional relationship. *European Journal of Immunology* **53**, 2149548 (2023).
191. M. McCully, J. Madrenas, Dendritic Cells as Arbiters of Peritoneal Immune Responses. *Peritoneal dialysis international : journal of the International Society for Peritoneal Dialysis* **26**, 8-25 (2006).
192. Y. Okabe, R. Medzhitov, Tissue-specific signals control reversible program of localization and functional polarization of macrophages. *Cell* **157**, 832-844 (2014).
193. A. J. Clarke, T. Riffelmacher, D. Braas, R. J. Cornall, A. K. Simon, B1a B cells require autophagy for metabolic homeostasis and self-renewal. *J Exp Med* **215**, 399-413 (2018).
194. M. Kobayashi *et al.*, Functional B-1 progenitor cells are present in the hematopoietic stem cell-deficient embryo and depend on Cbf $\beta$  for their development. *Proc Natl Acad Sci U S A* **111**, 12151-12156 (2014).
195. E. E. Ghosn, Y. Yang, J. Tung, L. A. Herzenberg, L. A. Herzenberg, CD11b expression distinguishes sequential stages of peritoneal B-1 development. *Proc Natl Acad Sci U S A* **105**, 5195-5200 (2008).
196. D. Parra *et al.*, Pivotal advance: peritoneal cavity B-1 B cells have phagocytic and microbicidal capacities and present phagocytosed antigen to CD4+ T cells. *J Leukoc Biol* **91**, 525-536 (2012).
197. J. B. Wong *et al.*, B-1a cells acquire their unique characteristics by bypassing the pre-BCR selection stage. *Nature Communications* **10**, 4768 (2019).
198. K. R. Alugupalli *et al.*, B1b lymphocytes confer T cell-independent long-lasting immunity. *Immunity* **21**, 379-390 (2004).

199. A. F. Cunningham *et al.*, B1b cells recognize protective antigens after natural infection and vaccination. *Front Immunol* **5**, 535 (2014).
200. R. Blandino, N. Baumgarth, Secreted IgM: New tricks for an old molecule. *J Leukoc Biol* **106**, 1021-1034 (2019).
201. G. F. Weber *et al.*, Interleukin-3 amplifies acute inflammation and is a potential therapeutic target in sepsis. *Science* **347**, 1260-1265 (2015).
202. B. G. Chousterman, F. K. Swirski, Innate response activator B cells: origins and functions. *Int Immunol* **27**, 537-541 (2015).
203. S. Fagarasan, K. Kinoshita, M. Muramatsu, K. Ikuta, T. Honjo, In situ class switching and differentiation to IgA-producing cells in the gut lamina propria. *Nature* **413**, 639-643 (2001).
204. F. L. Smith, N. Baumgarth, B-1 cell responses to infections. *Curr Opin Immunol* **57**, 23-31 (2019).
205. G. Composto *et al.*, Peritoneal T lymphocyte regulation by macrophages. *Immunobiology* **216**, 256-264 (2011).
206. J. F. Wijffels, R. J. Hendrickx, J. J. Steenbergen, I. L. Eestermans, R. H. Beelen, Milky spots in the mouse omentum may play an important role in the origin of peritoneal macrophages. *Res Immunol* **143**, 401-409 (1992).
207. D. A. Christian *et al.*, cDC1 coordinate innate and adaptive responses in the omentum required for T cell priming and memory. *Sci Immunol* **7**, eabq7432 (2022).
208. M. J. Skeen, H. K. Ziegler, Induction of murine peritoneal gamma/delta T cells and their role in resistance to bacterial infection. *J Exp Med* **178**, 971-984 (1993).
209. O. Ibdapo-Obe *et al.*, Mucosal-Associated Invariant T Cells Redistribute to the Peritoneal Cavity During Spontaneous Bacterial Peritonitis and Contribute to Peritoneal Inflammation. *Cell Mol Gastroenterol Hepatol* **9**, 661-677 (2020).
210. C. Summers *et al.*, Neutrophil kinetics in health and disease. *Trends Immunol* **31**, 318-324 (2010).
211. R. C. Furze, S. M. Rankin, The role of the bone marrow in neutrophil clearance under homeostatic conditions in the mouse. *Faseb j* **22**, 3111-3119 (2008).
212. E. Coppin *et al.*, Splenic hematopoietic stem cells display a pre-activated phenotype. *Immunol Cell Biol*, (2018).
213. V. Bronte, M. J. Pittet, The spleen in local and systemic regulation of immunity. *Immunity* **39**, 806-818 (2013).
214. L. Biswas *et al.*, Lymphatic vessels in bone support regeneration after injury. *Cell* **186**, 382-397.e324 (2023).
215. C. Fahlquist-Hagert, O. Sareila, S. Rosendahl, R. Holmdahl, Variants of beta-glucan polysaccharides downregulate autoimmune inflammation. *Commun Biol* **5**, 449 (2022).
216. I. Kwok *et al.*, Combinatorial Single-Cell Analyses of Granulocyte-Monocyte Progenitor Heterogeneity Reveals an Early Uni-potent Neutrophil Progenitor. *Immunity* **53**, 303-318.e305 (2020).
217. L. Kalafati, A. Hatzioannou, G. Hajishengallis, T. Chavakis, The role of neutrophils in trained immunity. *Immunological Reviews* **314**, 142-157 (2023).
218. K. Vanickova *et al.*, Hematopoietic stem cells undergo a lymphoid to myeloid switch in early stages of emergency granulopoiesis. *Embo j* **42**, e113527 (2023).

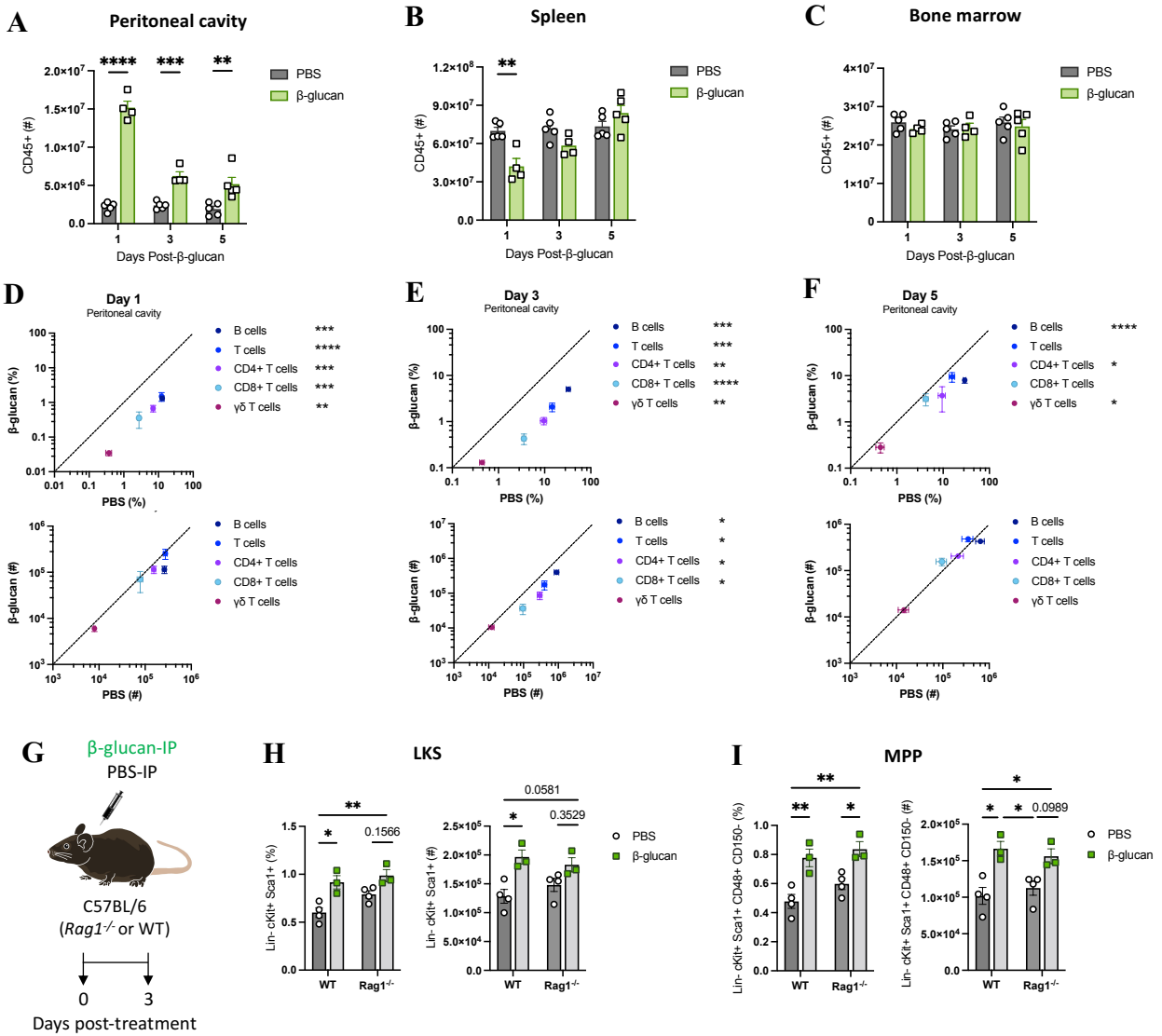
219. Y. Sasaki *et al.*, IL-6 Generated from Human Hematopoietic Stem and Progenitor Cells through TLR4 Signaling Promotes Emergency Granulopoiesis by Regulating Transcription Factor Expression. *J Immunol* **207**, 1078-1086 (2021).
220. F. Borriello *et al.*, Innate Immune Modulation by GM-CSF and IL-3 in Health and Disease. *Int J Mol Sci* **20**, (2019).
221. H. Takizawa *et al.*, Pathogen-Induced TLR4-TRIF Innate Immune Signaling in Hematopoietic Stem Cells Promotes Proliferation but Reduces Competitive Fitness. *Cell Stem Cell* **21**, 225-240.e225 (2017).
222. Y. Ueda, K. Yang, S. J. Foster, M. Kondo, G. Kelsoe, Inflammation controls B lymphopoiesis by regulating chemokine CXCL12 expression. *J Exp Med* **199**, 47-58 (2004).
223. E. E. Irons *et al.*, B cells suppress medullary granulopoiesis by an extracellular glycosylation-dependent mechanism. *Elife* **8**, (2019).
224. H. Andualem, E. Hollams, T. R. Kollmann, N. Amenyogbe, BCG-Induced Immune Training: Interplay between Trained Immunity and Emergency Granulopoiesis. *Journal of Molecular Biology* **435**, 168169 (2023).
225. B. Brook *et al.*, BCG vaccination–induced emergency granulopoiesis provides rapid protection from neonatal sepsis. *Science Translational Medicine* **12**, eaax4517 (2020).
226. M. G. Netea, A. Schlitzer, K. Placek, L. A. B. Joosten, J. L. Schultze, Innate and Adaptive Immune Memory: an Evolutionary Continuum in the Host’s Response to Pathogens. *Cell Host & Microbe* **25**, 13-26 (2019).
227. J. Quintin *et al.*, *Candida albicans* infection affords protection against reinfection via functional reprogramming of monocytes. *Cell Host Microbe* **12**, 223-232 (2012).
228. C. von Loeffelholz *et al.*, Increased Peritoneal B1-like Cells during Acute Phase of Human Septic Peritonitis. *iScience*, (2024).
229. P. A. Louwe *et al.*, Recruited macrophages that colonize the post-inflammatory peritoneal niche convert into functionally divergent resident cells. *Nature Communications* **12**, 1770 (2021).
230. F. G. Thies *et al.*, Cross Talk between Peritoneal Macrophages and B-1 Cells In Vitro. *PLOS ONE* **8**, e62805 (2013).
231. D. S. Nelson, Reaction to antigens in vivo of the peritoneal macrophages of guinea-pigs with delayed type hypersensitivity. Effects of anticoagulants and other drugs. *Lancet* **2**, 175-176 (1963).
232. D. G. Goswami *et al.*, Large Peritoneal Macrophages and Transitional Premonocytes Promote Survival during Abdominal Sepsis. *Immunohorizons* **5**, 994-1007 (2021).
233. L. C. Davies *et al.*, Distinct bone marrow-derived and tissue-resident macrophage lineages proliferate at key stages during inflammation. *Nature Communications* **4**, 1886 (2013).
234. E. L. Gautier, S. Ivanov, P. Lesnik, G. J. Randolph, Local apoptosis mediates clearance of macrophages from resolving inflammation in mice. *Blood* **122**, 2714-2722 (2013).
235. N. Zhang *et al.*, Expression of factor V by resident macrophages boosts host defense in the peritoneal cavity. *J Exp Med* **216**, 1291-1300 (2019).
236. P. Liu *et al.*, *Escherichia coli* and *Candida albicans* induced macrophage extracellular trap-like structures with limited microbicidal activity. *PLoS One* **9**, e90042 (2014).

237. A. Grant, Master's thesis, McGill University, (2022).
238. E. L. Gautier *et al.*, Gata6 regulates aspartoacylase expression in resident peritoneal macrophages and controls their survival. *J Exp Med* **211**, 1525-1531 (2014).
239. E. Kolaczkowska, P. Kubes, Neutrophil recruitment and function in health and inflammation. *Nat Rev Immunol* **13**, 159-175 (2013).
240. J. Yang *et al.*, Targeted gene disruption demonstrates that P-selectin glycoprotein ligand 1 (PSGL-1) is required for P-selectin-mediated but not E-selectin-mediated neutrophil rolling and migration. *J Exp Med* **190**, 1769-1782 (1999).
241. W.-B. Lee *et al.*, Mincle activation enhances neutrophil migration and resistance to polymicrobial septic peritonitis. *Scientific Reports* **7**, 41106 (2017).
242. Y. Song *et al.*, E. coli induced larger neutrophils in the peritoneal cavity of mice with severe septic peritonitis. *Molecular Immunology* **105**, 86-95 (2019).
243. C. Théroude *et al.*, Trained Immunity Confers Prolonged Protection From Listeriosis. *Front Immunol* **12**, 723393 (2021).
244. B. Ratitong, M. Marshall, E. Pearlman,  $\beta$ -Glucan-stimulated neutrophil secretion of IL-1 $\alpha$  is independent of GSDMD and mediated through extracellular vesicles. *Cell Rep* **35**, 109139 (2021).
245. P. Rider *et al.*, IL-1 $\alpha$  and IL-1 $\beta$  Recruit Different Myeloid Cells and Promote Different Stages of Sterile Inflammation. *The Journal of Immunology* **187**, 4835-4843 (2011).
246. A. D. Jerome *et al.*, Characterization of Zymosan-Modulated Neutrophils With Neuroregenerative Properties. *Frontiers in Immunology* **13**, (2022).
247. C. Bono *et al.*, GM-CSF Programs Hematopoietic Stem and Progenitor Cells During *Candida albicans* Vaccination for Protection Against Reinfection. *Frontiers in Immunology* **12**, (2021).
248. A. V. Ferreira *et al.*, Limited role of the spleen in a mouse model of trained immunity: Impact on neutrophilia. *Journal of Leukocyte Biology* **111**, 9-17 (2022).
249. C. M. Koh, Preparation of cells for microscopy using cytopsin. *Methods Enzymol* **533**, 235-240 (2013).
250. J. Wang *et al.*, Visualizing the function and fate of neutrophils in sterile injury and repair. *Science* **358**, 111-116 (2017).
251. A. E. Geller *et al.*, The induction of peripheral trained immunity in the pancreas incites anti-tumor activity to control pancreatic cancer progression. *Nat Commun* **13**, 759 (2022).
252. Y. Masuda *et al.*, Oral administration of soluble  $\beta$ -glucans extracted from *Grifola frondosa* induces systemic antitumor immune response and decreases immunosuppression in tumor-bearing mice. *Int J Cancer* **133**, 108-119 (2013).
253. P. Mata-Martínez, M. Bergón-Gutiérrez, C. del Fresno, Dectin-1 Signaling Update: New Perspectives for Trained Immunity. *Frontiers in Immunology* **13**, (2022).
254. M. J. Marakalala *et al.*, Dectin-1 plays a redundant role in the immunomodulatory activities of  $\beta$ -glucan-rich ligands in vivo. *Microbes and Infection* **15**, 511-515 (2013).
255. T. Chavakis, I. Mitroulis, G. Hajishengallis, Hematopoietic progenitor cells as integrative hubs for adaptation to and fine-tuning of inflammation. *Nature Immunology* **20**, 802-811 (2019).

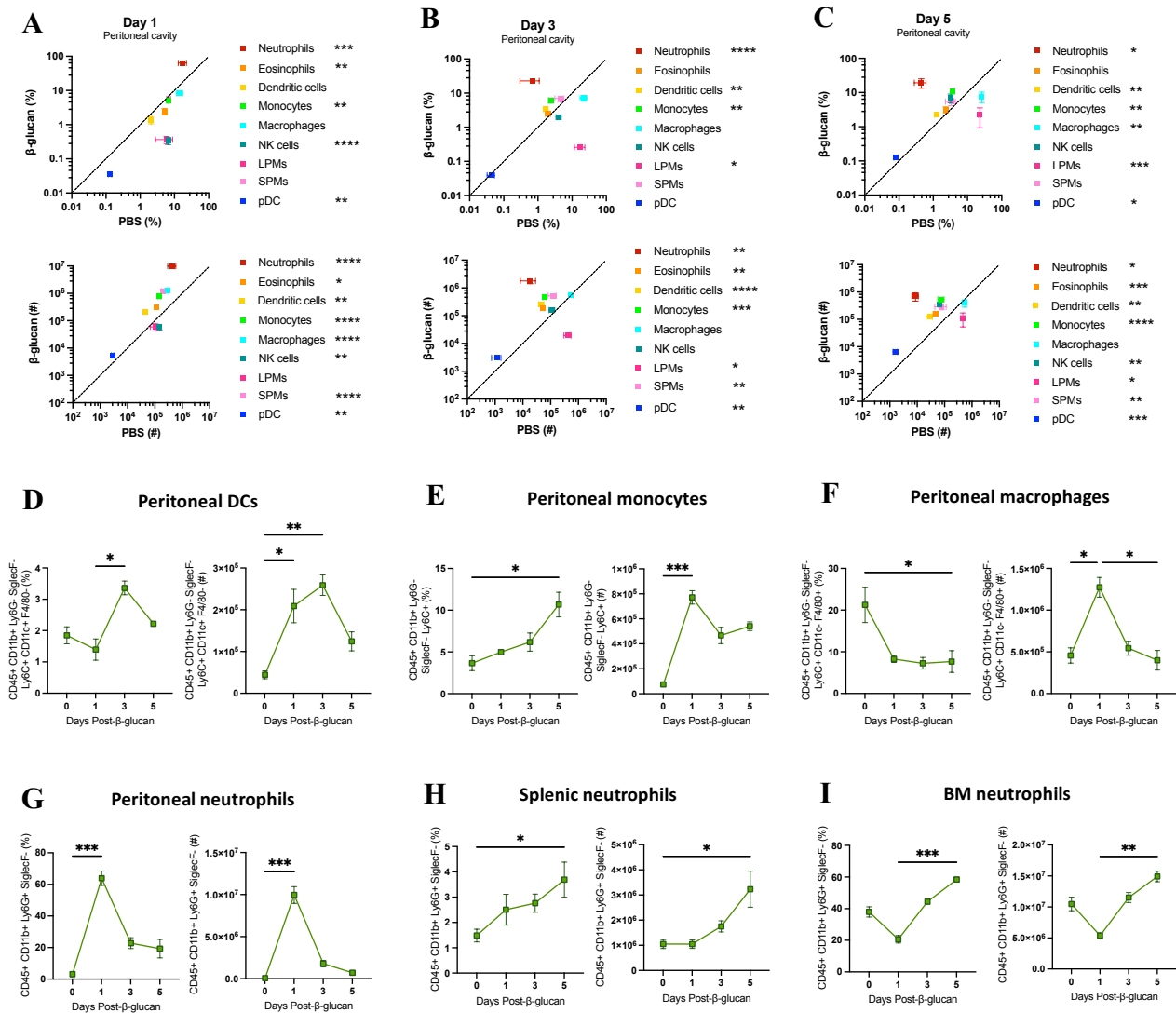
## APPENDIX A: FIGURES AND FIGURE LEGENDS



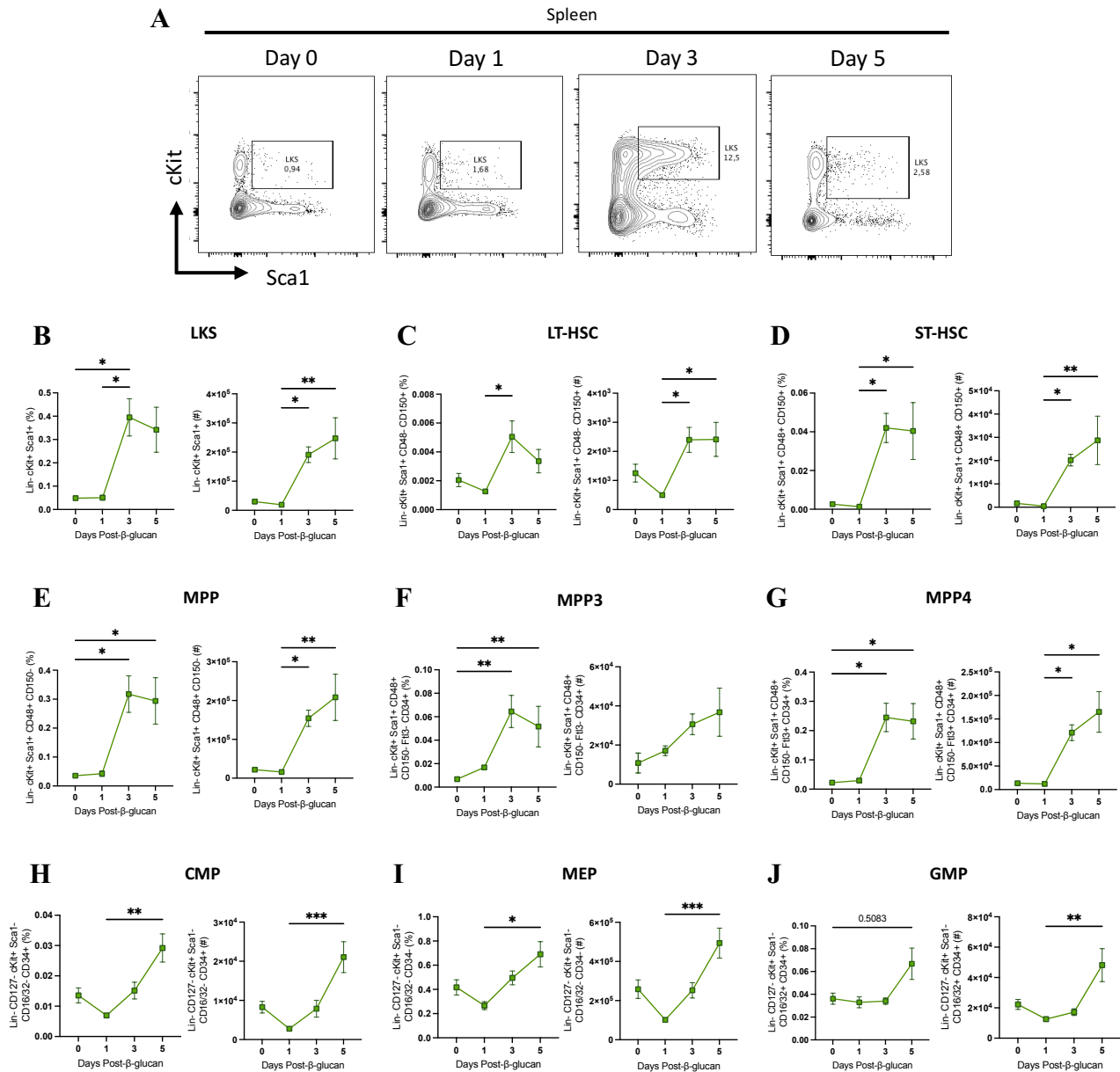
**Figure 3.  $\beta$ -Glucan expands HSPC populations in the BM.** (A) 6–10-week-old male wildtype C57BL/6 mice ( $n=4-5$ ) were treated with  $\beta$ -glucan-IP (1 mg) or PBS control (100  $\mu$ l). BM was collected at day 1, 3 and 5 after treatment. (B) Representative FACS plots of LKS population in BM at days 1, 3 and 5 post- $\beta$ -glucan treatment. (C–K) Frequency (left) and total cell number (right) of (C) LKS, (D) LT-HSC, (E) ST-HSC, (F) MPP, (G) MPP3, (H) MPP4, (I) CMP, (J) MEP, and (K) GMP in the BM after  $\beta$ -glucan treatment. Kruskal-Wallis test followed by Dunn's multiple comparison test; data are presented as Mean  $\pm$  SEM.



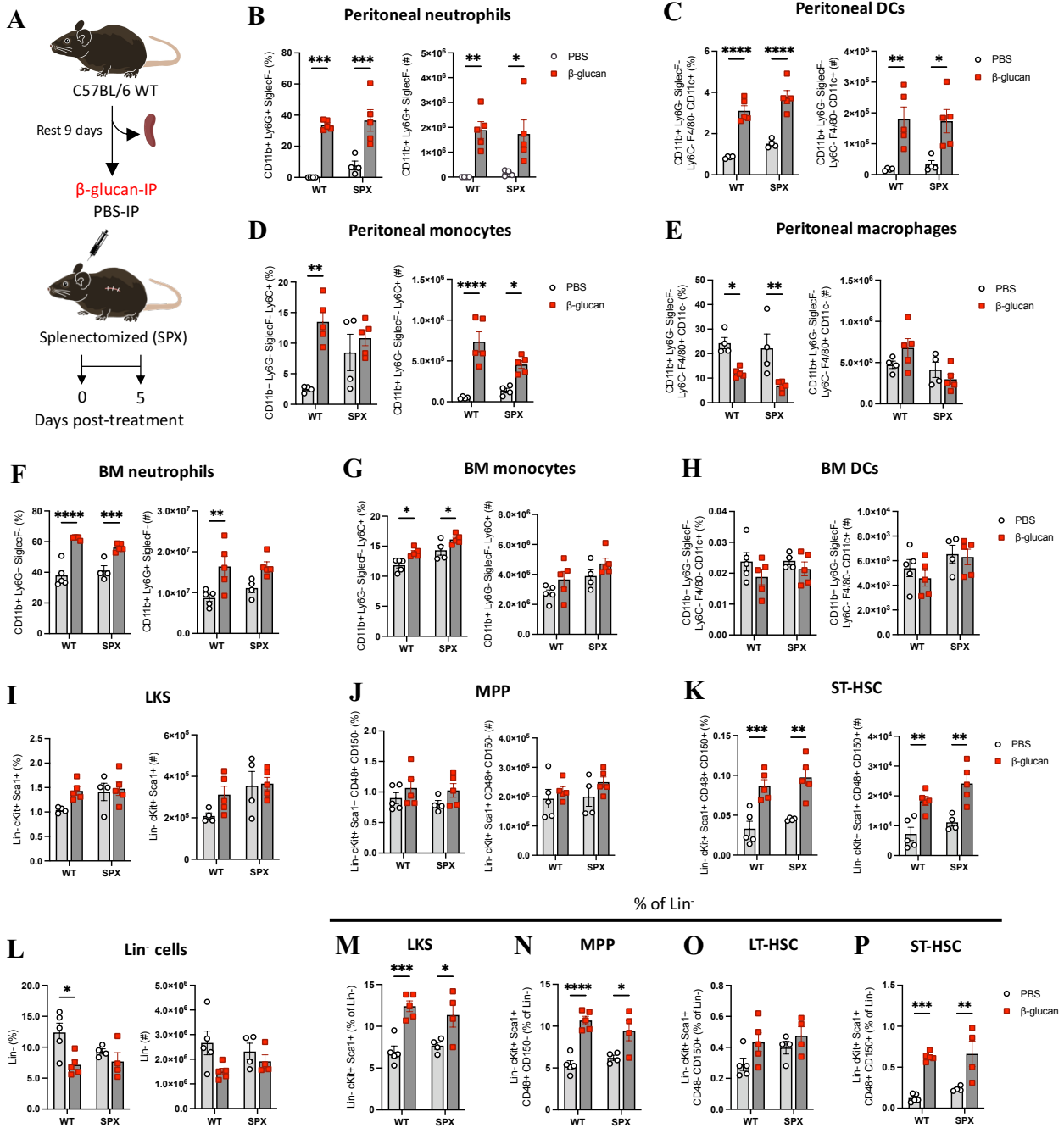
**Figure 4. β-Glucan-induced HSC expansion is independent of adaptive immunity.** (A-C) Total CD45<sup>+</sup> cell counts by flow cytometry in the (A) peritoneal cavity, (B) spleen and (C) BM after β-glucan treatment. (D-F) Frequency (top) and absolute cell counts (bottom) of peritoneal innate immune populations at (D) day 1, (E) day 3, and (F) day 5 post-β-glucan treatment. Each dot represents the Mean ± SEM. Dotted line represents where PBS and β-glucan frequencies or cell counts are equal. Analyzed using independent student T test. (G) 6–10-week-old male WT C57BL/6 and *Rag1*<sup>-/-</sup> mice (n=3-4) were treated with β-glucan-IP (1 mg) or PBS control (100 μl). BM was collected at day 3 post-treatment. (H-I) Frequency (left) and total cell number (right) of (H) LKS and (I) MPP in the BM after β-glucan treatment. Two-way ANOVA followed by Sidak's multiple comparison test; data are presented as Mean ± SEM.



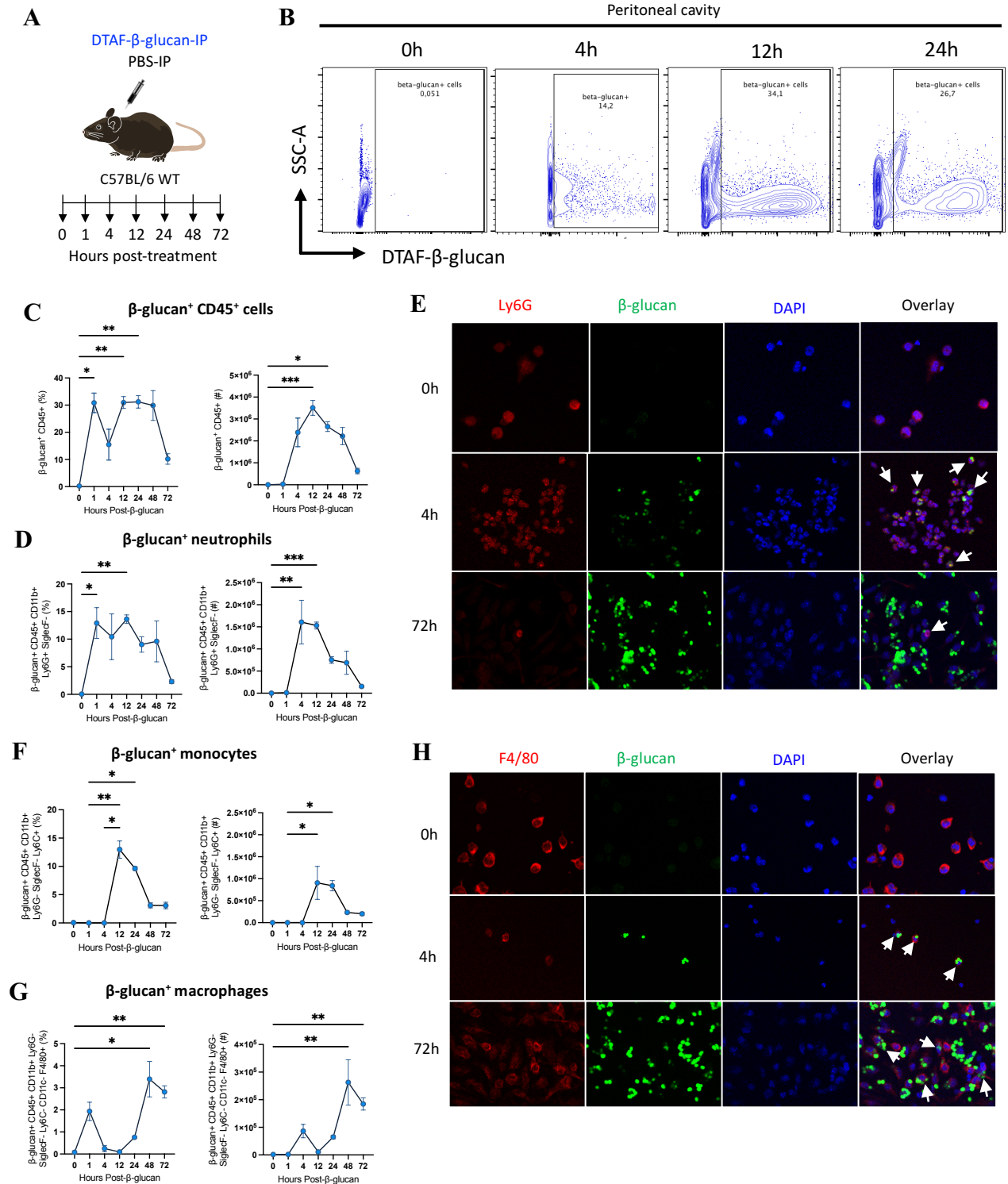
**Figure 5.  $\beta$ -Glucan increases innate cell populations in the peritoneal cavity.** (A-C) Frequency (top) and absolute cell counts (bottom) of peritoneal innate immune populations at (A) day 1, (B) day 3, and (C) day 5 post- $\beta$ -glucan treatment. Each dot represents the Mean  $\pm$  SEM. Dotted line represents where PBS and  $\beta$ -glucan frequencies or cell counts are equal. Analyzed using independent student T test. (D-G) Frequency (left) and absolute cell counts (right) of (D) dendritic cells, (E) monocytes, (F) macrophages and (G) neutrophils in the peritoneal cavity after  $\beta$ -glucan treatment. (H-I) Frequency (left) and absolute cell counts (right) of neutrophils in the (H) spleen and (I) BM. Kruskal-Wallis test followed by Dunn's multiple comparison test; data are presented as Mean  $\pm$  SEM.



**Figure 6.  $\beta$ -Glucan expands HSPC populations in the spleen. (A)** Representative FACS plots of LKS population in the spleen at days 1, 3 and 5 post- $\beta$ -glucan treatment. **(B-D)** Frequency and total cell number of splenic **(B)** LKS, **(C)** LT-HSC, **(D)** ST-HSC, **(E)** MPP, **(F)** MPP3, **(G)** MPP4, **(H)** CMP, **(I)** MEP, and **(J)** GMP in the spleen after  $\beta$ -glucan treatment. Kruskal-Wallis test followed by Dunn's multiple comparison test; data are presented as Mean  $\pm$  SEM.



**Figure 7. The role of the spleen in  $\beta$ -glucan-mediated trained immunity.** (A) WT C57BL/6 mice were (n=4-5) splenectomized, rested for 9 days and treated with  $\beta$ -glucan-IP (1 mg) or PBS control for 5 days. (B-E) Frequency (left) and absolute cell counts (right) of (D) neutrophils, (E) DCs, (F) monocytes and (G) macrophages in the peritoneal cavity after  $\beta$ -glucan treatment. (F-L) Frequency (left) and absolute cell counts (right) of (F) neutrophils, (G) monocytes, (H) DCs, (I) LKS, (J) MPP, (K) ST-HSC, and (L)  $\text{Lin}^-$  cells in BM after  $\beta$ -glucan treatment. (M-P) Frequency of  $\text{Lin}^-$  cells of (M) LKS, (N) MPP, (O) LT-HSC, and (P) ST-HSC in BM after  $\beta$ -glucan treatment. Two-way ANOVA followed by Sidak's multiple comparison test; data are presented as Mean  $\pm$  SEM.

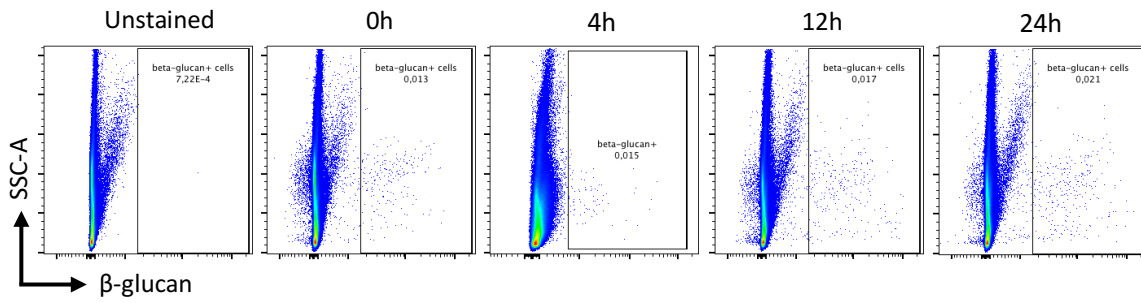
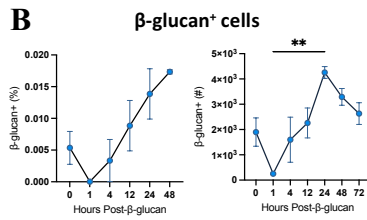
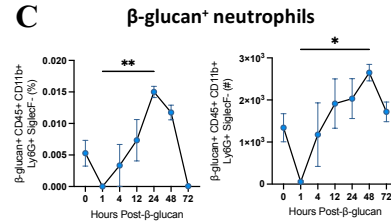
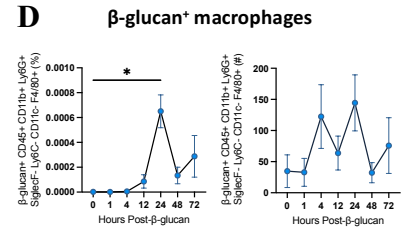


**Figure 8. Peritoneal neutrophils and macrophages recognize and ingest β-glucan.** (A) 6–10-week-old male wildtype C57BL/6 mice (n=3-6) were treated with DTAF-stained β-glucan-IP (1 mg). (B) Representative FACS plots of β-glucan<sup>+</sup> cells in the peritoneal cavity at 0h, 4h, 12h and 24h post-β-glucan-IP treatment. Gated on viable single cells. (C-D) Frequency (left) and absolute

cell counts (right) of **(D)**  $\beta$ -glucan<sup>+</sup> CD45<sup>+</sup> cells and **(E)**  $\beta$ -glucan<sup>+</sup> neutrophils. **(F)** Confocal microscopy images (magnification 20X) of murine peritoneal cells after 4h and 72h treatment with  $\beta$ -glucan-DTAF *in vivo*. Arrows represent  $\beta$ -glucan-internalized Ly6G<sup>+</sup> cells. **(F-G)** Frequency (left) and absolute cell counts (right) of  $\beta$ -glucan<sup>+</sup> **(F)** monocytes and **(G)** macrophages. **(H)** Confocal microscopy images (magnification 20X) of murine peritoneal cells after 4h and 72h treatment with  $\beta$ -glucan-DTAF *in vivo*. Arrows represent  $\beta$ -glucan-internalized F4/80<sup>+</sup> cells. Kruskal-Wallis test followed by Dunn's multiple comparison test; data are presented as Mean  $\pm$  SEM.

**A**

Bone marrow

**B****C****D**

**Figure 9. β-Glucan is likely not directly accessing BM via a cell intermediate. (A)** Representative FACS plots of β-glucan<sup>+</sup> cells population in the spleen at 0h, 4h, 12h and 24h post-β-glucan treatment. Gated on viable single cells. **(B-D)** Frequency (left) and total cell number (right) of β-glucan<sup>+</sup> **(B)** cells **(C)** neutrophils, and **(D)** macrophages in the BM after β-glucan treatment. Kruskal-Wallis test followed by Dunn's multiple comparison test; data are presented as Mean ± SEM.

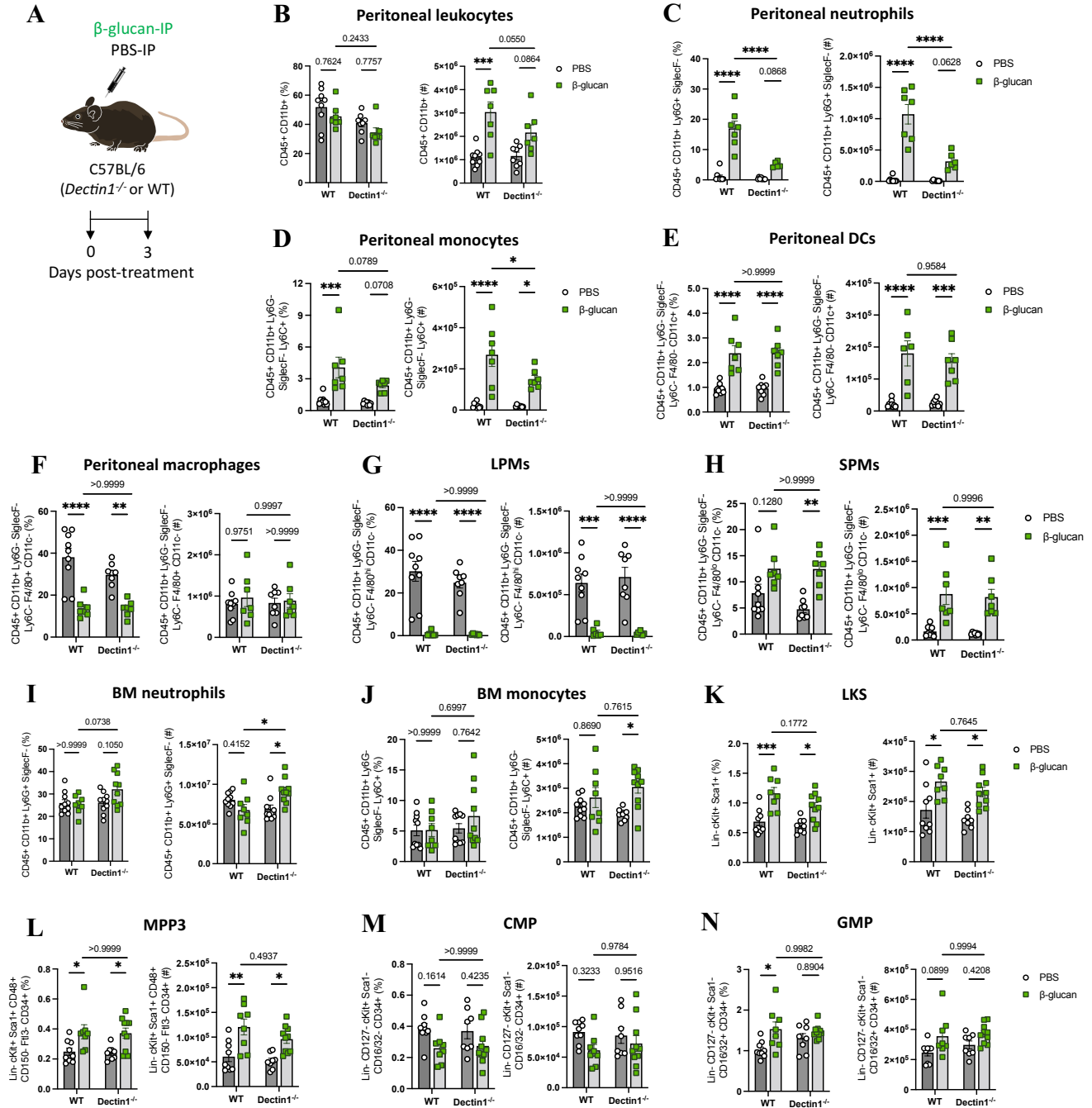


**Figure 10.  $\beta$ -Glucan-induced LKS expansion is likely independent of dectin-1 signaling.** (A) 6–10-week-old male wildtype C57BL/6 and *Dectin1*<sup>-/-</sup> mice (n=7-9) were treated with  $\beta$ -glucan-IP (1 mg) or PBS control (100  $\mu$ l). BM and peritoneal lavages were collected at day 3 post-treatment. (B–H) Frequency (left) and absolute cell counts (right) of (D) neutrophils, (B) leukocytes, (C) neutrophils, (D) monocytes, (E) DCs, (F) macrophages, (G) LPMs and (H) SPMs in the peritoneal cavity after  $\beta$ -glucan treatment. (I–N) Frequency (left) and absolute cell counts (right) of (I) neutrophils, (J) monocytes, (K) LKS, (L) MPP3, (M) CMP and (N) GMP in the BM after  $\beta$ -glucan treatment. Data pooled from two experiments. Two-way ANOVA followed by Sidak's multiple comparison test; data are presented as Mean  $\pm$  SEM.

## APPENDIX B: SUPPLEMENTARY FIGURES AND FIGURE LEGENDS

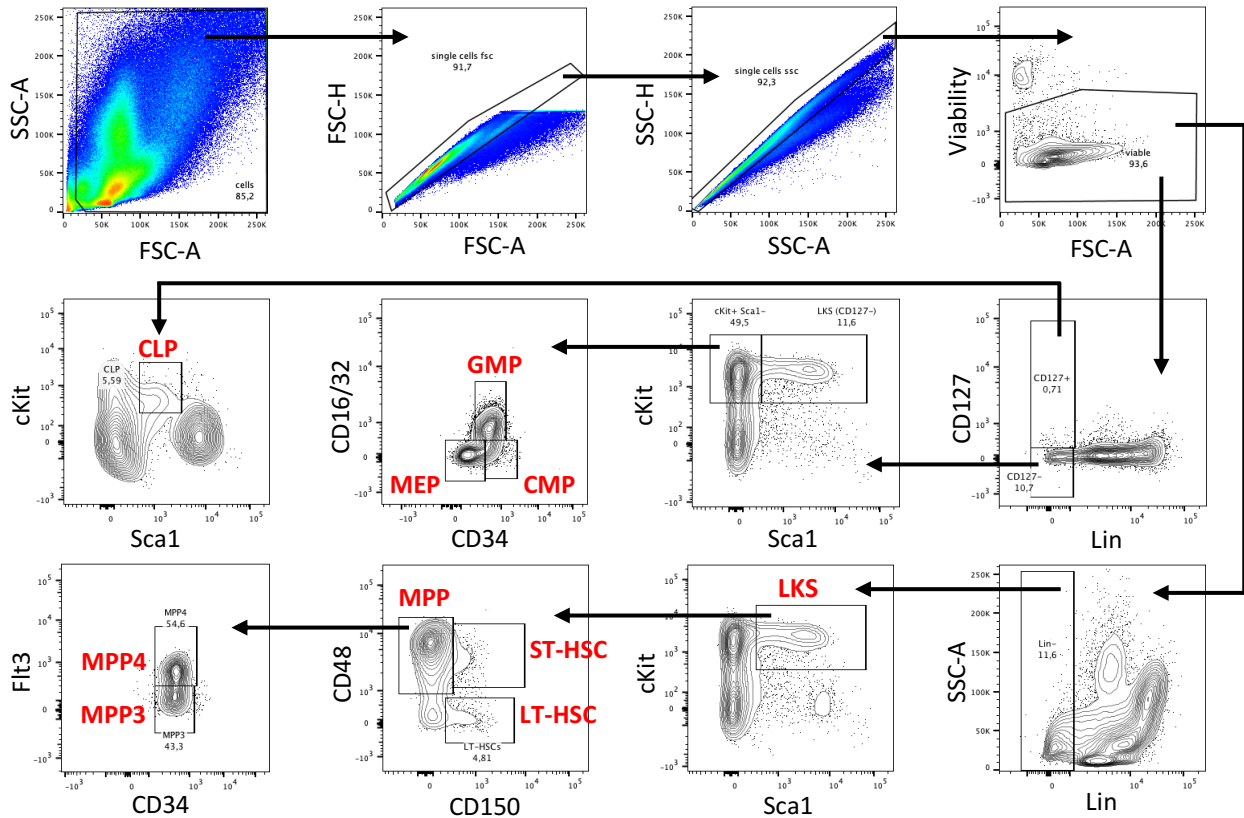


**Figure S1. Gating strategy for HSPC populations.** Cells were gated for FSC-A against SSC-A. Doublets were excluded using FSC-H against FSC-A followed by SSC-H against SSC-A. Viable cells were gated and lineage-committed (Lin: CD11b, Ly6C/G, Ter119, CD5, CD8, CD4, B220) cells were excluded. In the first gating strategy, Lin<sup>-</sup> cells were gated for cKit<sup>+</sup> Sca1<sup>+</sup> and defined as LKS cells. Within the LKS population, cells were identified based on CD48 and CD150 surface expression. CD48<sup>-</sup> CD150<sup>+</sup> cells were LT-HSCs; CD48<sup>+</sup> CD150<sup>+</sup> cells were ST-HSCs; and CD48<sup>+</sup> CD150<sup>-</sup> cells were MPPs. MPPs were further divided into MPP3 (Flt3<sup>-</sup> CD34<sup>+</sup>) and MPP4 (Flt3<sup>+</sup> CD34<sup>+</sup>). In the second gating strategy, Lin<sup>-</sup> cells were gated based on CD127 expression. Lin<sup>-</sup> CD127<sup>+</sup> were defined as CLP by cKit<sup>lo</sup> Sca1<sup>lo</sup> expression. Within the Lin<sup>-</sup> CD127<sup>-</sup> populations, cKit<sup>+</sup> Sca1<sup>-</sup> cells were subdivided into MEP, GMP and CMP based on CD16/32 and CD34 surface expression. CD16/32<sup>-</sup> CD34<sup>+</sup> were MEPs; CD16/32<sup>+</sup> CD34<sup>+</sup> were GMPs; and CD16/32<sup>-</sup> CD34<sup>+</sup> were CMPs.

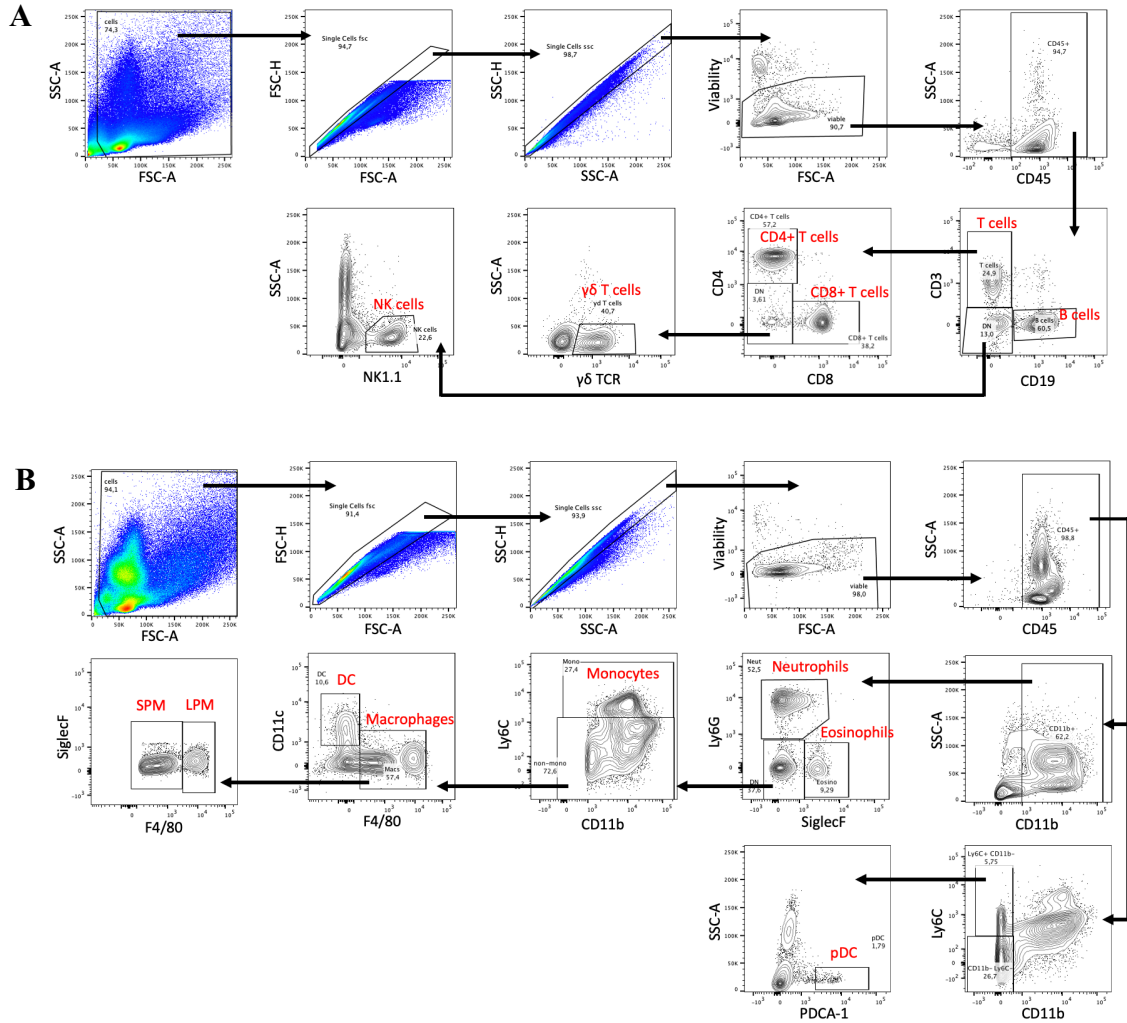


**Figure S2. Gating strategies for innate and adaptive immune cell subsets.** Cells were gated for FSC-A against SSC-A. Doublets were excluded using FSC-H against FSC-A followed by SSC-H against SSC-A. Viable cells were gated. Immune cells (CD45<sup>+</sup>) were gated. **(A)** For adaptive immune cells, cells were divided based on CD3 and CD19 expression. B cells were defined as CD3<sup>-</sup> CD19<sup>+</sup>. Within the CD3<sup>+</sup> CD19<sup>-</sup> population, CD4<sup>+</sup> T cells and CD8<sup>+</sup> T cells were identified based on CD4 and CD8 expression. Double negative cells for CD4 and CD8 were further gated for  $\gamma\delta$  TCR<sup>+</sup> cells to define  $\gamma\delta$  T cells or for NK1.1<sup>+</sup> to define NK cells. **(B)** For innate immune cells, cells defined as CD11b<sup>+</sup> cells were gated and further divided based on Ly6G and SiglecF expression. Neutrophils were characterized as CD45<sup>+</sup> CD11b<sup>+</sup> Ly6G<sup>+</sup>. Eosinophils were characterized as CD45<sup>+</sup> CD11b<sup>+</sup> SiglecF<sup>+</sup>. Double negative cells for Ly6G and SiglecF cells were gated on Ly6C. Ly6C<sup>+</sup> cells were defined as monocytes. Ly6C<sup>-</sup> cells were further characterized based on CD11c and F4/80 expression. Macrophages were defined as CD45<sup>+</sup> CD11b<sup>+</sup> Ly6G<sup>-</sup> SiglecF<sup>-</sup> Ly6C<sup>-</sup> F4/80<sup>+</sup> CD11c<sup>-</sup> and dendritic cells (DC) were defined as CD45<sup>+</sup> CD11b<sup>+</sup> Ly6G<sup>-</sup> SiglecF<sup>-</sup> Ly6C<sup>-</sup> F4/80<sup>-</sup> CD11c<sup>+</sup>. In the peritoneal cavity, macrophages can be further divided into large peritoneal macrophages (LPMs) and small peritoneal macrophages based on F4/80<sup>hi</sup> and F4/80<sup>lo/mid</sup> expression, respectively. For pDCs, CD11b<sup>-</sup> Ly6C<sup>+</sup> were gated on CD45<sup>+</sup> cells and further identified based on PDCA-1 expression.

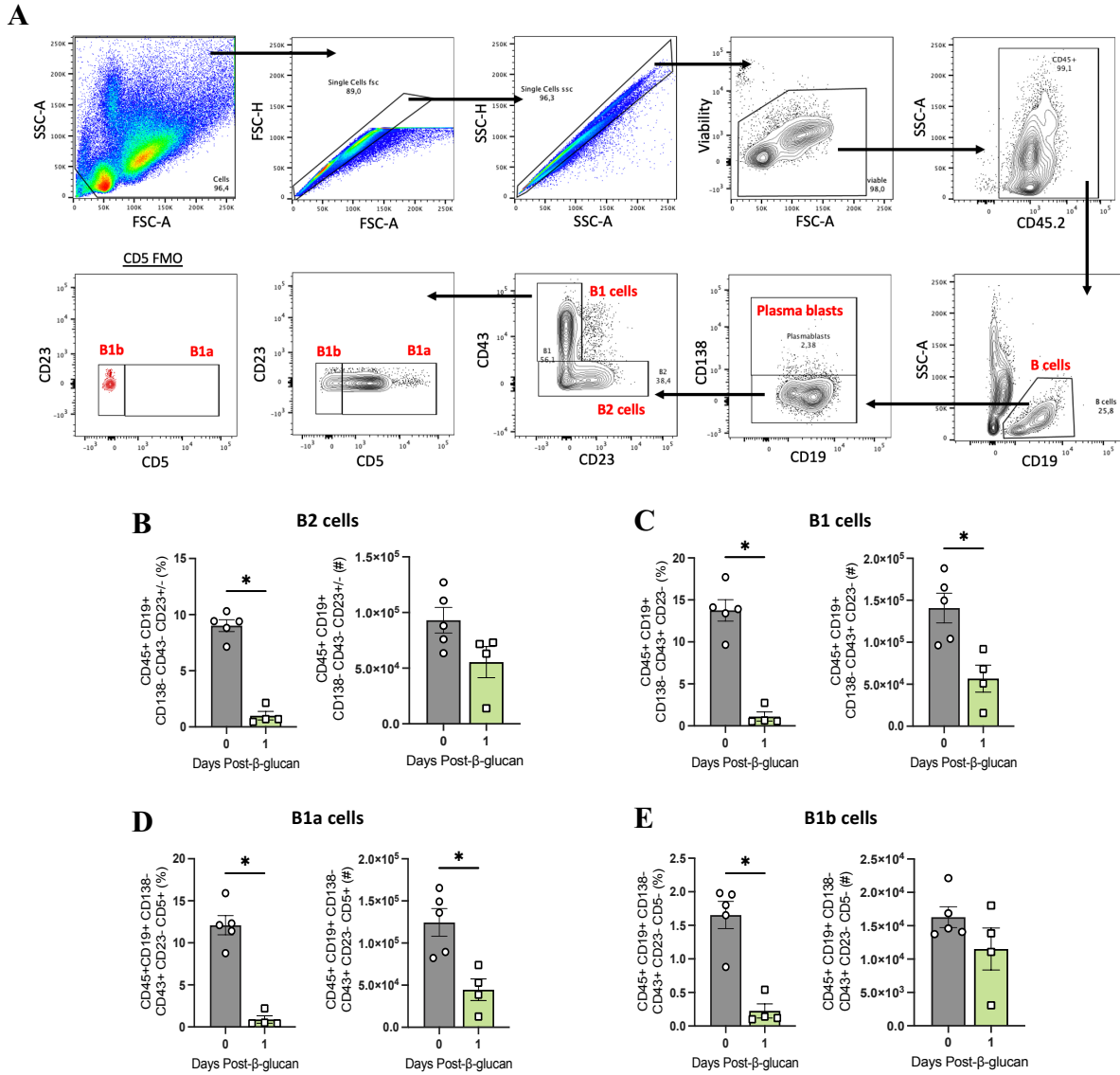


**Figure S3. Peritoneal B1 cells after  $\beta$ -glucan treatment.** (A) Gating strategy for peritoneal B1 cells. Cells were gated for FSC-A against SSC-A. Doublets were excluded using FSC-H against FSC-A followed by SSC-H against SSC-A. Viable cells were gated. Immune cells (CD45<sup>+</sup>) were gated. B cells were gated as CD19<sup>+</sup> cells. Plasma blasts were gated for CD138<sup>+</sup> and CD138<sup>-</sup> cells were further divided based on CD43 and CD23 expression. B1 were characterized as CD45<sup>+</sup> CD19<sup>+</sup> CD138<sup>-</sup> CD43<sup>+</sup> CD23<sup>-</sup>. B2 were characterized as CD45<sup>+</sup> CD19<sup>+</sup> CD138<sup>-</sup> CD43<sup>-</sup> CD23<sup>+/-</sup>. B1 cells were subdivided into B1a and B1b based on CD5 expression. (B-E) Frequency (left) and total cell counts (right) of peritoneal (B) B2 cells, (C) B1 cells, (D) B1a cells and (E) B1b cells at 1 day post- $\beta$ -glucan treatment. Mann-Whitney test; data are presented as Mean  $\pm$  SEM.

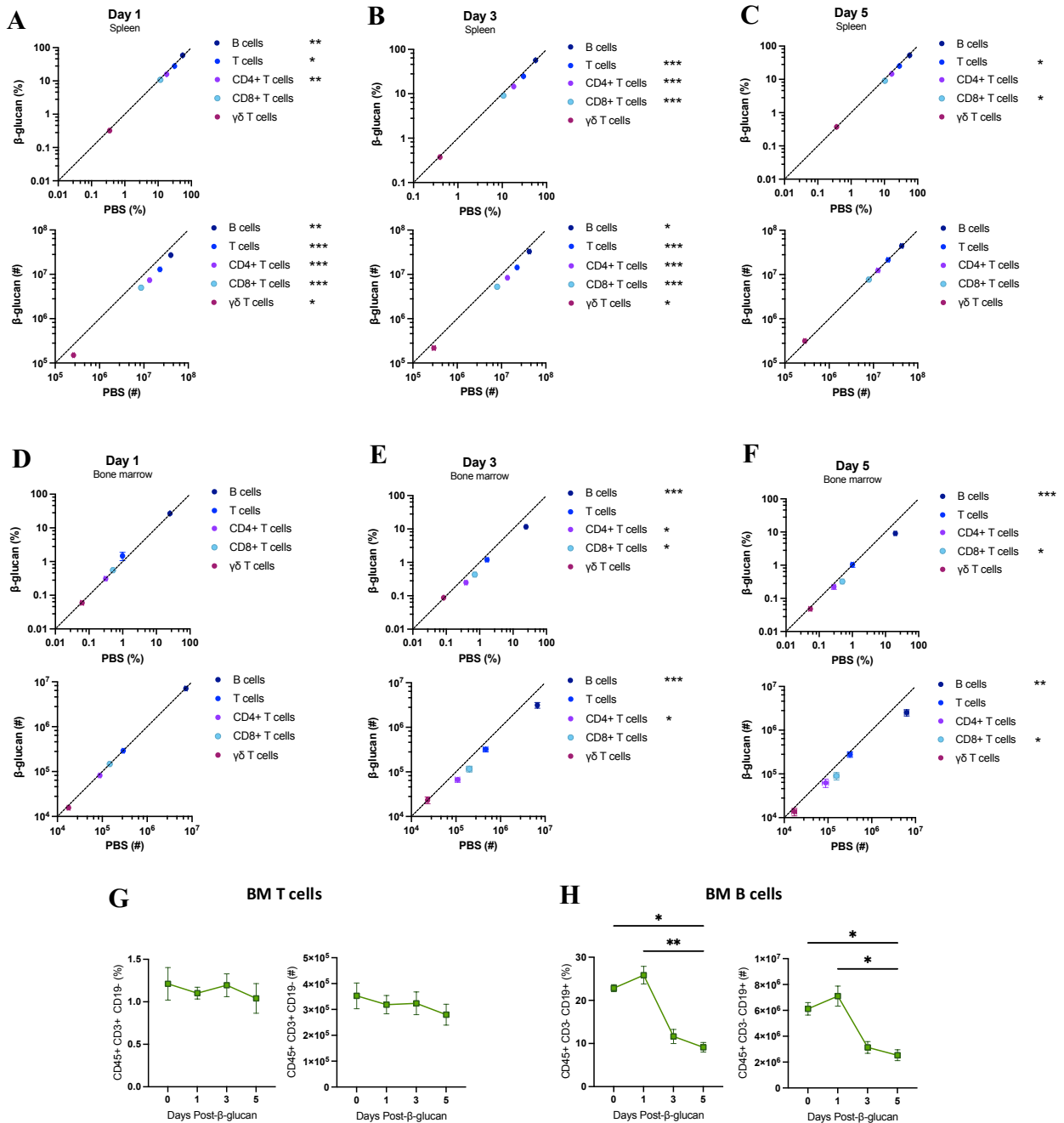


**Figure S4. Adaptive immune cell subsets in the BM and spleen after  $\beta$ -glucan treatment.** (A-C) Frequency (top) and absolute cell counts (bottom) of adaptive immune populations in the spleen at (A) day 1, (B) day 3, and (C) day 5 post- $\beta$ -glucan treatment. (D-F) Frequency (top) and absolute cell counts (bottom) of adaptive immune populations in the BM at (D) day 1, (E) day 3, and (F) day 5 post- $\beta$ -glucan treatment. Each dot represents the Mean  $\pm$  SEM. Dotted line represents where PBS and  $\beta$ -glucan frequencies or cell counts are equal. Analyzed using independent student T test. (G-H) Frequency (left) and absolute cell counts (right) of (G) T cells and (H) B cells in BM after  $\beta$ -glucan treatment. Kruskal-Wallis test followed by Dunn's multiple comparison test; data are presented as Mean  $\pm$  SEM.

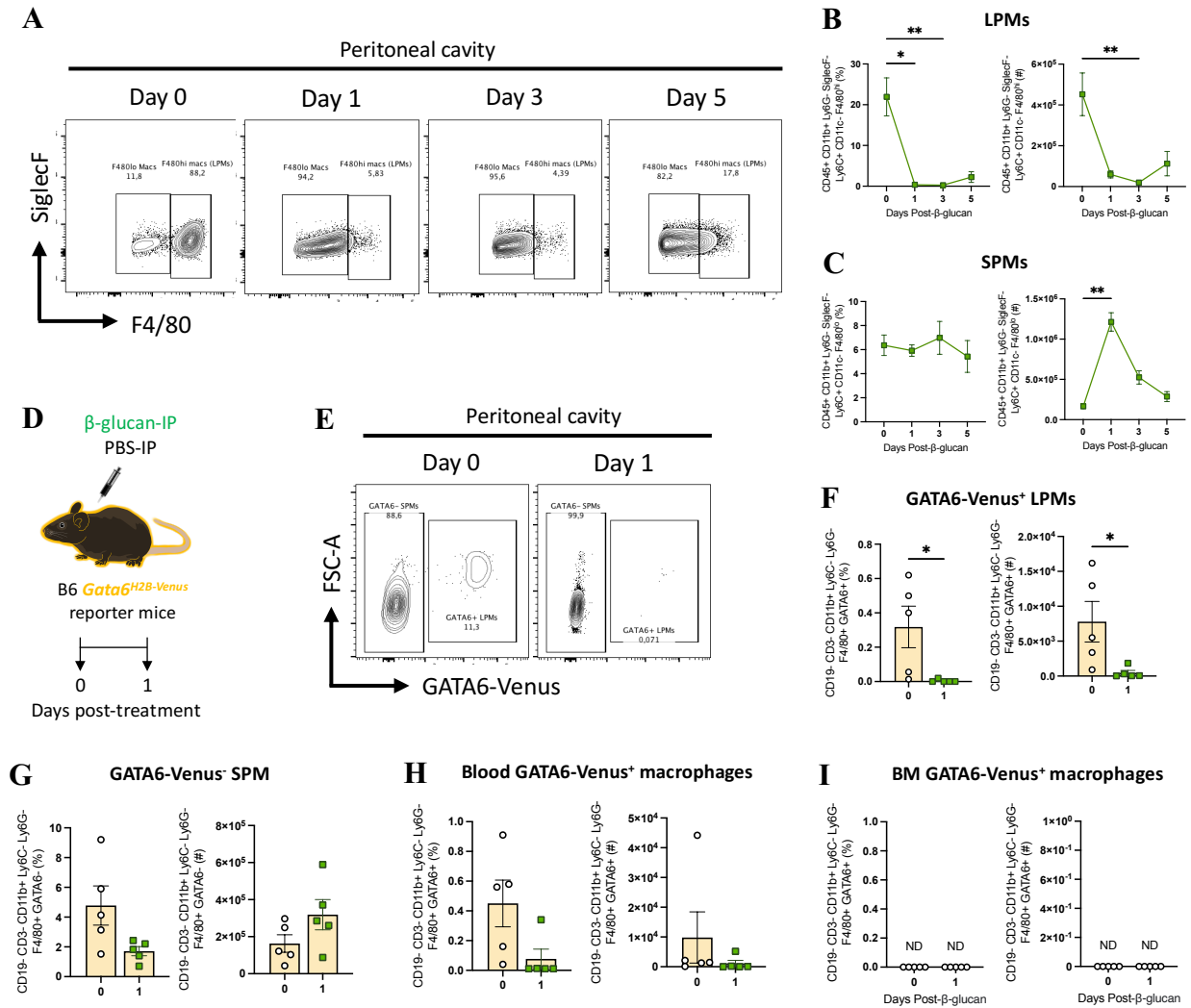


**Figure S5. LPMs do not egress from the peritoneal cavity at 1 day post- $\beta$ -glucan treatment.** (A) Representative FACS plots of LPM and SPM populations in the peritoneal cavity of WT mice at days 1, 3 and 5 post- $\beta$ -glucan treatment. Gated on CD45<sup>+</sup> CD11b<sup>+</sup> Ly6G<sup>-</sup> SiglecF<sup>-</sup> Ly6C<sup>-</sup> CD11c<sup>-</sup> F4/80<sup>+</sup> cells. (B-C) Frequency (left) and total cell counts (right) of (B) LPMs and (C) SPMs. (D) GATA6 reporter mice (n=4-5) treated with  $\beta$ -glucan-IP (1 mg) or PBS control for 1 day. (E) Representative FACS plots of LPM and SPM populations in the peritoneal cavity of GATA6 reporter mice at day 1 post- $\beta$ -glucan treatment. Gated on CD19<sup>-</sup> CD3<sup>-</sup> CD11b<sup>+</sup> Ly6G<sup>-</sup> SiglecF<sup>-</sup> Ly6C<sup>-</sup> CD11c<sup>-</sup> F4/80<sup>+</sup> cells; LPMs are GATA6-Venus<sup>+</sup> and SPMs are GATA6-Venus<sup>-</sup>. (F-G) Frequency (left) and total cell counts (right) of (F) LPMs, (G) SPMs, (H) GATA6-Venus<sup>+</sup> macrophages in the blood, and (I) GATA6-Venus<sup>+</sup> macrophages in the BM. Mann-Whitney test; data are presented as Mean  $\pm$  SEM. ND; not detected.

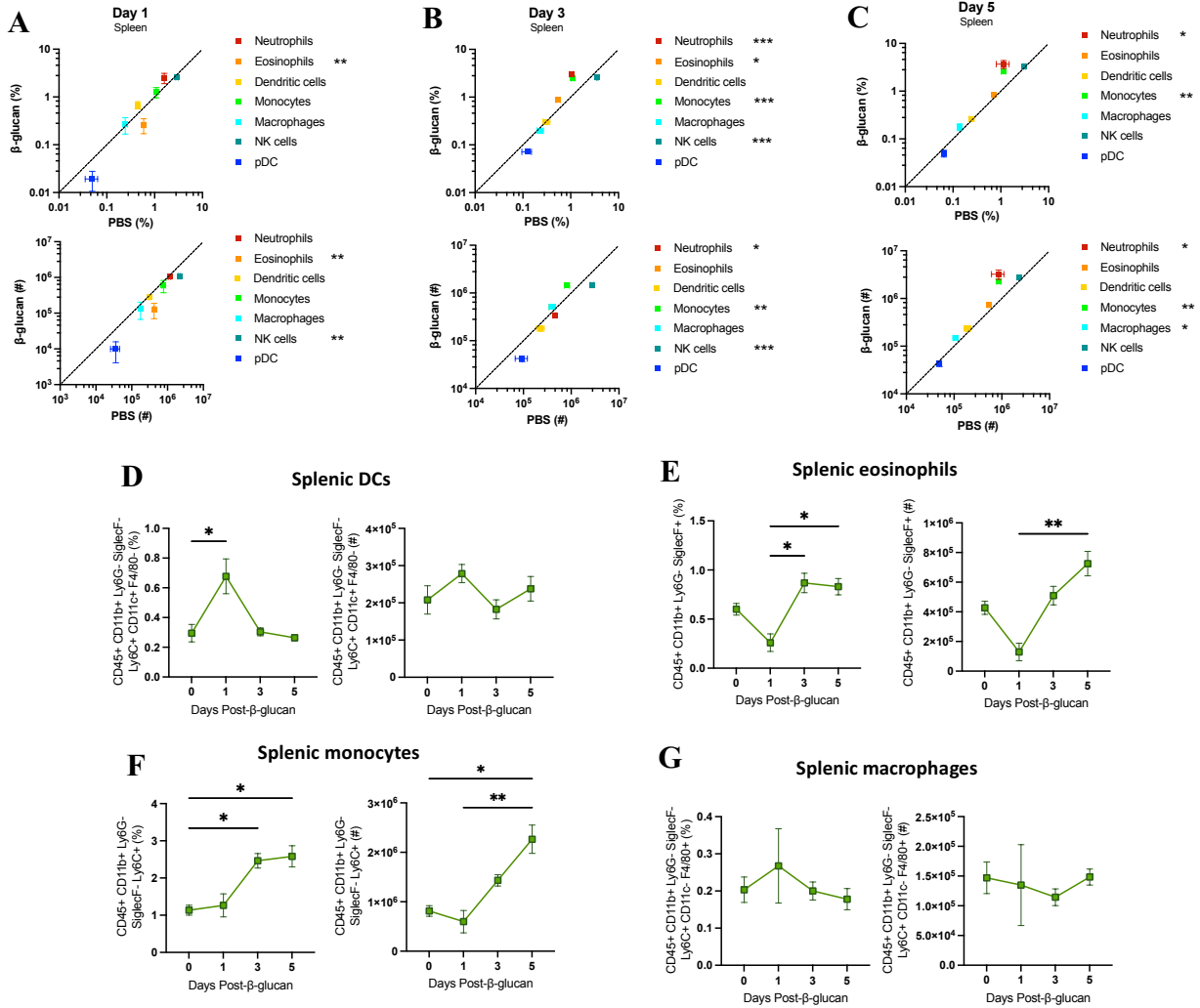


**Figure S6. Innate immune cell subsets in the spleen after  $\beta$ -glucan treatment.** (A-C) Frequency (top) and absolute cell counts (bottom) of innate immune populations in the spleen at (A) day 1, (B) day 3, and (C) day 5 post- $\beta$ -glucan treatment. Each dot represents the Mean  $\pm$  SEM. Dotted line represents where PBS and  $\beta$ -glucan frequencies or cell counts are equal. Analyzed using independent student T test. (D-F) Frequency (left) and absolute cell counts (right) of splenic (D) DCs, (E) eosinophils, (F) monocytes and (G) macrophages after  $\beta$ -glucan treatment. Kruskal-Wallis test followed by Dunn's multiple comparison test; data are presented as Mean  $\pm$  SEM.

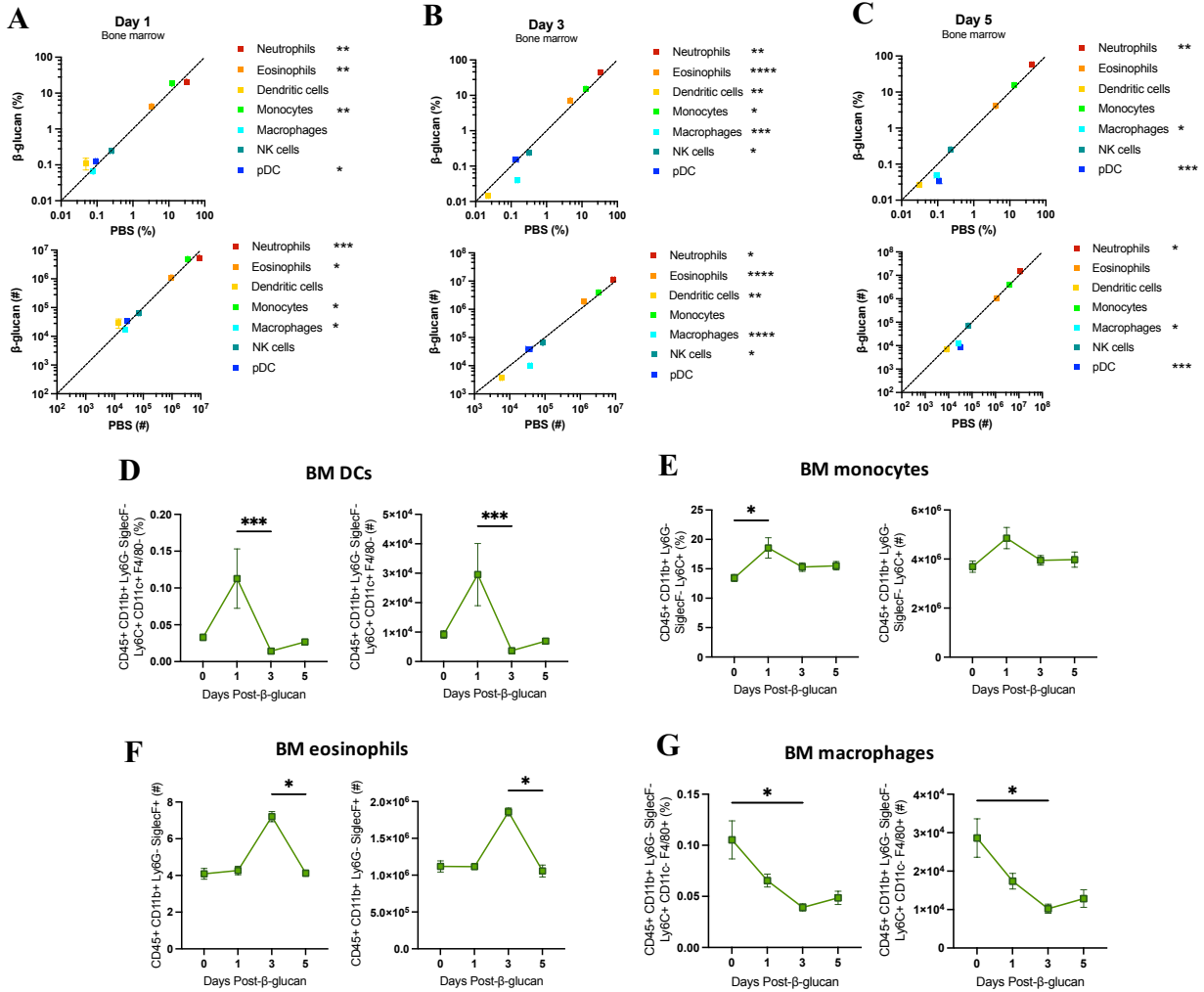


**Figure S7. Innate immune cell subsets in the BM after  $\beta$ -glucan treatment.** (A-C) Frequency (top) and absolute cell counts (bottom) of innate immune populations in the BM at (A) day 1, (B) day 3, and (C) day 5 post- $\beta$ -glucan treatment. Each dot represents the Mean  $\pm$  SEM. Dotted line represents where PBS and  $\beta$ -glucan frequencies or cell counts are equal. Analyzed using independent student T test. (D-F) Frequency (left) and absolute cell counts (right) of (D) DCs, (E) monocytes, (F) eosinophils and (G) macrophages in BM after  $\beta$ -glucan treatment. Kruskal-Wallis test followed by Dunn's multiple comparison test; data are presented as Mean  $\pm$  SEM.